

Dear Dr. Browne,

In addition to the suggested changes from the reviewers, we have also made the following changes based upon conversations with various collaborators while this paper was in the discussion stage.

Table with values of parameters used in model

We have now included an additional table in the manuscript (Table 2) that presents the values of parameters used in the model to help readers easily see which observations we have used for model input.

Removal of NRF_{τ_z} from manuscript

Joël Savarino and Joseph Erbland (LGGE, France) have recently used a snow chemistry column model to investigate nitrogen recycling between the air and snow at Dome C, Antarctica (manuscript was in review in ACPD at the time of writing). Conversations with them, initiated by a reviewer of their manuscript, convinced all of us that NRF_{yr} (not NRF_{τ_z}) represents the total number of nitrogen recyclings between the air and snow archived in ice cores. We have decided to remove NRF_{τ_z} from our manuscript and have changed NRF_{yr} to simply NRF . In sum, it is not necessary to multiply NRF by τ_z to calculate the degree of recycling archived in ice-core records because the majority of recycling happens in the first year after deposition to the ice sheet. Most of the recycling occurs between the air and the snow surface layer (~ top 2 cm) because snow-sourced HNO_3 is re-deposited only to the surface layer. In contrast, loss of nitrate occurs throughout the snow photic zone. Model-estimates of nitrogen recycling at Dome C in Erbland et al. [2015] (4 recycling events) and in this study (9 recycling events) are now more similar in magnitude. The difference (4 versus 9 may be due to the assumption in Erbland et al. that 20% of snow-sourced nitrate is transported away via katabatic winds ($f_{exp} = 0.2$). We are able to calculate f_{exp} in our modeling framework, and we calculate that 25% of snow-sourced nitrate is transported away at Dome C ($f_{exp} = 0.25$), which is slightly larger than the assumption in Erbland et al. Larger values of f_{exp} will lead to larger loss of snow nitrate, which may also lead to a larger number of recycling events via transport and redeposition of snow-sourced NO_x throughout East Antarctica. Additionally, the NRF values calculated for East Antarctica ($NRF=5-10$) are within the uncertainty of NRF values estimated by Davis et al. [2008]. These comparisons are described in section 3.3.

Since NRF_{τ_z} is now removed from the manuscript, we have moved the discussion of τ_z to later in the manuscript because τ_z is needed to calculate f . Additionally, in section 3.6., f is now compared to NRF across Antarctica instead of NRF_{τ_z} , which leads to a different relationship between spatial patterns of nitrogen recycling and photolysis-driven loss of snow nitrate. This relationship is discussed in the text, but the change does not significantly alter our conclusions.

Figure 7 now shows only NRF and Figure 9 now shows τ_z in addition to f and $\delta^{15}N(NO_3^-)$. We have moved τ_z into Figure 9 because τ_z is still used to calculate f and is no longer used to estimate the degree of nitrogen recycling (NRF_{τ_z}). Figure 10 now shows NRF vs.

f instead of NR_{τ_z} vs. f . Instead of separating the data into East and West Antarctica, we have separated the data by the number of years that nitrate remains in the snow photic zone.

Thank you for considering this manuscript for publication.

Sincerely,

Maria Zatko, Lei Geng, Becky Alexander, Eric Sofen, Katharina Klein

References:

Davis, D. D., Seelig, J., Huey, G., Crawford, J., Chen, G., Wang, Y., Buhr, M., Helmig, D., Neff, W., Blake, D., Arimoto, R., Eisele, F.: A reassessment of Antarctic plateau reactive nitrogen based on ANTCI 2003 airborne and ground based measurements. *Atmos. Environ.*, 42, 2831-2848, doi:10.1016/j.atmosenv.2007.07.039, 2008.

Erbland, J., Savarino, J., Morin, S., France, J.L., Frey, M.M., King, M.D.: Air-snow transfer of nitrate on the East Antarctic plateau – Part 2: An isotopic model for the interpretation of deep ice-core records. *Atmos. Chem. Phys. Discuss.*, 15,6886-6966, doi:10.5194/acpd-15-6887-2015, 2015.

Author Responses to Reviewer 1:

Thank you for all of these thoughtful and helpful comments and suggestions. These suggestions, along with suggestions from Reviewer 2, have led us to now refer to the modeled snowpack as “idealized”, largely because we agree that this study is based on several assumptions about the spatial variability of snow physical and optical properties. As mentioned in our responses to Reviewer 2, the goal of this research is to investigate the potential spatial variability in the flux of snow-sourced NO_x associated with snow nitrate photolysis along with the recycling, loss, and spatial redistribution of nitrogen across Antarctica, an environment in which observations of these parameters over large spatial scales are difficult to obtain. This modeling study is used to perform sensitivity studies aimed to guide future lab and field campaigns. We have clearly stated this goal in the abstract and also in the last paragraph of the introduction.

The phrase ‘comparable to observations’ is used frequently to compare a large range of result from the model to the very limited observations available across the Antarctic continent, and overall a strong case is not made that the model is comparable.

We have removed all references of model-measurement agreement in the manuscript although observations are still overplotted where available.

Sensitivity of the model’s parameters are tested for the calculation of the average flux of NO_x from the snow, and the model is most sensitive to the quantum yield and fraction assumed for nitrate that is “photolabile”. However, the sensitivity of the calculations is not tested for wet and dry deposition parameterizations, accumulation rate, and boundary layer height, which should all be expected to be very important.

Thank you for these suggestions. In a sense, accumulation rate is varied when concentrations of black carbon (C_{BC}) are changed because snow accumulation rate influences the flux of snow-sourced NO_x (F_{NO_x}) through its impacts on C_{BC} and thus the depth of the snow photic zone. Snow nitrate concentrations are also somewhat influenced by accumulation rate, so changes in snow nitrate concentrations also reflect changes in snow accumulation rate. Although we have not directly changed the rates of wet and dry deposition, we have performed sensitivity studies where only dry deposited nitrate (instead of total nitrate) is photolabile (see section 3.2). Unfortunately, we have not performed sensitivity studies where boundary layer heights are varied because arbitrary variation in the model boundary layer height would lead to inconsistent model physics and thus may give an inaccurate estimate of the impact of boundary layer height on the transport and redistribution of snow-sourced NO_x .

In some ways this simulation highlights to me a great deal that we lack in terms of understanding of photochemistry in and above snow-covered surfaces.

We hope that the results of our sensitivity studies will give readers a sense of which parameters influence snow-sourced NO_x the most. Many of these parameters are uncertain, such as the concentration of photolabile nitrate, which is one of the most influential parameters for F_{NO_x} . Since this parameters are very important for snow-

sourced NO_x , we hope that this study echoes other studies that have called for further field and laboratory studies aimed to better quantify the fraction of total nitrate that is photolabile.

This paper could be significantly improved upon if more detailed comparisons were made at sites such as South Pole and Dome C, where a great deal of data exists (for the environment) in terms of surface snow concentration, gas phase concentrations, and boundary layer conditions. Then the model would be much more believable for scaling up to the entire continent.

Thank you for this suggestion. In an earlier version of this manuscript, we compared boundary layer nitrate and ozone mixing ratios to modeled mixing ratios of these species. Modeled mixing ratios of nitrate and ozone are to a large degree dependent upon the height of the model boundary layer. Unfortunately, it is difficult to determine how well modeled boundary layer heights compare to observations because observations often span a large range at many stations (see Table 1 below for more detail). Additionally, other photochemical reactions in the snowpack that influence oxidant concentrations in the polar boundary layer (e.g., photolysis of H_2O_2 , production of reactive halogens) that are not included in the model at present will impact NO_3^- , HNO_3 , and O_3 through oxidant cycling reactions. Although we have not compared modeled boundary layer mixing ratios to observations in the manuscript, we have calculated factor increases in NO_x , NO_3^- , O_3 , OH for a model run with snow photochemistry compared to a model run without snow photochemistry in order to demonstrate how this one snow photochemical reaction alone (photolysis of snow nitrate) impacts, in a relative sense, the mixing ratios of NO_3^- , HNO_3 , OH, and O_3 .

Additionally, more careful comparisons with specific sites where isotopic data is available in the snow and in the atmosphere would also help to more fully evaluate the model and whether it is worth considering the quantified results in the paper.

We unfortunately do not simulate atmospheric $\delta^{15}\text{N}(\text{NO}_3^-)$ in the model and also cannot simulate vertical profiles of $\delta^{15}\text{N}(\text{NO}_3^-)$ in the snow since the model does not contain an explicit snow-column model. We are unsure of other ways to more carefully compare observed isotopic data to available model output from this study besides comparing modeled and observed $\delta^{15}\text{N}(\text{NO}_3^-)$ below the photic zone. Fortunately, these observations cover a large range of snow accumulation rates, which is the predominate factor governing its variability across the Antarctic continent.

Specific comments:

P18972, L14-15: This is a very big assumption. Laboratory, field, and box modeling studies all suggest that a very small portion of nitrate can explain the fluxes of NO_x out of the snow at South Pole and Summit (Greenland). Further, several studies suggest that a significant portion of the photolyzed nitrate products remain in the aqueous phase. Indeed, using isotopes of nitrate in laboratory and field studies, there are multiple suggestions of in situ reactions requiring water (or something isotopically similar) in the reformation of nitrate following photolysis (McCabe et al., Frey et al., Erbland et al., Shi et al., - all already cited in this paper) and this is

likely happening in the snow (as opposed to in the boundary layer). How is it that these studies, or what they suggest, should be ignored in this context?

The fraction of snow nitrate that is photolyzed in the model is limited by the use of a low quantum yield ($\phi=0.002$ [Chu and Anastasio, 2003]) and by the assumption that only dry-deposited nitrate is available for photolysis. These limit the fraction of total nitrate in the snow that is photolyzed in this study. Using this approach, there is order-of-magnitude agreement between modeled and measured snow-sourced NO_x . In contrast, using the quantum yield presented in Zhu et al. [2010] results in an overestimate of modeled F_{NO_x} by 3 orders of magnitude. The recombination of the NO_x photoproducts in the condensed phase has been observed in the references cited above, and will influence lab- and field-based estimates of the quantum yield.

The recombination effects within ice grains suggested in Erbland et al. [2013] will lower the flux of snow-sourced NO_x and influence oxygen isotopes, although nitrogen isotopes are not influenced by this ‘cage effect’. There are uncertainties in the amount of NO_x that is trapped within the ice grain. Erbland et al. [2015] suggest that 15% of NO_x experiences cage effects, but this fraction is an estimate and there are large uncertainties associated with the amount of NO_x that experiences recombination chemistry.

Nitrate that has been wet deposited to the snow likely has a higher probability of being trapped in the ice grain (and thus experience ‘cage effects’ or ‘recombination chemistry’) compared to dry deposited nitrate, although there may be some diffusion of nitrate in the snow grain after deposition. We have assumed that all wet deposited nitrate is unavailable for photolysis. We now specifically discuss recombination chemistry in the manuscript in section 2.1.3 in light of the potential influence that this process has on modeled snow-sourced NO_x fluxes.

P18974, L26 – P18975, L9: The phrase “likely from the redistribution of nitrate resulting from photolysis and subsequent recycling” is a major conclusion from this work and it is therefore inappropriate to state this here unless it is referenced in some way to other work that provides evidence for this.

There is evidence that nitrate concentrations vary considerably across the Antarctic ice sheet (for example for ITASE plus individual smaller scale studies) There is evidence that nitrate is much more concentrated in the top 2 cm of snow than below. But to what depth? The remainder of the “photic-zone depth” is very loose terminology here, since later the model will be used to calculate e-folding depths. If the concentrations in the surface snow are an artifact of nitrate redistribution than it seems that the model would be better compared with atmospheric concentrations (aerosols, fresh snow) than snow concentrations alone. Further, this would make the scaling below (P18975, L20-25) based upon dry versus wet deposition much more acceptable if the simulated results were similar to observations in the atmosphere. We have removed the phrase ‘likely from the redistribution of nitrate resulting from photolysis and subsequent recycling’ from this paragraph.

Nitrate concentration profiles generally show an enhancement in the top several centimeters of snow and then a sharp decrease to a stable equilibrium value throughout the remainder of the snow column, which in the vast majority of cases is at least as deep as 1 e-folding depth of UV actinic flux. In this manuscript, the full photic zone (3 e-folding depths of UV actinic flux) is used to calculate fluxes of NO_x from the snow. Since nitrate concentrations in the top 2 cm are enhanced by a factor of 6 compared to nitrate concentrations below, nitrate concentrations are decreased by an equal amount from the full photic zone (3 e-folding depths of UV actinic flux) for mass balance. Later in the manuscript, specifically when τ_z is calculated, an 'effective' photic zone depth is used (1 e-folding depth of UV actinic flux) because 87-91% of snow-sourced NO_x is produced within the top 1 e-folding depth.

For reasons stated above, it is difficult to interpret the model-measurement agreement for boundary layer mixing ratios. Through various sensitivity studies, we have explored the implications for snow-sourced NO_x on our assumptions about both snow nitrate concentration and the assumption that only dry deposited nitrate is photolabile (see section 3.2.).

P18976, L1-9: It does indeed seem unnecessary for a global model to include a liquid like region and distribute nitrate based upon this since there is still a fair amount of uncertainty regarding this within the laboratory based literature. It is clear from the Thomas et al. study (and studies by Boxe et al. such as ACP, 2008 and J. Phys. Chem. A., 2005) that the flux of NO_x from the snow in different places can be accounted for by only photolyzing a very small percentage of the nitrate in the snow, because it is concentrated in the LLR. This is an important distinction from blowing away/recycling all of the nitrate in the photic zone. This is a critical point that needs to be better evaluated in the context of whether it is worthwhile to even consider the simulated results as having any bearing in the real world if it cannot reconcile this. In other words, parameterizing the loss of nitrate from snow may be necessary at this scale, but this does not mean that work suggesting a great deal of nitrate is reformed within the snow (see comments above also) or that the loss of nitrate is minor compared to the bulk nitrate concentration in snow when including a LLR can be ignored.

Thank you for this comment, as well as the related comment above. As also mentioned above, we have used the quantum yield from Chu and Anastasio [2003] and additionally have only assumed that dry-deposited nitrate is available for photolysis. In these ways, only a fraction of the total nitrate in the snow is photolyzed in this study over the course of a year and there is at least order-of-magnitude agreement between modeled and measured snow-sourced NO_x when taking this approach. The modeling studies mentioned above represent calculations for a single location, and thus are able to "tune" their model to produce the desired results for that single location (e.g., Thomas et al. [2011] need to assume that only 6% of snow nitrate is photolabile to match observations at Summit). Since we do not have observations at every grid box in the model, we need to make more process-based assumptions about the fraction of snow nitrate that is photolabile. There are essentially no laboratory or field based observations of the fraction of nitrate that is photolabile that allow us to examine the validity of our assumptions

about this parameter. Hence, we perform sensitivity simulations that effectively change this fraction (changing the quantum yield, removing the dry-deposition limitation) to evaluate the importance of these assumptions.

As mentioned above, Thomas et al. [2011] find that only 6% of the nitrate in snow must be photolyzed to match modeled and observed NO mixing ratios in the boundary layer. In this study, there are places where a similar fraction of nitrate in snow is photolabile (e.g., 10-15% around the coasts, Figure 3c), and the fluxes of NO_x calculated in these region are on the order of 10⁸ molec cm⁻² s⁻¹, which is the same order of magnitude as most snow-sourced NO_x flux observations.

We have added discussion about recombination chemistry and nitrate concentrations in the LLR into the manuscript in sections 2.3.1. In regions where wet deposition is dominant, we feel that we are attempting to take recombination chemistry into account (albeit crudely).

P18977, section 2.3.1. There is a great deal of uncertainty associated with the assumptions made in this section. Several aspects of the assumptions are tested via sensitivity studies. But it is critical to better understand how sensitive the calculations are to the amount of deposition taking place in the model (wet versus dry, total deposition overall). Further it is also very important to test sensitivity to accumulation rate as this should be very important for how long nitrate remains in the photic zone. Studies that directly work to quantify accumulation rate are limited and often fraught with the difficulty of dealing with blowing snow, drafting, density changes etc. So a simple comparison with a few values that “seem” to fit the model is weak at best, and it should be understood how important this parameter is to determining simulated values. Finally, changes in boundary layer height should be tested for sensitivity. In section 3.4., the authors are dismissive about comparing the model to observed boundary layer heights, as they vary over a large range and don’t agree well. How important is this? A priori I would expect this to play a very important role in determining how much of this NO_x is transported away versus recycled and “re”deposited locally, which applies to all of the results computed in this work.

Thank you for these suggestions. It is true that we have not performed sensitivity studies varying wet and dry deposition, boundary layer height, or snow accumulation rate specifically. At least two of these parameters (snow accumulation rate and the fraction of wet versus dry deposition of nitrate) have considerable spatial variability in the model, allowing us to examine their influence without the need for arbitrary changes. The biggest influence that the snow accumulation rate will have on F_{NO_x} is via its impacts on snow black carbon and nitrate concentrations, and we have performed sensitivity studies varying both of these parameters. Although we have not directly changed the relative rates of wet and dry deposition, we have performed sensitivity studies where only dry deposited nitrate influences snow-sourced NO_x. We have not performed sensitivity studies where boundary layer heights are varied because changes in boundary layer height would lead to inconsistencies with model physics (e.g., temperatures, winds). It would be difficult to associate changes in our results solely with changes in the boundary

layer height, and interpretation of arbitrary changes in boundary layer height may be misleading due to associated inconsistencies in model physics as described above.

Below is a table that shows observed boundary layer heights compared to monthly-averaged model boundary layer heights for several stations in Antarctica. Unfortunately it is difficult to tell how well the boundary layer is represented in the model because there is such a large range of observed boundary layers at many locations. The observations are generally averaged value over the course of the measurement period. Several observations span the full range of diurnal values, and these observations have been noted in the table below.

Table 1. Observed and modeled boundary layer heights in Antarctica

Location	Observed BL (m)	Modeled BL (m)	References
Neumayer	10-300 (summer)	460 (Dec) 285 (Jan) 300 (Feb)	Handorf [1996] Konig-Langlo et al. [1998] Davis et al. [2004] Weller et al. [1999]
South Pole	50-600 (Dec-Jan) 200-375 (Mar-Nov) 100-300 (Mar-Aug) 25-300 (Nov-Dec)	50 (Dec,Jan,Feb) 40-45 (Mar-Nov)	Oncley et al. [2004] Travouillon et al. [2008] Neff et al. [2008]
Dome C	0-300 m (summer, with diurnal variation) 10-300 m (summer, with diurnal variation) 25-40 m (winter)	65 (Jan) 50 (Feb) 40 (Mar-Oct) 50 (Nov) 104 (Dec)	King et al. [2006] Lawrence et al. [2004] Trinquet et al. [2008] Casanta et al. [2014]
Halley	200-300 (summer) 40-110 (summer) 200-400 (winter) 50-150 (winter)	190 (Jan) 270 (Feb) 200 (Mar) 160 (Apr) 125 (May) 80 (Jun) 170 (Jul) 120 (Aug)	King et al. [2006] Jones et al. [2008] Jones et al. [2006] Anderson [2003]
Kohnen	200-500 (Nov-Dec, diurnal variation)	80 (Nov) 130 (Dec)	Kodama et al. [1989]

P18979, L22-23: How, on the timescale of ice cores (e.g., glacial/interglacial cycles) would it ever be assumed that factors that influence snow photochemistry would remain the same? The fraction lost from year to year seems like it would be highly variable, not “stable from year to year”. In fact, snowpit profiles from Antarctica (studies cited here such as Rothlisberger, Frey, Dibb, Shi) show quite a significant amount of variability in concentration with depth.

Over the timescales of ice cores, we would definitely expect there to be changes in many parameters that would influence snow photochemistry, such as changes in snow accumulation rates with climate or changes in the concentration of light-absorbing impurities. However, over the number of years that nitrate remains in the photic zone (up to 7.5 years in Antarctica in the present day), these parameters remain relatively constant. f can be calculated for present-day snow and for glacial-period snow separately, using an appropriate number of years that nitrate remains in the photic zone for each period. In this study, we are focusing on the present climate.

P18982, L15-20: It needs to be made clear here and in several other places what below 2 cm means. To what depth is the model calculating over? To what depth is being compared to with the observations? Below surface could be to 3km!, please quantify this here and in table 2 and in the figure captions.

Why is it that a constant concentration is assumed? Above, there is direct discussion of the evidence for variability in nitrate concentrations at the surface. Justification should be made as to why it is important to use a constant concentration.

Please report concentration (or actually, it’s mass fraction when reported as ng/g) in consistent units

Why are only ITASE measurements compared here? The isotope results are seemingly compared with more data, but those studies must all have concentration data available also. Given the much more limited data on the East Antarctica Ice Sheet, it seems worthwhile to compare with Frey, Erbland, and Shi transect concentration data as well.

Thank you for suggesting that we make the depth terminology “below 2 cm” more clear throughout the manuscript. Throughout the manuscript (sections 2.1.3., Table 1, Figure 3 caption, Figure 4 caption) we have clarified “below 2 cm” to mean “from 2-cm depth to the bottom of the photic zone (z_{3e})”. In Table 2 and Table 3 we now use the variable “[NO_3^-] $_{bot}$ ”, which has been clearly defined in Table 1.

We have assumed spatially constant concentrations of nitrate across Antarctica ($[NO_3^-]_{bot} = 60 \text{ ng g}^{-1}$, $[NO_3^-]_{bot} = 360 \text{ ng g}^{-1}$). Although there is a wide range of multi-year, sub-surface snow nitrate concentrations measured across Antarctica during the ITASE campaign [Bertler *et al.*, 2005], there is not a clear spatial pattern associated with these observations. Although we use constant snow nitrate concentrations across Antarctica, a number of sensitivity studies are performed to investigate the impact of snow nitrate concentration on snow-sourced NO_x . In sensitivity studies, snow nitrate concentrations are halved and doubled, the nitrate enhancement factor is varied from 1 to 10, and it is

assumed that all nitrate is photolabile (see section 3.2.). We have now slightly rearranged the beginning of section 2.1.3. and added two sentences to explain why we use constant nitrate concentrations across Antarctica.

Erbland et al. [2015] and Shi et al. [2014] provided snow nitrate concentration data in tabular form and we have now included this data in Figure 3d and have updated the text and figure caption accordingly.

P18986: At the top and bottom of this page there are important disagreements with Davis et al. (2000) and Erbland et al. (2015), and both seem to be dismissed as “varying approaches”. Why are the calculated values so different? Given the understanding the authors believe they are developing from the sensitivity studies, what most likely explain the difference in results?

Thank you for addressing this issue. While this manuscript was in the review process, we have had some discussions with Joël Savarino and Joseph Erbland about how to best calculate $NR_{F_{\tau_z}}$ in light of the reviews of their paper, which at the time was in the review stages in ACPD. We have now removed $NR_{F_{\tau_z}}$ from the manuscript and compared our calculated $NR_{F_{yr}}$ (now just NR_{F}) with the NR_{F} values calculated in Erbland et al. [2015] and Davis et al. [2008]. The reason that $NR_{F_{\tau_z}}$ was not valid is because although loss of nitrate occurs throughout the snow photic zone, the recycling happens mainly at the surface via re-deposition of snow-sourced NO_x . Our modeled $NR_{F_{yr}}$ (not just NR_{F}) values are similar in magnitude to the NR_{F} values reported in Erbland et al. [2015] and Davis et al. [2008]. We have outlined changes made to the nitrogen recycling part of this manuscript in the “Letter to the Editor” and have copied this information below. The last paragraph in section 3.3. has also been updated to reflect this change and compares the NR_{F} values from these different studies.

P18988, L11 and L19-20: What does sub-photic zone mean? What depth range is this? Why not compare with surface observations (i.e. some mean of the top few cm or a mean of the model calculated photic zone for each observation point. The comparison here seems not justified or worse, artificially constructed. Furthermore, on line 20 it is suggested that the ice core measurements are representative of observations “well below the snow photic zone”. But, upon deposition, the snow nitrate was exposed to light (before it was archived in the “sub-photic zone”). Better terminology is needed here to help the reader understand what is being referred to and why this is an important comparison to make. Unless it is an instant in time below the photic zone, the nitrate is not necessarily lacking in influence of exposure to photolytic processing. In fact, here and below, it seems important to consider comparing with atmospheric observations – i.e. the primary signal that is then processed in the surface snow – rather than that that has already been photolytically altered.

Sub-photic zone is the depth in snow below the bottom of the photic zone, which is any depth interval below 3 e-folding depths of UV actinic flux in this study. Below this depth, ~95% of the radiation has been attenuated.

The $\delta^{15}\text{N}(\text{NO}_3^-)$ calculated in this study represents snow below the photic zone (below 3 e-folding depths of actinic flux) because it is indicative of the loss of snow nitrate over the total time that it spent in the snow photic zone. When nitrate is buried below the snow photic zone, no more photolysis or alteration of $\delta^{15}\text{N}(\text{NO}_3^-)$ occurs; hence, the $\delta^{15}\text{N}(\text{NO}_3^-)$ (referred to as asymptotic $\delta^{15}\text{N}(\text{NO}_3^-)$ in Erbland et al. [2013]) is further unaltered and is preserved in the ice-core record. The chemical and physical properties of snow within the photic zone are used to estimate what the enrichment in $\delta^{15}\text{N}(\text{NO}_3^-)$ would be in ice cores at depths below the photic zone (below z_{3e}).

Since we have not incorporated a detailed snow chemistry column model into GEOS-Chem, we are unfortunately not able to simulate vertical profiles of $\delta^{15}\text{N}(\text{NO}_3^-)$ in snow or calculate surface $\delta^{15}\text{N}(\text{NO}_3^-)$ values. Since we are only able to calculate $\delta^{15}\text{N}(\text{NO}_3^-)$ values in this study that are relevant for ice-cores or snow that is below the photic zone, we compare our modeled $\delta^{15}\text{N}(\text{NO}_3^-)$ values with $\delta^{15}\text{N}(\text{NO}_3^-)$ observations from snow below the photic zone, which is a region without snow photochemistry.

P18988, L25-26: “The modeled $\delta^{15}\text{N}(\text{NO}_3^-)$ values are generally higher than observations, however, boundary layer $\delta^{15}\text{N}(\text{NO}_3^-)$ observations are negative over much of Antarctica (Erbland et al., 2013; Frey et al., 2009; Morin et al., 2009; Savarino et al., 2007), making modeled $\delta^{15}\text{N}(\text{NO}_3^-)$ values biased high by up to 40%”. A few questions here. What is being compared? Snow nitrate $\delta^{15}\text{N}(\text{NO}_3^-)$ values to snow nitrate $\delta^{15}\text{N}(\text{NO}_3^-)$ values, atmosphere to atmosphere, or snow to atmosphere? The link between the negative atmosphere values and the model being biased high is not making sense here to me. In addition, “over much of Antarctica” is a stretch – the Erbland and Frey studies include atmospheric observations at Dome C, Savarino at DDU and Morin in the Weddell Sea. 3 sites hardly count as over much of Antarctica, given it’s size. Still, it seems important to compare, at those sites, the model versus observations in the atmosphere to better constrain the simulation.

Thank you for asking us to clarify whether we are discussing atmospheric or snow $\delta^{15}\text{N}(\text{NO}_3^-)$ values in this sentence. We are comparing modeled and observed sub-photoc zone/ice-core $\delta^{15}\text{N}(\text{NO}_3^-)$ values here, not atmospheric $\delta^{15}\text{N}(\text{NO}_3^-)$ values. We have updated this sentence as shown below:

“The modeled enrichments in ice-core $\delta^{15}\text{N}(\text{NO}_3^-)$ values are generally higher than the sub-photoc zone $\delta^{15}\text{N}(\text{NO}_3^-)$ observations presented in Figure 9c, however, boundary layer $\delta^{15}\text{N}(\text{NO}_3^-)$ observations are negative over much of Antarctica [Erbland et al., 2013, Frey et al., 2009, Morin et al., 2009, Savarino et al., 2007], making modeled $\delta^{15}\text{N}(\text{NO}_3^-)$ values biased high by up to ~40‰ since we assume that the $\delta^{15}\text{N}$ of atmospheric nitrate (NO_3^- and HNO_3) deposited to the snow surface is always equal to 0‰”.

In the equation used to calculate enrichments in ice-core $\delta^{15}\text{N}(\text{NO}_3^-)$ (equation 11), the $\delta^{15}\text{N}$ of NO_3^- in the atmosphere is required. In this way, atmospheric $\delta^{15}\text{N}(\text{NO}_3^-)$ influences the value of ice-core $\delta^{15}\text{N}(\text{NO}_3^-)$. We have set the atmospheric $\delta^{15}\text{N}(\text{NO}_3^-)$ in equation 11 equal to 0 because we only examining the impacts of snow nitrate photolysis

on enrichment in ice-core $\delta^{15}\text{N}(\text{NO}_3^-)$. Where observations of atmospheric $\delta^{15}\text{N}(\text{NO}_3^-)$ are available in Antarctica, the measured values are generally negative (up to -40‰). Since we have set $\delta^{15}\text{N}(\text{NO}_3^-)$ equal to 0, rather than a negative number, this leads to the high bias in ice-core $\delta^{15}\text{N}(\text{NO}_3^-)$ that was mentioned in the text.

We have removed the terminology “over much of Antarctica”. This sentence now reads: “The modeled enrichments in ice-core $\delta^{15}\text{N}(\text{NO}_3^-)$ values are generally higher than the sub-photic zone $\delta^{15}\text{N}(\text{NO}_3^-)$ observations presented in Figure 9c, however, boundary layer $\delta^{15}\text{N}(\text{NO}_3^-)$ observations are negative in both coastal [Morin *et al.*, 2009, Savarino *et al.*, 2007, Wagenbach *et al.*, 1998] and continental [Erbland *et al.*, 2013, Frey *et al.*, 2009] Antarctica, making modeled $\delta^{15}\text{N}(\text{NO}_3^-)$ values biased high by up to ~40‰.”

Due to the lack of a snow chemistry column model, we are unable to simulate atmospheric $\delta^{15}\text{N}(\text{NO}_3^-)$ in the model and thus cannot compare this model output to observations.

P18990, L3-6: Two aspects of the $\delta^{15}\text{N}(\text{NO}_3^-)$ work should be tested for sensitivity. How sensitive are the results to the photolytic fractionation factor? How sensitive are the results to the initial starting values of 0‰. Berhanu *et al.*'s laboratory study is much better developed than previous work, but the results therein (and the companion paper by Meusinger *et al.*) look nothing like what is suggested in the model here. For instance, in the laboratory study the e-folding depth is only a few to several centimeters (or less) and the amount of nitrate lost is fairly minimal even given long exposure times. In addition, the Frey *et al.* (2009), Erbland *et al.* (2013), and Shi *et al.* (2015) work suggest that the apparent fractionation factors, base on snowpits in the field, vary considerably (Frey *et al.* report -49.8 and -71.0 for field based snow, and theoretically predict -44.8; Shi *et al.* report values from -93.1 to -50.2 for the apparent fractionation factor at low accumulation sites in the 0-20 cm depth and higher values at the higher accumulation sites; Erbland *et al.* report -74.3 to -40.0 for Dome C, Vostok, and similar sites, higher values again for higher accumulation sites). The field based values reflect a number of processes, even if they are dominated by photolytic loss. Still, the balance of evidence suggests that sensitivity to the photolytic fractionation factor should be tested within a fairly wide range (or at least at much more negative values too).

For the last sentence here, can an example be show as to how d15N could be used to estimate the degree of recycling and loss for a different point in time than present? What values need to be known to perform this calculation? Do constant conditions need to be assumed over time (e.g., concentration, deposition, LAI, overhead sun, etc)? Looking at figure 10, how would one know the f value for their site if the nitrate is heavily processed?

Additionally my read of this section is that field work is needed to better understand the atmospheric isotopic values across Antarctica, both in terms of what might be primary input and what is secondary formation over the continent because of snow emissions of NO_x . Depending on the results of the suggested sensitivity analyses

above this may be worth including in the conclusions as a focus of future work as well.

Changes in the photolytic fractionation factor and air $\delta^{15}\text{N}(\text{NO}_3^-)$ both influence ice-core $\delta^{15}\text{N}(\text{NO}_3^-)$ values considerably. We assume air $\delta^{15}\text{N} = 0\text{‰}$ in this study as we are only examining the enrichment in snow $\delta^{15}\text{N}(\text{NO}_3^-)$ due to photolysis. The magnitude of the fractionation factor will certainly impact our calculations of the enrichment in snow $\delta^{15}\text{N}(\text{NO}_3^-)$ due to photolysis, though it will not impact our calculations of other parameters in this study (e.g., F_{NO_x} , f , and NRF). We have varied the photolytic fractionation factor from -90‰ to -10‰ and found that ice-core $\delta^{15}\text{N}(\text{NO}_3^-)$ by increases by a factor of 2 and decreases by a factor of 5, respectively, across Antarctica. We have added the following sentence to the end of section 3.5.:

“The modeled ice-core $\delta^{15}\text{N}(\text{NO}_3^-)$ values resulting from the photolysis-driven loss of snow nitrate are sensitive to the fractionation constant (ϵ). The fractionation constant is varied over the full range of values reported in Erbland et al [2013], Frey et al., [2009], and Shi et al. [2014]; an ϵ of -90‰ increases $\delta^{15}\text{N}(\text{NO}_3^-)$ by a factor of 2 and an ϵ of -10‰ decreases $\delta^{15}\text{N}(\text{NO}_3^-)$ by a factor of 5 across Antarctica.”

Thank you for suggesting that we provide an example of how $\delta^{15}\text{N}(\text{NO}_3^-)$ could be used to estimate the degree of recycling and loss for a different point in time than the present. In section 3.6. we now discuss which values must be known to perform this calculation (e.g., snow accumulation rate and light-absorbing concentrations in snow) and how these parameters may change under different climate scenarios.

We agree that more measurements of atmospheric isotopic values across Antarctica would be incredibly valuable.

P18890, L19-21: The pattern is suggested to be dependent about the patterns of snow accumulation rate and LAI across the continent, yet the sensitivity to accumulation rate is not tested, and the sensitivity to LAI is limited so why is this so important to the pattern?

In this study, the spatial pattern of F_{NO_x} is dependent on the spatial patterns of LAI in snow, and the spatial patterns of LAI are dependent on snow accumulation rate. The spatial pattern is also dependent on the fraction of photolabile nitrate, which we have now included in this section as well (thank you for bringing this to our attention).

This part of the text now reads: “The modeled spatial pattern of the flux of snow-sourced NO_x is determined by the patterns of light-absorbing impurity concentrations in snow and the fraction of photolabile NO_3^- across Antarctica. The spatial pattern of light-absorbing impurities is strongly influenced by snow accumulation rates and the spatial pattern of photolabile NO_3^- in the model is influenced by the amount of wet deposited NO_3^- compared to total deposited NO_3^- across Antarctica. Snow NO_3^- concentrations were kept constant for this simulation; however, spatial variations in snow NO_3^- concentrations would also influence the spatial pattern of F_{NO_x} across Antarctica.”

P18991, L10: Not clear how a conclusion can be drawn about preservation in the coastal region when the model is limited in its ability to reproduce observations in the region. While the reason for this limitation is explained in the paper, how can conclusions be drawn about what the modeling is producing if there is no way to verify its realism?

Thank you very much for this comment. We have removed this sentence from the conclusions.

Technical Comments/corrections:

P18964, L5: nitrate photolysis is not a direct source of ozone, remove mention of this in the ().

Ozone has been removed from these parentheses.

P18964, L5: I disagree with the use “disturbs the preservation of NO₃⁻ in ice cores”. It needs to be clear here that nitrate photolysis changes what is preserved or changes what is ultimately archived in the snow such that ice cores may not reflect a primary atmospheric signal (or loading). The phrase as it is now (and later in the text) implies that nitrate can be affected after it is preserved, and I do not understand the term “disturbs” in this context.

We have changed this sentence to: “Nitrate (NO₃⁻) photolysis in snow provides a source of oxidants (e.g., hydroxyl radical) and oxidant precursors (e.g., nitrogen oxides) to the overlying boundary layer, and alters the concentration and isotopic (e.g., δ¹⁵N) signature of NO₃⁻ preserved in ice cores.”

We have also made similar updates in the introduction and in section 2.3.

P18965, L13: Levy et al. 1999 is one of the few modeling studies that actually shows the temporal and spatial dependence of the NO_x lifetime against loss. Be more specific here in terms of what is relevant to this study – eg. mid to high southern latitudes where the lifetime is typically longer than only a day, especially in winter.

We have changed this sentence to include the NO_x lifetimes in polar regions as presented in Appendix A5 of Levy et al. [1999]. The sentence now reads: “Oxidation to form nitrate (HNO₃/NO₃⁻) is the main sink for NO_x in the troposphere [Logan, 1983], and the lifetime of NO_x against oxidation to nitrate is 1-3 days in polar regions [Levy et al., 1999]”.

P18965, L15: There are much more recent studies that are relevant here than Logan 1983. For instance, Xu, Penner et al. suggest the global average lifetime of nitrate (particulate and HNO₃) is about 5 days.

Thank you for bringing this more recent paper to our attention. This sentence now reads: “NO₃⁻ is lost from the atmosphere through dry and wet deposition to the Earth’s surface, and has an atmospheric lifetime of roughly 5 days [Xu and Penner, 2012].”

P18965, L19: So as not to confuse the reader later replace “recycles” with “returns” (ie this is only speaking to the atmospheric impact and not the recycling back to snow nitrate).

We have replaced “recycled” with “returns” in this sentence.

P18967, L13: In the above equation, everything is listed as in the aqueous phase. It needs to be clear here that NO₂ and NO can then be lost to the gas phase and THEN pumped out of the snowpack.

The sentence below E1 and E2 now reads: “The aqueous phase NO₂ produced in E1 is can be transferred to the gas phase and subsequently transported into the interstitial air [Boxe *et al.*, 2005] and then released to the atmosphere.”

P18967, L15-16: The local abundance of NO_x is also dependent upon how much NO_x is transported away from the site. If you look at any of the studies referenced here in terms of NO_x fluxes, almost none of them understand the NO_x budgets at individual locations.

In this sentence, we are specifically addressing the relative abundance of NO and NO₂, not the total local abundance of NO_x. We agree that the local abundance of NO_x is subject to local transport patterns.

P18968, L4: Please remove the use of the phrase “disturbs the preservation”. See above comments in the abstract, and consider that this process makes what is preserved not necessarily reflect atmospheric loading of nitrate.

We have removed this phrase and the sentence now reads: “The photolysis of snow NO₃⁻ and subsequent recycling between the air and snow alters the concentration and isotopic (e.g., δ¹⁵N) signature of NO₃⁻ that is ultimately preserved in polar ice sheets, which hampers the interpretation of ice-core NO₃⁻ records [Wolff *et al.*, 2008].”

P18968, L19: Given the timescale of the model simulations in this study, this sentence is a bit iffy. While the model is compared with some ice core data, this seems to be because the data is limited not because the model is actually being aimed at reconstructing ice core δ¹⁵N.

One of the major goals of this modeling study is to calculate ice core δ¹⁵N in the present climate, which is explained in more detail in some of the comments above. Since this is a main goal of our work, we would like to keep this sentence in the manuscript.

P18974, L12: Some justification as to why a value from coastal Alaska is applicable to the Antarctic ice sheet should be made here (even if the insoluble material plays a small role in the results).

We have added a phrase to the end of the sentence starting with “To our knowledge..”. This sentence now reads: “To our knowledge, observations of soluble light-absorbing impurities in Antarctic snow are unavailable. We use soluble LAI observations from the Arctic to provide a general estimate of the importance of soluble LAI in polar snow.”

P18978, L4: This fits with the earlier assumption that the photolabile nitrate is located closer to the surface. The range of % NO_x produced is different here than in the caption of Figure 1.

In this section of the text, we mention that 87-91% percent of snow-sourced NO_x is produced in the top 1 e-folding depth. In Figure 1, we mention that 30-65% of the snow-sourced NO_x is produced in the top 2 cm of snow. In this study, the top e-folding depths of UV actinic flux extends below the top 2 cm of snow.

P18981, L13: Suggest moving “Fig. 3” into the () so as not to cause confusion with Figure 3 of this paper.

Thank you for this suggestion. We have moved Fig. 3 into the parentheses.

P18984, L25: “peroxyacl” is a misspelling.

Thank you for catching this misspelling. We have corrected it in the latest version of the manuscript.

Figure 1: Why does it appear that nitrate formed locally is deposited, snowed upon, and then photolyzed to NO_x? Not that % snow-sourced NO_x in the top 2 cm is different here than in the text.

As mentioned in the comments above, the % in the Figure 1 caption refers to the top 2 cm and the % in the text refers to the top 1 e-folding depth. This has been made more explicit in the figure caption.

In Figure 1, F_{PRI} represents long-range transport of nitrate and input from the stratosphere and F_R represents the nitrate that has been photolyzed in the snow, exported as NO_x into the boundary layer, and then re-deposited back to the snow. To illustrate that not all of the nitrate formed in the atmosphere is re-deposited to the original site of photolysis, we have now added another arrow to simulate transport of nitrate away from the original site of NO_x emission from snow.

Figure 3: Why not also compare with surface snow concentrations (rather than just $[NO_3^-]_{bot}$ scaled by F_p)

The snow nitrate concentration measurements that have been included in Figure 3d are sub-surface snow nitrate concentration measurements. For consistency, we have compared these observations to $[NO_3^-]_{bot}$. Due to the rapid decrease of snow nitrate concentrations in the top 2 cm, observations of “surface” snow nitrate concentrations are difficult to interpret, as some observations represent the average over the top 2 cm, while other represent observations in the surface skin layer (~ 1 mm).

Figure 6a and 6b are not particularly useful; the ratios in c and d are much more helpful for understanding how much difference this can make.

Figures 6a and 6b show where F_{NO_x} has been set to 0 in these sensitivity studies, which is helpful for quickly visualizing how much recycled nitrate is present in regions where F_{NO_x} has been set to 0. For example, although F_{NO_x} is set to 0 across West Antarctica, Figure 6d shows that some recycled nitrate is still present in West Antarctica.

Figure 9a: It seems the figure caption here should be rephrased. I find it very confusing to look at negative values as a fraction of nitrate lost by photolysis. In the model it seems it should be possible to account for or track how much nitrate is lost and then how much nitrate is deposited to the site as a result of secondary formation on the continent from snow-sourced NO_x. Maybe then the fraction of nitrate that is the result of photolytic processes (i.e. some amount is lost + some amount is returned as result of snow-sourced NO_x becoming nitrate) could be quantified and illustrated, rather than just a fraction that is lost (which again does not actually describe what is pictured).

Thank you for this comment. The variable, f , described in this study is used to calculate the amount of nitrate lost (or gained) from the snow associated with snow nitrate photolysis. We have decided to change the sign of equation 9 (E9) so that negative f values now represent loss of nitrate from the snow and positive f values represent gain of nitrate to the snow. We have rephrased the figure caption and also the description of this figure in the text (section 3.5) to reflect these changes. Since negative f values now represent net loss of snow-sourced nitrate, equation 11 (E11) has been slightly altered to reflect this sign change.

Figure 10: Can the sizes of the text on the axes and in the equations be made larger? They are difficult to read now and will be worse if resized for a different format

The text size in Figure 10 has been made larger.

References:

- Anderson, P.S.: Fine-scale structure observed in a stable atmospheric boundary layer by sodar and kite-borne tetheredsonde. *Boundary-Layer Meteorology*, 107, 323-351, 2003.
- Casasanta, G., Pietroni, I., Petenko, I., Argentini, S.: Observed and modelled convective mixing-layer height and Dome C, Antarctica. *Boundary-Layer Meteorol*, 151, 597-608, doi:10.1007/s10546-014-9907-5, 2014.
- Davis, D., Chen, G., Buhr, M., Crawford, J., Lenschow, D., Lefer, B., Shetter, R., Eisele, F., Mauldin, L., Hogan, A.: South Pole NO_x Chemistry: an assessment of factors controlling variability and absolute levels. *Atmos. Environ.*, 38, 5375-5388, 2004.
- Handorf, D., Foken, T., Kottmeier, C.: The stable atmospheric boundary layer over an Antarctic ice sheet. *Boundary-Layer Meteorol*, 91, 165-189, 1999.
- Jones, A.E., Anderson, P.S., Wolff, E.W., Turner, J., Rankin, A.M., Colwell, S.R.: A role for newly forming sea ice in springtime polar tropospheric ozone loss? Observational evidence from Halley station, Antarctica. *J. Geophys. Res.*, 111, D08306, doi:10.1029/2005JD006566, 2006.
- Jones, A.E., Wolff, E.W., Salmon, R.A., Bauguitte, S.J.-B., Roscoe, H.K., Anderson, P.S., Ames, D., Clemitshaw, K.C., Fleming, Z.L., Bloss, W.J., Heard, D.E., Lee, J.D., Read, A.K., Hamer, P., Shallcross, D.E., Jackson, A.V., Walker, S.L.,

- Lewis, A.C., Mills, G.P., Plane, J.M.C., Saiz-Lopez, A., Sturges, W.T., Worton, D.R.: Chemistry of the Antarctic Boundary Layer and the Interface with Snow: an overview of the CHABLIS campaign. *Atmos. Chem. Phys.*, 8, 3789-3803, 2008.
- King, J.C., Argentini, S.A., Anderson, P.S.: Contrasts between the summertime surface energy balance and boundary layer structure at Dome C and Halley stations, Antarctica. *J. Geophys. Res.*, 111, D02105, doi:10.1029/2005JD006130, 2006.
- Kodama, Y., Wendler, G., Ishikawa, N.: The diurnal variation of the boundary layer in summer in Adelie Land, Eastern Antarctica. *J. Appl. Met.*, 28, 16-24, 1989.
- Konig-Langlo, G., King, J., Pettre, P., Climatology of the three coastal Antarctic stations Durmont D'urville, Neumayer, and Halley. *J. Geophys. Res.*, D9, 103, 10935-10946, 1998.
- Lawrence, J.S., Ashley, M.C.B., Tokovinin, A., Travouillon, T.: Exceptional astronomical seeing conditions above Dome C in Antarctica. *Nature*, 431, 278-281, doi: 10.1038/nature02929, 2004.
- Neff, W., Helmig, D., Grachev, A., Davis, D.: A study of boundary layer behaviour associated with high concentrations at the South Pole using a minisoder, tethered balloon, and a sonic anemometer. *Atmos. Environ.*, 42, 2762-2779, 2008.
- Oncley, S., Buhr, M., Lenschow, D., Davis, D., Semmer, S.: Observations of summertime NO fluxes and boundary-layer height at the South Pole during ISCAT 2000 using scalar similarity. *Atmos. Environ.*, 38, 5389-5398, doi:10.1016/j.atmosenv.2004.05.053, 2004.
- Travouillon, T., Ashley, M.C.B., Burton, M.G., Storey, J.W.V., Loewenstein, R.F.: Atmospheric turbulence at the South Pole and its implications for astronomy. *Astronom. And Astrophys.*, 400, 1163-1172, doi:10.1051/0004-6361:20021814, 2003.
- Thomas, J.L., Stutz, J., Lefer, B., Huey, L.G., Toyota, K., Dibb, J.E., von Glasow, R.: Modeling chemistry in and above snow at Summit, Greenland – Part 1: Model description and results. *Atmos. Chem. Phys.*, 11, 4899-4914, doi:10.5194/acp-11-4899-2011, 2011.
- Trinquet, H., Agabi, A., Vernin, J., Azouit, M., Aristidi, E., Fossat, E.: Nighttime optical turbulence vertical structure above Dome C in Antarctica. *Publ. Astron. Soc. Pac.*, 120, 864, 203-211, 2008.
- Weller, R., Minikin, A., Konig-Langlo, G., Schrems, O., Jones, A.E., Wolff, E.W., Anderson, P.S.: *Geophys. Res. Lett.*, 26, 18, 2853-2856, 1999.

Author Responses to Reviewer 2:

Thank you for taking the time to provide thoughtful comments about this manuscript. We agree that it would be best to take the approach where we stress that this manuscript examines nitrogen recycling and redistribution using an *idealized* snowpack that accounts for spatial variability in parameters important to snow nitrate photolysis (snow accumulation rates, snow black carbon concentration, fraction of photolabile nitrate). The goal of this research is to investigate the potential spatial variability in the flux of snow-sourced NO_x associated with snow nitrate photolysis along with the recycling, loss, and spatial redistribution of nitrogen across Antarctica, an environment in which observations of these parameters over large spatial scales are difficult to obtain. This modeling study is used to perform sensitivity studies aimed to guide future lab and field campaigns. We have clearly stated this goal in the abstract and also in the last paragraph of the introduction.

My impression is that a global model with a 2 x 2.5 degree grid, no realistic treatment of the atmospheric boundary layer, and no snow actually in the model is not the right tool to advance understanding of these issues.

Although there are disadvantages associated with using a global chemical transport model with relatively coarse ($2^\circ \times 2.5^\circ$) resolution, this type of modeling framework is the only way to examine the large scale transport and redistribution of nitrogen associated with snow nitrate photolysis. For example, Erbland et al., ACPD, 2015 took a very different approach to this problem by using a snow column model with the atmosphere as a boundary condition. In order to calculate snow $\delta^{15}\text{N}(\text{NO}_3^-)$ in their model, they had to assume a fraction of snow-sourced NO_x that is transported away from a given ice-coring site, something for which there is no observational constraint. Our modeling approach can at least provide an estimate of the potential range of this fraction. Indeed, we have included a figure showing this calculation across the Antarctic continent for use in future snow modeling studies.

Additionally, the parameterization that has been incorporated into GEOS-Chem can easily be updated as more is learned about these reactions. The model can also be run at finer resolution in the future to assist in the interpretation of observations from a specific field campaign.

This mismatch is exacerbated by the small number of observations across Antarctica (and tendency for the few that exist to cluster in space) of the critical parameters the team attempts to model, making it nearly impossible to assess whether the model has any skill.

Although observations of chemicals associated with or important for snow nitrate photolysis are sparse across Antarctica, we feel that it is important to compare modeled parameters with observations despite the idealized nature of the snowpack. For example, it is useful to compare modeled F_{NO_x} with observations when using two very different values of the quantum yield, as one clearly deviates from the observations by several orders of magnitude. Despite the idealized treatment of the snowpack, comparing model output to observations can at least allow the authors and readers to get an order of

magnitude sense of model-measurement agreement. Including observations in these plots allows for a quick visualization of this agreement. Additionally, readers are able to see where observations exist for various parameters. However, we now have removed all statements about how well the modeling results agree with observations.

On the other hand, the simulations, and especially the sensitivity studies may be useful if the authors admit that they are creating an idealized Antarctic ice sheet...

Thank you for suggesting that we acknowledge that this simulation uses an idealized snowpack. This has been our thought all along, and we thank the reviewer for helping us to better articulate our approach. We now use terminology such as “idealized snowpack” throughout the manuscript, especially in the abstract, introduction, and the conclusions to make this point clear.

In section 2.1.2. the team outlines key parameters that control the depth dependence of actinic flux into the off-line snowpack.

The model snowpack is embedded within GEOS-Chem and some of the chemical and optical properties in the snow are updated at every time step.

Troublesome assumptions include that insoluble LAI are always strictly externally mixed with the snow grains and homogeneously distributed in the full depth of the photic zone

We have made simplifying assumptions about the location of light-absorbing impurities (LAI) in snow because observations of this parameter across Antarctica are limited. A detailed snow module (e.g. SNICAR) would likely be able to simulate the location of LAI with respect to a snow grain and also the heterogeneity of LAI throughout the snowpack. However, the incorporation of a detailed snow chemical and physical model would greatly increase computation time in GEOS-Chem and is beyond the scope of this project. We have performed numerous sensitivity studies that evaluate the impact of changing LAI concentration in snow and also alteration of snow grain shape (see section 2.2 and 3.2). While these sensitivity studies do not directly address the location of LAI in snow, they provide a sense of the influence that changes in LAI have on the flux of snow-sourced NO_x .

The depth profile of effective radius of snow grains measured at one location is applied to the entire ice sheet

Thank you for bringing up this point. While there have been a number of satellite-based snow grain radius (r_e) in Antarctica (e.g., Jin et al., 2008), ground observations are limited [Gallet et al., 2011, Grenfell et al., 1994, Klein, 2014].

We use an r_e scheme that allows for vertical r_e variation (r_e increases with increasing snow depth) and temporal r_e variation (snow surface r_e increases throughout summer) based upon measurements at Dome C, Antarctica [Gallet et al., 2011] and in Dronning Maud Land, Antarctica [Klein, 2014]. We have varied r_e in sensitivity studies to assess the influence of r_e on snow-sourced NO_x fluxes. Section 2.1.2. provides a description of the r_e profiles used in this study and sections 2.2. and 3.2. describe the r_e sensitivity studies.

Measurements of BC at a single location are applied to the entire continent by assuming constant deposition flux modeled by variations in snow accumulation (as predicted by the model)

The authors tested a variety of techniques to calculate annual mean snow black carbon (C_{BC}) in GEOS-Chem. In addition to scaling C_{BC} by accumulation rate, anchored to C_{BC} observations at Vostok, a regression equation between annual mean snow black carbon concentration observations and modeled snow accumulation rates was developed, however this method would be more appropriate if many C_{BC} observations were available. Additionally, snow C_{BC} was calculated by dividing the total annual wet and dry deposition of hydrophilic and hydrophobic black carbon (ng yr^{-1}) by the total annual accumulation rate (g yr^{-1}) in each grid box. The spatial pattern and magnitude of snow C_{BC} calculated using black carbon deposition and accumulation rates are similar to the observed spatial pattern and magnitude of C_{BC} presented in Figure 3b (see Figure 1 below).

Since the dilution of insoluble black carbon in snow with increasing snow accumulation rates is well-documented (e.g., Doherty et al., 2010), we feel that scaling black carbon concentration in snow is appropriate. Additionally, the modeled C_{BC} and observed C_{BC} are in general agreement (see Table 1 below), although specific comments on how well the model agrees with the observations have been removed from the text due to the idealized nature of the snowpack. Also shown below is a table comparing modeled accumulation rates to observed accumulation rates (Table 2). In section 3.2., sensitivity studies are described where concentrations of C_{BC} are halved and doubled and the implications for snow-sourced NO_x are assessed.

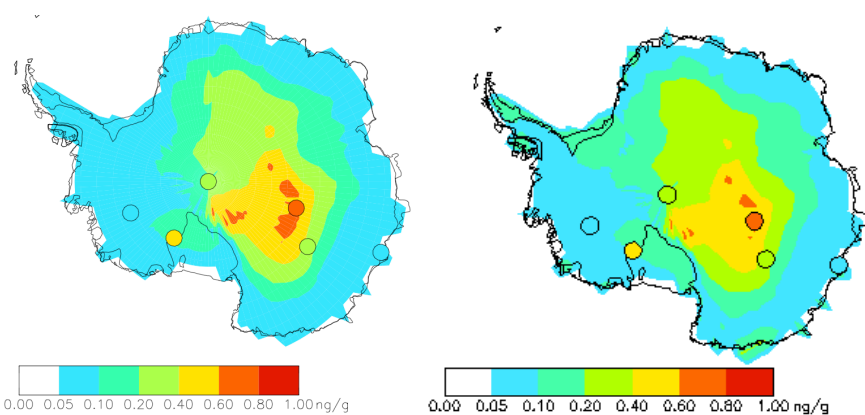


Figure 1. Annual mean snow black carbon concentrations (C_{BC} , ng g^{-1}) calculated by (a) scaling C_{BC} by snow accumulation rate tied to C_{BC} observations at Vostok (Figure 3b) and (b) by dividing the total annual wet and dry deposition of hydrophilic and hydrophobic black carbon (ng yr^{-1}) by the total annual accumulation rate (g yr^{-1}) in each grid box.

Table 1. Annual mean snow black carbon concentrations (ng g⁻¹)

Location	Observed	Modeled	Reference
WAIS-Divide	0.08	0.08	Bisiaux et al. [2012]
Law Dome	0.08	0.08	Bisiaux et al. [2012]
Siple Dome	0.5	0.08	Chylek et al. [1992]
South Pole	0.1	0.2	Warren et al. [1990]
Dome C	0.3	0.4	Warren et al. [2006]
Vostok	0.6	0.6	Grenfell et al. [1994]

Table 2. Total annual snow accumulation rate (kg m⁻² a⁻¹)

Longitude	Latitude	Observed ^a	Modeled
139.8	-66.7	558	366
138.6	-67.4	515	149
136.7	-67.9	334	167
135.2	-68.5	246	186
134.3	-69.3	216	77
134.1	-70.3	160	32
133.0	-71.6	121	33
132.8	-71.5	96	33
130.5	-72.3	68	36
128.7	-74.0	53	17
126.9	-73.8	43	17
124.5	-74.7	34	19
123.3	-75.1	25	19
123.3	-75.1	25	19
123.3	-75.1	25	19
123.3	-75.1	25	19
123.3	-75.1	25	19
120.2	-75.7	28	12
113.0	-76.7	22	13
110.6	-77.7	29	14
106.8	-78.5	21	13
106.8	-78.5	21	13
106.8	-78.5	21	13
0	-90	80	47
-112.1	-79.3	220	114

^aObserved or inferred total annual snow accumulation rates from Erbland et al. [2013], Fegyveresi et al. [2011]., Grenfell et al., [1994].

In section 2.1.3, the depiction of how nitrate is distributed across the ice sheet, and partitioned between photolabile and more stable forms is presented. Extreme simplifications include the decision to assume uniform concentration (60 ng g^{-1}) below 2 cm and 360 ng g^{-1} 0-2 cm everywhere. The first number is based on wide ranging surface traverses where 60 was the median of a distribution that ranges from 4 to 800 ng g^{-1} , and the surface amplification is a mid range value of observations that range from near zero in some places to 100 or more at others. Although there is a wide range of multi-year, sub-surface snow NO_3^- concentrations measured across Antarctica during the ITASE campaign [Bertler *et al.*, 2005], there is no clear spatial pattern associated with these observations. NO_3^- concentrations in snow are influenced both by snow accumulation rates and by post-depositional processing and associated redistribution of snow-sourced NO_x and NO_3^- . We have chosen to apply the median value of observed sub-surface snow NO_3^- concentration (60 ng g^{-1}) in our idealized snowpack. However, we have performed a number of sensitivity studies to investigate the impact of snow NO_3^- concentration on snow-sourced NO_x . In sensitivity studies, snow NO_3^- concentrations are halved and doubled, the NO_3^- enhancement factor is varied from 1 to 10, and, in an additional sensitivity study, it is assumed that all NO_3^- is photolabile (see section 3.2.).

There is a wide range of NO_3^- enhancement factors in the top 2 cm of snow. This range can be even larger if the NO_3^- concentrations in the snow skin layer (very top surface, $\sim 1 \text{ mm}$) are compared to NO_3^- concentrations in sub-surface layers. An enhancement factor of 6 has been chosen because it is a mid-range value of many observed enhancement factors (see references in 2.1.3.), and this enhancement factor is applied across Antarctica. Similar to snow NO_3^- and LAI concentrations, the NO_3^- enhancement factor in the top 2 cm of snow is varied from 1 to 10 in sensitivity studies to investigate the impacts of this parameter on snow-sourced NO_x (see section 3.2.).

Regarding whether the nitrate is photolabile or relatively stable, it is assumed that the dry deposited fraction is on surface of snow grain, hence readily photolyzed, but the partitioning between wet and dry deposited nitrate is model defined with no validation that the model is anywhere close to correct on this critical factor.

Unfortunately, no observational constraints on the relative importance of wet- and dry-deposited NO_3^- across Antarctica exist for model assessment. However, both the wet deposition scheme [Amos *et al.*, 2012] and dry deposition schemes over snow [Fisher *et al.*, 2011] have been recently updated in GEOS-Chem. The spatial pattern of wet deposition in the model is at least qualitatively what we would expect; the amount of wet deposited nitrate is highest at the coasts (closest to ocean) and lowest on the East Antarctic plateau (furthest from ocean).

These decisions guarantee that the model is dealing with snow that has some resemblance to that which is found in Antarctica, but the spatial and vertical distributions in the model snowpack intentionally smooth variations that are known to exist across the actual Antarctic snowpack.

Thank you for mentioning this fact. We agree and have made sure to mention that this study uses an idealized snowpack. Additionally, we have included an appendix that illustrates the spatial variability in F_{NO_x} associated with a variety of sensitivity studies.

It is particularly puzzling why the authors assume a constant flux of BC but impose constant concentrations on nitrate. They could have made the same choice for both, or they could have combined the model estimates of spatially distributed deposition (combined wet and dry) of both BC and nitrate with modeled snow accumulation that would at least have internally consistent spatial variations in these parameters. Snow NO_3^- concentrations are altered by both post-depositional processing associated with snow NO_3^- photolysis and snow accumulation rates, while snow black carbon concentrations are only influenced by snow accumulation rates (i.e., black carbon does not undergo photolytic recycling, and is thought to be well-preserved in ice as long as there is no surface melting). Therefore, it is necessary to make different assumptions about modeled snow NO_3^- and black carbon.

However, given that the team starts with a snowpack that is not like Antarctica (by choice), I see no point in comparing model predictions smoothed in an undefined way to relatively few spot observations in the series of maps shown in Fig. 2, 3, 4, and 9. It is also a problem that these comparisons are all described as “good” with no objective criteria, but if the figures go away this issue will too.

We have removed all model-measurement comparison statements in this manuscript although we feel that it is still instructive to compare model output to observations where available. This allows readers to obtain a rough ‘order-of-magnitude’ idea of model-measurement agreement. Additionally, these observations are laid out spatially, which allows readers to see where observations exist for various parameters.

I think this paper needs a major rewrite that admits the simulations are based on highly idealized snowpack that may be more like Antarctica than Greenland or smaller icecaps in other parts of the world and focuses on an expanded discussion of the sensitivity studies and what they may reveal about fundamental processes and where more focused studies would be most fruitful.

Thank you for all of these suggestions. We now refer to the snowpack as ‘idealized’ throughout the manuscript. Additionally, throughout the text we describe the main results of our sensitivity studies and how these results can be used to shape future field and laboratory experiments (see section 3.2 and conclusions). The flux of snow-sourced NO_x is most sensitive to the quantum yield and the concentration of photolabile nitrate, and these parameters are likely related to each other. We have also included an appendix (Appendix A) that shows the spatial pattern of F_{NO_x} for many of our sensitivity studies.

Specific technical edits and comments:

18964/25 to 18965/3: Not sure that this last statement in the abstract is supported by the rest of the manuscript. There is no clear advice on how ice-core N-15 is going to answer these questions.

We have updated section 3.6. to describe the significant correlations between NRF , f , and $\delta^{15}\text{N}(\text{NO}_3^-)$ in more detail. Additionally, in the conclusions section we have included a sentence about one possible application of this work for ice-core NO_3^- interpretation.

18966/13-14: Not sure what is meant by “partially transferred to the gas phase during transport from the LLR to interstitial air”. Seems only NO_2 that leaves aqueous phase could get into the interstitial air. Related point is that here you cite work that suggests some stays in the LLR, but the model pushes all of it directly into the bottom layer of the atmosphere. In addition to retention in LLR, is there not also a fraction that could recycle to nitrate in the interstitial air and redeposit before getting out of the snow.

We have reworded this statement to “The aqueous phase NO_2 produced in E1 can be transferred to the gas phase and subsequently transferred to the interstitial air”. For simplicity, we have assumed that all NO_2 produced through the photolysis of snow NO_3^- can escape from the LLR into the boundary layer and have specifically stated this assumption in section 2.1.1.

The efficiency of transport of NO_2 from the interstitial air to the overlying boundary layer was evaluated in Zlatko et al. [2013] by comparing the lifetime of NO_x against escape out of the snow (diffusion and windpumping) to the lifetime of NO_x against chemical decay (combination of NO_x with BrO , IO , OH) at a variety of polar locations. The lifetime of NO_x against escape was always shorter than the lifetime of NO_x against chemical conversion, so we assume that all NO_x in the interstitial air can escape to the atmosphere. Although there have been numerous laboratory studies aimed to learn more about the LLR (or QLL), there are still many uncertainties associated with nitrate photolysis in the LLR [Domine et al., 2013].

18966/21: 0.003-0.44 does not span the full range (0.003-0.6) mentioned in the 2 preceding sentences

Thank you for catching this. We have reworded this sentence to ‘In a recent study by Meusinger et al. [2014], $\phi=0.003-0.44$ molec photon⁻¹ for E1, which nearly spans the full range of previously reported quantum yields.’

18966/23: “as well as and” should be “and” or “as well as”

Thank you for catching this as well. We have removed ‘and’ from the sentence.

18971/10: Seems you need to say something about how the model was tweaked to deal with the compression of longitude at very high latitude. Are there really 144 grid cells between 88 and 90 S, and how are they all forced to agree at the pole?

There are 144 grid cells between 88 and 90 S. In the advection scheme that GEOS-Chem uses, there is special treatment at the poles because the scheme is based on calculation of

the slopes between neighboring grid boxes. The grid boxes at the poles are treated as one circular grid cell.

18971/12: I think this should be May 2009

Yes, thank you for catching this typo.

18971/23-25: Is this statement correct? Looking at a bunch of short lived stuff with surface source and it does not matter if you dilute this into a 100 versus 300 m deep BL? If it is accurate, it really reinforces my very early statement that a CTM run at 2x2.5 degree resolution is the wrong tool for the problem

Thank you for questioning this statement because we found a minor error in this part of the code. The mixing ratios of these species are dependent on which vertical grid boxes are considered. We have now removed this sentence from the manuscript.

18972/14-15: see earlier comment about citation of Boxe et al. [2005]

We have changed this sentence to “We assume that all NO_x formed in E7 is immediately desorbed into the gas-phase and transported from the LLR to the interstitial air and then into the overlying boundary layer [Zatko et al., 2013].” Additionally, at the end of section 2.1.3., we discuss the implications of assuming that all NO_x from the LLR is transferred to the gas-phase for the flux of snow-sourced NO_x .

18973/3: It is unusual to have the figure callouts out of order. You have not referred to Fig 2 yet, so perhaps what is now Fig 3 needs to be Fig 2.

We have removed the figure callouts (Figure 2a and Figure 3c) that are out of order in section 2.1.2 and 2.1.3.

18975/11: here (and consistently afterward through the rest of the manuscript) you say 0.0013 for the yield found by Chu and Anastasio, but in the intro you say 0.003. These authors actually document both pH and temperature dependencies and quote 0.0017-0.0054 from 239 to 268K as the yield from nitrate doped ice. It seems something closer to 0.003 might be more appropriate for a lot of the Antarctica in the summer. However, later it says that based on the sensitivities studies you decide to use 0.0013 for all following analyses. Please check what value was used, and explain why you used something lower than Chu and Anastasio, if that is correct.

Thank you very much for pointing out this error. We use $\phi=0.002$ (corresponding to $T=244\text{K}$, $\text{pH}=5$) for the following analyses, not $\phi=0.0013$. Table 3 has been updated to reflect this change.

18976/10 Section 2.2.: really ought to be more than this short paragraph and Table 2. It is the most useful part of this study and needs to be the focus of the discussion.

Section 2.2. and Table 3 have been expanded in the latest version of this manuscript. We have also included an appendix in the manuscript that shows mean austral summer F_{NO_x} for a variety of sensitivity studies.

18979/23-24: While this statement may be true in the model as it is set up, I doubt that the photolabile fraction of nitrate in real snow will remain constant as a layer

slowly sinks lower in the photic zone. Easily photolyzed nitrate will be, and if it is recycled and dry deposited, it will be in the current surface layer. So, I would expect the stable fraction to grow in the original due to loss of photolabile molecules (some have discussed this photobleaching).

We agree that the fraction of photolabile nitrate will likely decrease as a layer sinks lower in the photic zone. The fraction (F_R/F_{NOx}) in the equation for f represents the fraction of nitrate lost in 1 year in the photic zone, not the fraction of photolabile nitrate in the snow. We have slightly updated this sentence in an attempt to provide more clarity:

“Provided that there are no major changes in parameters that influence snow photochemistry (e.g., LAI, overhead ozone abundance) from year to year, the fraction of photolabile NO_3^- lost from the snow **over 1 year** will be stable from year to year.”

18981/8-10: Who says this is “good” agreement. On what basis? More importantly, what do you really mean by “total snow accumulation rates” in the model. Is this just snowfall, or does it consider sublimation, diamond dust, fog, drifting and blowing snow? I can not imagine that these BL processes are well captured in the model, so I am guessing that you are comparing accumulation to model precip, which is not really appropriate. However, as noted earlier, there are way too few observations to make this comparison very rigorous and I suggest you not even try. I will not make similar comments related to subsequent statements about model/observation comparisons, but you should be assured that I noted them in the marginalia.

We have removed all judgments about model-measurement agreement from this manuscript due to the idealized nature of the model snowpack.

The model does not simulate sublimation, diamond dust, fog, drifting and blowing snow in the boundary layer. Observed or inferred snow accumulation rates are compared to modeled total annual precipitation (mm liquid water equivalent year⁻¹) that has been converted to total snow accumulation (kg m⁻² yr⁻¹) using a typical Antarctic snow density (360 kg m⁻³).

A related comment that applies throughout section 3, and probably also in section 2. If you are going to keep all of the maps (against my advice) I think you need to describe how the gridded data were contoured. There is a lot of fine structure in some of these that probably is not really captured at 2 x 2.5 degrees.

GEOS-Chem calculates one value for each grid box (2° x 2.5°) and this data is then smoothed using bilinear interpolation algorithms in the GAMAP plotting routines. The TVMAP GAMAP routine uses the TVIMAGE function, which in turn uses the (http://acmg.seas.harvard.edu/gamap/doc/by_alphabet/gamap_t.html#TVIMAGE) TV routine (http://www.exelisvis.com/docs/TV_Procedure.html), a core routine in IDL.

We have included a sentence about the smoothing algorithm in section 2.1.1. Figure 2 shows both gridded and smoothed data. The fine structure in the data is not lost when gridded data is smoothed, as can be seen in the two plots below.

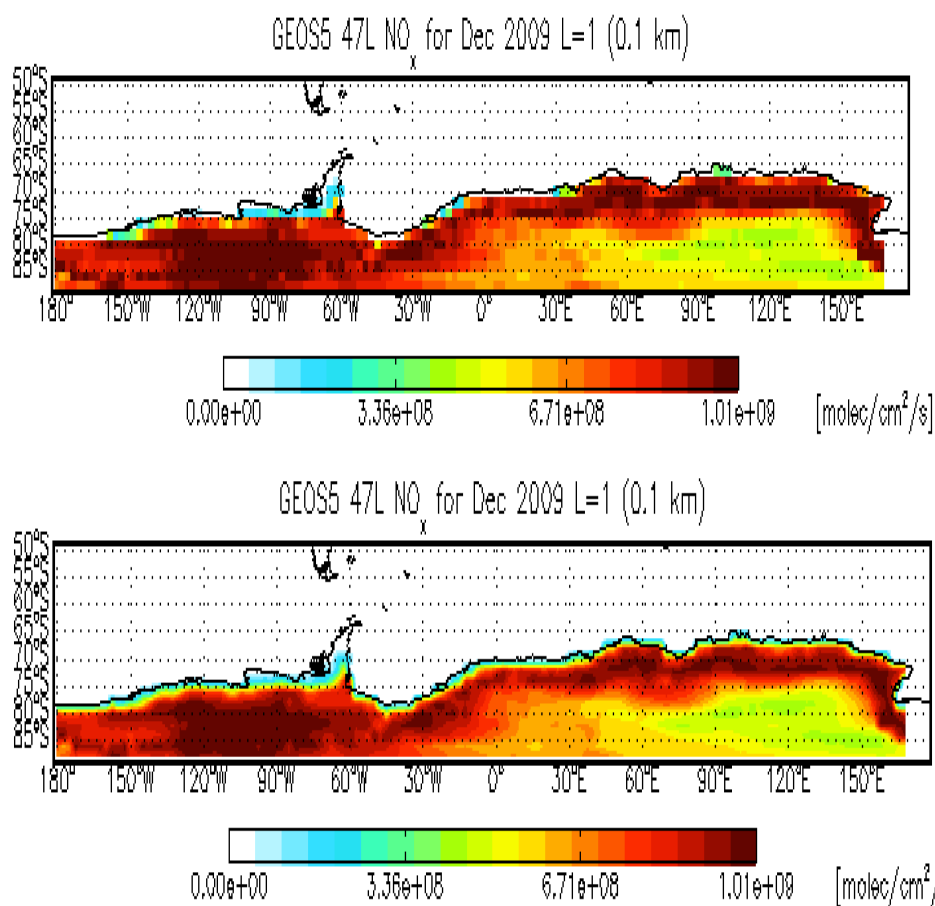


Figure 2. (top) gridded data. (bottom) smoothed data.

18984/1: Does it really make sense to average fluxes purporting to be peak noon values and 24 hour averages and weeks or months long campaign averages together?? I do not think so.

In order to overplot observations onto the model results, we need to have one single value for each station. Due to the idealized nature of the snowpack in the model, an order-of-magnitude level comparison is relevant here. Station-averaged NO_x flux values in Figures 4c and 4d allow for such a comparison. However, we have removed all model-measurement NO_x flux comparisons in section 3.2. and have provided the full range of observed NO_x fluxes at each station in section 3.2.

18984/7: Not being able to take advantage of all the work at Halley and Neumayer because the model grid is too coarse goes back to a familiar point, is a global CTM the right tool? More generally, given the huge gradients in just about everything

within 2 degrees of the coast of Antarctica having a lot of contaminated grid cells in this very interesting region seems a pretty big problem

The incorporation of snow nitrate photolysis into a global chemical transport model is perhaps the only way to assess the large scale nitrogen recycling and redistribution associated with snow nitrate photolysis across Antarctica. Global chemical transport models, including GEOS-Chem, may be run with much finer resolution than $2^\circ \times 2.5^\circ$, which would allow one to better resolve the coast as well as small scale features throughout the entire continent, although with much greater computational cost.

Although the e-folding depths, and thus F_{NO_x} are not properly resolved directly at the coast in this modeling project, much of Antarctica is not on the coast and is therefore unaffected by mixed surface grid boxes. Additionally, we have removed a sentence from the conclusion that mentioned a possible result in coastal Antarctica.

18989/8: I assume that section 3.6. is supposed to justify the final sentence in the abstract but it does not succeed for me.

There is a strong relationship between the degree of photolysis-driven loss of snow NO_3^- and the degree of nitrogen recycling between the air and snow in regions of Antarctica with a snow accumulation rate greater than $85 \text{ kg m}^{-2} \text{ a}^{-1}$ in the present day. We have expanded on this analysis in section 3.6 and have added a sentence in the conclusions section about how this relationship could be used to aide in the interpretation of nitrate in ice core records. Please also see our response to your other comment above.

References:

- Bertler, N., Mayewski, P. A., Arístarain, A., Barrett, P., Becagli, S., Bernardo, R., Bo, S., Xiao, C., Curran, M., Qin, D., Dixon, D., Ferron, F., Fischer, H., Frey, M., Frezzotti, M., Fundel, F., Genthon, C., Gragnani, R., Hamilton, G., Handley, M., Hong, S., Isaksson, E., Kang, J., Ren, J., Kamiyama, K., Kanamori, S., Karkas, E., Karlof, L., Kaspari, S., Kreutz, K., Kurbatov, A., Meyerson, E., Ming, Y., Zhang, M., Motoyama, H., Mulvaney, R., Oerter, H., Osterberg, E., Proposito, M., Pyne, A., Ruth, U., Simoes, J., Smith, B., Sneed, S., Teinila, K., Traufetter, F., Udisti, R., Virkkula, A., Watanabe, O., Williamson, R., Winther, J-G., Li, Y., Wolff, E., Li, Z., Zielinski, A.: Snow chemistry across Antarctica, *Annals of Glaciology*, 41(1), 167- 179, 2005.
- Bisiaux, M. M., Edwards, R., McConnell, J. R., Curran, M. A. J., Van Ommen, T. D., Smith, A. M., Neumann, T. A., Pasteris, D. R., Penner, J. E., Taylor, K.: Changes in black carbon deposition to Antarctica from two high-resolution ice core records, 1850-2000 AD. *Atmos. Chem. Phys.*, 12, 4107-4115, doi: 10.5194/acp-12-4107-2012, 2012.
- Chu, L., and Anastasio, C.: Quantum Yields of Hydroxyl Radicals and Nitrogen Dioxide from the Photolysis of Nitrate on Ice. *J. Phys. Chem. A.*, 107, 9594-9602, 2003.
- Chylek, P., Johnson, B., Wu, H.: Black carbon concentration in Byrd station ice core – From 13,000 to 700 years before present. *Ann. Geophys.*, 10, 625-629, 1992.

- Doherty, S. J., Warren, S. G., Grenfell, T. C., Clarke, A. D., and Brandt, R. E.: Light-absorbing impurities in Arctic snow. *Atmos. Chem. Phys.*, 10, 11647-11680, doi:10.5194/acp-10-11647-2010, 2010.
- Erbland, J., Vicars, W.C., Savarino, J., Morin, S., Frey, M.M., Frosini, D., Vince, E., Martins, J.M.F.: Air-snow transfer of nitrate on the East Antarctic Plateau – Part 1: Isotopic evidence for a photolytically driven dynamic equilibrium in summer. *Atmos. Chem. Phys.*, 13, 6403-6419, doi:10.5194/acp-13-6403-2013, 2013.
- Domine, F., Bock, J., Voisin, D., Donaldson, D. J.: Can we model snow photochemistry? Problems with the current approaches. *J. Phys. Chem. A*, 117, 4733-4749, doi: 10.1021/jp3123314 2013.
- Fegyveresi, J.M., Alley, R.B., Spencer, M.K., Fitzpatrick, J.J., Steig, E.J., White, J.W.C., McConnell, J.R., Taylor, K.C.: Late-Holocene climate evolution at the WAIS Divide site, West Antarctica: bubble number-density estimates. *J. Glaciol.*, 57, 204, 2011.
- Gallet, J.-C., Domine, F., Arnaud, L., Picard, G., and Savarino, J.: Vertical profiles of the specific surface area and density of the snow at Dome C and on a transect to Dumont D'Urville, Antarctica – albedo calculations and comparison to remote sensing products. *The Cryosphere.*, 5, 631-649, doi: 10.5194/tc-5-631-2011, 2011.
- Grenfell, T.C., Warren, S.G., Mullen, P.C.: Reflection of solar radiation by the Antarctic snow surface at ultraviolet, visible, and near-infrared wavelengths. *J. Geophys. Res.*, 99, D9, 18669-18684, 1994.
- Klein, K.: Variability in dry Antarctic firn; Investigations on spatially distributed snow and firn samples from Dronning Maud Land, Antarctica. Ph.D. Thesis, Universitat Bremen. hdl: 10013/epic.44893. <http://nbn-resolving.de/urn:nbn:de:gbv:46-00104117-15>, date last access: April 15, 2014.
- Jin, Z., Charlock, T.P., Yang, P., Xie, Y., Miller, W.: Snow optical properties for different particle shapes with application to snow grain size retrieval and MODIS/CERES radiance comparison over Antarctica. *Remote. Sens. Environ.*, 112, 3563-3581, 2008.
- Warren, S.G., Clarke, A.D.: Soot in the atmosphere and snow surface of Antarctica. *J. Geophys. Res.*, 95, 1811-1816, 1990.
- Warren, S. G., Brandt, R. E., and Grenfell, T. C.: Visible and near-ultraviolet absorption spectrum of ice from transmission of solar radiation into snow. *Appl. Opt.*, 45, 5320-5334, 2006.

The impact of snow nitrate photolysis on boundary layer chemistry and the recycling and redistribution of reactive nitrogen across Antarctica in a global chemical transport model

Zatko, M.C.¹, Geng, L.¹, Alexander, B.¹, Sofen, E.D.², Klein, K.³

¹Department of Atmospheric Sciences, University of Washington, Seattle, United States

²Department of Chemistry, University of York, York, United Kingdom

³Division of Glaciology, Alfred Wegener Institute Helmholtz Centre for Polar and Marine Research, Bremerhaven, Germany

Correspondence to Becky Alexander (beckya@uw.edu)

1 **Abstract**

2 The formation and recycling of reactive nitrogen (NO, NO₂, HONO) at the air-snow
3 interface has implications for air quality and the oxidation capacity of the atmosphere in
4 snow-covered regions. Nitrate (NO₃⁻) photolysis in snow provides a source of oxidants
5 (e.g., hydroxyl radical) and oxidant precursors (e.g., nitrogen oxides) to the overlying
6 boundary layer, and alters the concentration and isotopic (e.g., δ¹⁵N) signature of NO₃⁻
7 preserved in ice cores. We have incorporated the photolysis of Antarctic snow NO₃⁻ into
8 a global chemical transport model (GEOS-Chem) to examine the implications of snow
9 NO₃⁻ photolysis for boundary layer chemistry, the recycling and redistribution of reactive
10 nitrogen across the Antarctic continent, and the preservation of ice-core NO₃⁻ in Antarctic
11 ice cores. This modeling framework uses an idealized snowpack that accounts for the
12 spatial variability in parameters that influence snow NO₃⁻ photolysis. The goal of this
13 research is to investigate the potential spatial variability of snow-sourced NO_x fluxes
14 along with the recycling, loss, and areal redistribution of nitrogen across Antarctica,
15 which is an environment in which observations of these parameters over large spatial
16 scales are difficult to obtain. The calculated potential fluxes of snow-sourced NO_x in
17 Antarctica range from 0.5 x 10⁸ to 7.8 x 10⁸ molec cm⁻² s⁻¹ and calculated e-folding depths
18 of UV actinic flux in snowpack range from 24 to 69 cm. Snow-sourced NO_x increases
19 mean austral summer boundary layer mixing ratios of total nitrate (HNO₃+NO₃⁻), NO_x,
20 OH, and O₃ in Antarctica by a factor of up to 32, 38, 7, and 2, respectively, in the model.
21 Model results also suggest that NO₃⁻ can be recycled between the air and snow multiple
22 times and that NO₃⁻ can remain in the snow photic zone for at least 7.5 years on the East
23 Antarctic plateau. The fraction of photolysis-driven loss of NO₃⁻ from the snow is
24 roughly -0.99 on the East Antarctic plateau, while areas of wind convergence (e.g., over
25 the Ronne Ice Shelf) have a net gain of NO₃⁻ due to redistribution of snow-sourced
26 reactive nitrogen across the Antarctic continent. The modeled enrichment in ice-core
27 δ¹⁵N(NO₃⁻) due to photolysis-driven loss of snow NO₃⁻ ranges from 0‰ to 363‰, with
28 the largest enrichments on the East Antarctic plateau. There is a strong relationship
29 between the degree of photolysis-driven loss of snow NO₃⁻ and the degree of nitrogen
30 recycling between the air and snow in regions of Antarctica with a snow accumulation
31 rate greater than 85 kg m⁻² a⁻¹ in the present day. This modeling framework study is also
32 used to perform a variety of sensitivity studies to highlight the largest uncertainties in our
33 ability to model these processes in order to guide future lab and field campaigns.

Maria Zatko 9/12/15 7:51 AM
Deleted: , ozone... and oxidant precu ... [1]

Maria Zatko 9/4/15 12:44 PM
Formatted: Not Superscript/ Subscript

Maria Zatko 9/4/15 12:44 PM
Deleted: NO3-

Maria Zatko 9/4/15 12:44 PM
Formatted: Not Superscript/ Subscript

Maria Zatko 9/4/15 12:44 PM
Deleted: NO3-...photolysis for bound ... [2]

Maria Zatko 9/4/15 12:44 PM
Formatted: ... [3]

Maria Zatko 9/4/15 12:44 PM
Deleted: ...he calculated potential flt ... [4]

Maria Zatko 10/16/15 5:36 PM
Formatted: ... [5]

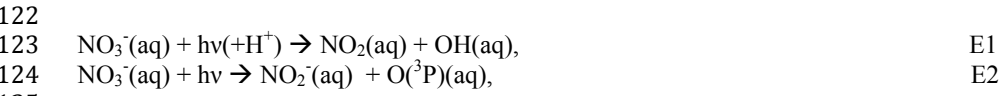
Maria Zatko 9/4/15 12:20 PM
Deleted: , suggesting that ice-core δ¹⁵N(NO₃⁻) observations can be used to assess the degree of nitrogen recycling and loss over much of Antarctica and aid in the interpretation of ice-core NO₃⁻ in terms of past atmospheric variability of reactive nitrogen.

86 **1. Introduction**

87 Nitrogen oxides (NO_x=NO+NO₂) emitted from fossil fuel combustion, biomass burning,
88 soil microbial activity, and lightning have adverse respiratory effects, contribute to the
89 formation of atmospheric acidity, and are a key ingredient in tropospheric oxidant cycling
90 leading to the formation of ground-level ozone (O₃). Ozone also has adverse respiratory
91 effects, is an effective greenhouse gas [UNEP, 2011], and its photolysis dominates
92 hydroxyl radical (OH) production in much of the troposphere [Thompson, 1992].
93 Oxidation to form nitrate (HNO₃/NO₃⁻) is the main sink for NO_x in the troposphere
94 [Logan, 1983], and the lifetime of NO_x against oxidation to nitrate is 1-3 days in polar
95 regions, [Levy et al., 1999]. NO₃⁻ is lost from the atmosphere through dry and wet
96 deposition to the Earth's surface, and has an atmospheric lifetime of roughly 5 days [Xu
97 and Penner, 2012]. In Antarctica, NO₃⁻ deposited to the snowpack originates from both
98 the troposphere (e.g., long-range transport) [Lee et al., 2014] and stratosphere [Frey et
99 al., 2009, Savarino et al., 2007]. In snow-covered regions, the deposition of NO₃⁻ is not a
100 permanent sink for NO_x, as the photolysis of snow NO₃⁻ returns reactive nitrogen
101 (N_r=NO_x, HONO) back to the atmosphere, with implications for other oxidants such as
102 OH and ozone [Domine and Shepson, 2002].

103
104 Snow photochemistry significantly influences boundary layer chemistry and plays an
105 important role in oxidant production and cycling, especially in pristine regions, such as
106 Antarctica [Bloss et al., 2007, Chen et al., 2004, Grannas et al., 2007, Helmig et al.,
107 2008]. Snow photochemistry may have more widespread impacts since up to 40% of land
108 on Earth is snow-covered at a given time [Grannas et al., 2007]. NO₃⁻ is not the only
109 photochemically-active species in snow. The photolysis of nitrite (NO₂⁻) in snow and the
110 photolysis of snow-sourced formaldehyde (CH₂O), nitrous acid (HONO), and hydrogen
111 peroxide (H₂O₂) provide additional sources of N_r and OH to the boundary layer. Bromine
112 (Br₂) is also produced in the snow via reactions involving bromide (Br⁻),
113 photochemically-active species (e.g., NO₃⁻), and photochemically-produced species (e.g.,
114 OH) within snow grains [Pratt et al., 2013].

115
116 In snow, NO₃⁻ photolysis likely occurs in the liquid-like region (LLR) on the surface of
117 ice grains, in cracks between ice grains, or in brine pockets embedded within ice grains
118 [Domine et al., 2013]. There are two channels for NO₃⁻ photolysis at wavelengths
119 (λ)=290-345 nm. In the aqueous phase, NO₃⁻ can photolyze to produce NO₂ and OH (E1),
120 or produce NO₂⁻ and O(³P) (E2), but E1 is the dominant pathway [Grannas et al., 2007,
121 Mack and Bolton, 1999, Meusinger et al., 2014].



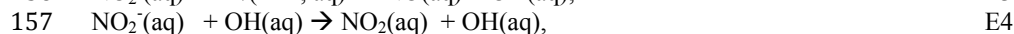
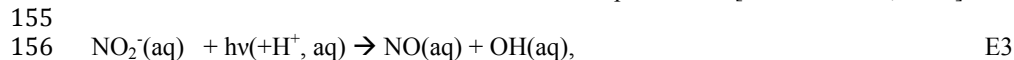
126 The aqueous phase NO₂ produced in E1 is can be transferred to the gas phase and
127 subsequently transported into the interstitial air, [Boxe et al., 2005] and then released to
128 the atmosphere. The quantum yield (φ) in E1 is strongly influenced by the location of
129 NO₃⁻ in an ice grain. Chu and Anastasio [2003] froze NO₃⁻-doped water in the lab and
130 measured the quantum yield for E1 (0.003, molec photon⁻¹ at T=253K) as frozen ice
131 grains were exposed to ultraviolet (UV) radiation. Zhu et al. [2010] deposited HNO₃ on

Maria Zatko 9/12/15 9:46 AM
Deleted: on the order of one day
Maria Zatko 9/12/15 10:21 AM
Deleted: on the order of several
Maria Zatko 9/12/15 10:21 AM
Deleted: Logan
Maria Zatko 9/12/15 10:21 AM
Deleted: 1983
Maria Zatko 9/12/15 10:25 AM
Deleted: recycles

Maria Zatko 9/8/15 11:18 AM
Deleted: partially
Maria Zatko 9/8/15 11:19 AM
Deleted: , NO₂(g), during transport from the LLR to the interstitial air
Maria Zatko 9/8/15 11:44 AM
Deleted: 3x10-3
Maria Zatko 9/8/15 11:50 AM
Deleted: 53

142 an ice film and measured ϕ for E1 (0.6 molec photon⁻¹ at T=253K), as the frozen surface
143 was irradiated with UV radiation. In a recent study by Meusinger et al. [2014], $\phi=0.003-$
144 | 0.44 molec photon⁻¹ for E1, which nearly spans the full range of previously reported
145 quantum yields. Results from Meusinger et al. [2014] suggest that ϕ is dependent on the
146 length of time that snow is exposed to UV radiation, as well as the location of NO₃⁻ in the
147 ice grain. Meusinger et al. [2014] suggest that two photochemical domains of NO₃⁻ exist:
148 photolabile NO₃⁻ and NO₃⁻ buried within the ice grain. The NO_x produced from the
149 photolysis of photolabile NO₃⁻ can escape the ice grain, while the NO_x produced from the
150 photolysis of buried NO₃⁻ is likely to undergo recombination chemistry within the snow
151 | grain, thus lowering the quantum yield of NO_x for NO₃⁻ photolysis.

152
153 The NO₂⁻ produced in E2 is quickly photolyzed at longer wavelengths ($\lambda=290-390$ nm) in
154 the LLR or can react with OH or H⁺ in the LLR to produce N_r [Grannas et al., 2007]:



159
160 HONO produced in E5 can rapidly photolyze to produce NO and OH in the interstitial air
161 or the atmospheric boundary layer [Anastasio and Chu, 2009]. Reactions involving NO₂⁻
162 are intermediate reactions for NO₃⁻ photolysis because NO₃⁻ photolysis is required for
163 NO₂⁻ formation and the end products of E1-E5 are all N_r. Once emitted, NO₂ and NO are
164 efficiently transported to the overlying atmosphere via windpumping [Zatko et al., 2013]
165 and enter into rapid NO_x-cycling reactions. In the atmosphere, the relative abundance of
166 NO and NO₂ will be determined by local atmospheric conditions, specifically oxidant
167 | concentrations (e.g., O₃, HO₂, RO₂, BrO, and ClO) [Frey et al., 2013]. The snow-sourced
168 NO_x is then re-oxidized to HNO₃ via E6 under sunlit conditions.



171
172 The HNO₃ produced in E6 can undergo wet or dry deposition to the snow surface [Dibb
173 et al., 2004] within a day [Slusher et al., 2002, Wang et al., 2008]. Evidence for HNO₃
174 re-deposition is seen in the snow NO₃⁻ concentration profile at many polar locations,
175 where NO₃⁻ concentrations are at least an order of magnitude higher in the top two
176 centimeters (cm) of snow compared to NO₃⁻ concentrations below [Dibb et al., 2004,
177 Frey et al., 2009, Mayewski and Legrand, 1990, Rothlisberger et al., 2000]. Once HNO₃
178 is deposited back to the snow, it is available for photolysis again. NO₃⁻ can be recycled
179 multiple times between the boundary layer and the snow before burial below the photic
180 zone [Davis et al., 2008, Erbland et al., 2015].

181
182 | The photolysis of snow NO₃⁻ and subsequent recycling between the air and snow alters
183 the concentration and isotopic (e.g., $\delta^{15}\text{N}$) signature of NO₃⁻ that is ultimately preserved
184 in polar ice sheets, which hampers the interpretation of ice-core NO₃⁻ records [Wolff et
185 al., 2008]. Such records have been sought to reconstruct the past history of the abundance
186 of NO_x in the atmosphere [Wolff, 1995]. It has also been suggested that the nitrogen
187 ($\delta^{15}\text{N}$) and oxygen ($\Delta^{17}\text{O} = \delta^{17}\text{O} - 0.52 \times \delta^{18}\text{O}$) isotopic composition of ice-core NO₃⁻ can

Maria Zatko 9/8/15 12:09 PM

Deleted: spans the range of

Maria Zatko 9/12/15 8:21 AM

Deleted: disturbs the preservation of NO₃⁻

Maria Zatko 9/12/15 8:22 AM

Deleted: and

Maria Zatko 9/12/15 8:22 AM

Deleted: concentration

192 provide information on past variability in atmospheric NO_x sources and oxidant
193 abundances [e.g., *Alexander et al.*, 2004, *Hastings et al.*, 2005]. Different sources of NO_x
194 have different δ¹⁵N signatures (~ -19‰ to 25‰, see summary in *Geng et al.*, 2014a),
195 giving ice-core δ¹⁵N(NO₃⁻) measurements the potential to track NO_x-source changes over
196 time. The oxygen-17 excess of NO₃⁻ (Δ¹⁷O(NO₃⁻)) is determined mainly by the relative
197 abundance of the oxidants involved in NO_x cycling and conversion of NO₂ to NO₃⁻ (i.e.
198 O₃, HO₂, RO₂, OH), giving ice-core Δ¹⁷O(NO₃⁻) measurements the potential to track
199 variability in the relative abundance of these oxidants over time. However, δ¹⁵N(NO₃⁻)
200 and Δ¹⁷O(NO₃⁻) in ice cores can also be influenced by post-depositional processing of
201 snow NO₃⁻ initiated by photolysis. In this study we focus on the impact of snow NO₃⁻
202 photolysis on ice-core δ¹⁵N(NO₃⁻).

203
204 Ice-core δ¹⁵N(NO₃⁻) values will be altered if there is photolysis-driven loss of NO₃⁻ from
205 the snow when snow-sourced NO_x is transported away from the site of primary
206 deposition. Nitrate photolysis in snow is associated with a large fractionation constant (ε)
207 of -47.9‰ [*Berhanu et al.*, 2014], providing the boundary layer with a source of NO_x that
208 is highly depleted in δ¹⁵N, leaving highly enriched δ¹⁵N(NO₃⁻) in the snow. In the
209 Weddell Sea, atmospheric δ¹⁵N(NO₃⁻) values are as low as -40‰, indicating transport of
210 snow-sourced NO_x from the continental interior [*Morin et al.*, 2009], while on the East
211 Antarctica plateau, snow δ¹⁵N(NO₃⁻) up to 480‰ has been reported [*Blunier et al.*, 2005,
212 *Erbland et al.*, 2013, *Frey et al.*, 2009, *Shi et al.*, 2014], indicating net loss of NO₃⁻ driven
213 by photolysis. If snow-sourced NO_x is simply re-deposited back to the snow surface at
214 the site of emission, a vertical profile in δ¹⁵N(NO₃⁻) within the snow photic zone will
215 develop due to vertical redistribution of NO₃⁻ [*Erbland et al.*, 2013, *Frey et al.*, 2009];
216 however, the depth-integrated δ¹⁵N(NO₃⁻) will not be impacted, even with active
217 photolysis-driven recycling between the atmosphere and the snow. Enrichment in
218 δ¹⁵N(NO₃⁻) in ice cores requires photolysis-driven loss from snow combined with
219 atmospheric transport of the resulting NO_x. In addition to photolysis, ice-core δ¹⁵N(NO₃⁻)
220 values are also influenced by evaporation of HNO₃ [*Mulvaney et al.*, 1998] from snow
221 and by atmospheric processing, such as NO_x cycling [*Freyer et al.*, 1993] and gas-particle
222 partitioning [*Heaton et al.*, 1997, *Geng et al.*, 2014a]; however, these impose a
223 fractionation in δ¹⁵N(NO₃⁻) at least an order of magnitude smaller than photolysis, and
224 are thus not able to explain the large enrichments in snow δ¹⁵N(NO₃⁻) observed on the
225 East Antarctic plateau [*Blunier et al.*, 2005, *Erbland et al.*, 2013, *Frey et al.*, 2009, *Shi et*
226 *al.*, 2014].

227
228 Here we incorporate a snowpack actinic flux parameterization used to calculate the
229 photolysis of snow NO₃⁻ into a global chemical transport model. The idealized Antarctic
230 ice sheet incorporated into GEOS-Chem has similar topography, climate, and weather as
231 the real Antarctic ice sheet, but is subject to assumptions about the chemical and physical
232 properties of the snow. The idealized snowpack in this modeling framework accounts for
233 the spatial variability in parameters important to snow NO₃⁻ photolysis in order to
234 investigate the potential spatial variability in snow-sourced NO_x fluxes and associated
235 reactive nitrogen recycling and redistribution across Antarctica, where observations of
236 these parameters over large spatial scales are difficult to obtain. The potential impacts of
237 nitrogen recycling between the air and snow on boundary layer chemistry as well as the

Maria Zatko 9/12/15 8:23 AM

Deleted: the preservation of

Maria Zatko 9/4/15 3:50 PM

Deleted: This modeling framework is use

Maria Zatko 9/4/15 1:24 PM

Deleted: d

Maria Zatko 9/4/15 1:28 PM

Deleted: evaluate the

Maria Zatko 9/4/15 1:28 PM

Deleted: impact of a

Maria Zatko 9/4/15 1:28 PM

Deleted: the

244 | [impacts of photolysis-driven loss of NO₃⁻ from the snow](#) on the preservation of ice-core
245 | NO₃⁻ across [Antarctica are examined in this study](#). A major advantage of using a global
246 | chemical transport model framework is the ability to examine the redistribution and loss
247 | of reactive nitrogen across large spatial scales [due to photolysis-driven loss of snow NO₃⁻](#)
248 | . Section 2 describes the inclusion of a snowpack actinic flux parameterization and NO₃⁻
249 | photolysis into a global chemical transport model, GEOS-Chem. Section 3 explores the
250 | implications of photolysis-driven reactive nitrogen recycling and redistribution for
251 | boundary layer chemistry and [the alteration of NO₃⁻ concentration and its isotopes](#)
252 | [ultimately archived](#) in ice cores. We end by using our model sensitivity studies to
253 | highlight the largest uncertainties in our ability to model these processes as a guide for
254 | future laboratory and field studies.

255

256 | 2. Methods

257

258 | 2.1. Incorporating Snow NO₃⁻ Photolysis into a Global Chemical Transport Model

259 | Table 1 provides a glossary of the variables used throughout this paper.

260

261 | 2.1.1. Global Chemical Transport Model Description

262 | GEOS-Chem is a global 3-dimensional (3-D) model of coupled aerosol-oxidant
263 | chemistry with detailed HO_x-NO_x-VOC-O₃-BrO_x tropospheric chemistry originally
264 | described in Bey et al. [2001]. The model uses assimilated meteorological data from the
265 | NASA Goddard Earth Observing System (GEOS-5) including winds, convective mass
266 | fluxes, boundary layer depths, temperature, precipitation, and surface properties.
267 | Meteorological data have 6-hour temporal resolution (3-hour for surface variables and
268 | mixing depths). [The TPCORE advection algorithm \[Lin and Rood, 1996\] is the transport](#)
269 | [routine in GEOS-Chem and is based on the calculation of the slopes between neighboring](#)
270 | [grid boxes. At the poles, neighboring grid boxes are used to estimate transport of](#)
271 | [chemical species into and out of the circular polar grid box. The spectral direct and](#)
272 | diffuse downwelling surface irradiance and photolysis frequencies are calculated using
273 | the Fast-JX radiative transfer module [Wild et al., 2000, Bian and Prather, 2002, Mao et
274 | al., 2010]. In GEOS-Chem, aerosols can be wet deposited via scavenging in convective
275 | updrafts and by rainout from convective anvils and large-scale precipitation [Liu et al.,
276 | 2001]. The wet deposition scheme for gases is described by Amos et al. [2012] and the
277 | scavenging of aerosol by snow and cold/mixed precipitation is described by Wang et al.
278 | [2011]. Dry-deposition velocities for coarse mode aerosols (radii between 1-10 μm) are
279 | calculated based on aerosol size and hygroscopic growth as described in Zhang et al.
280 | [2001]. Aerosol deposition to snow and ice surfaces is described by Fisher et al. [2011].
281 | For smaller aerosols (radii less than 1 μm), dry deposition velocities are calculated with a
282 | standard resistance-in-series scheme [Wang et al., 1998, Wesely, 1989].

283

284 | Anthropogenic NO_x emissions are from the EDGAR 3.2-FT2000 global inventory for the
285 | year 2000 [Oliver et al., 2005], scaled by country on the basis of energy statistics as
286 | described by van Donkelaar et al. [2008]. The monthly inventory of emissions from
287 | biomass burning are from the Global Fire Emissions Database (GFED2) [van der Werf et
288 | al., 2009]. Soil NO_x emissions are computed using a parameterization described in
289 | Hudman et al. [2012], which is a function of vegetation type, temperature, soil moisture,

Maria Zatko 9/4/15 1:45 PM

Deleted: boundary layer chemistry and

Maria Zatko 9/4/15 1:46 PM

Deleted: the A

Maria Zatko 9/4/15 1:46 PM

Deleted: continent

Maria Zatko 9/4/15 1:37 PM

Deleted: , such as the Antarctic continent,

Maria Zatko 9/12/15 8:26 AM

Deleted: .

Maria Zatko 9/12/15 8:28 AM

Deleted: preservation

296 precipitation, and fertilizer emissions. Emissions of NO_x from lightning are linked to
 297 deep convection following the parameterization of *Price and Rind* [1992] and are scaled
 298 globally as described by Murray et al. [2012] to match OTD/LIS climatological
 299 observations of lightning flashes. The stratospheric source of NO_y (=NO_x+HNO₃) utilizes
 300 monthly climatological 3-D production and loss rates from the Global Modeling Initiative
 301 (GMI) model [*Allen et al.*, 2010], which captures the formation of the polar vortex and
 302 PSC sedimentation [*Murray et al.*, 2012].

303
 304 For this work, GEOS-Chem version v9-01-01 was run at 2°x2.5° horizontal resolution
 305 with 72 hybrid vertical levels using GEOS-5 meteorology from May 2009 to May 2010.
 306 The model was spun up for six months prior to May 2009. There are no sub-surface
 307 (snow) layers in GEOS-Chem and the three lowest vertical levels are each roughly 100
 308 meters in height above Antarctica. The boundary layer in GEOS-Chem is calculated
 309 using a parameterization involving the bulk Richardson number with surface friction, a
 310 turbulent velocity scale, and non-local fluxes of heat and moisture [*Holtstlag and Boville*,
 311 1993] as implemented by Lin and McElroy [2010]. The mixing of emissions, dry
 312 deposition, and concentrations of individual species within the boundary layer are
 313 determined by static instability. In a stable boundary layer, the local scheme based on
 314 eddy diffusivity-theory is used, and the mixing is weak. In an unstable boundary layer,
 315 boundary layer mixing is triggered by large eddies. Average boundary layer mixing ratios
 316 (ppbv) of species reported in this study (e.g., NO₃⁻, NO_x, OH, O₃) are mixing ratios in the
 317 lowest vertical grid box (total height ~ 100 m).

318
 319 Figure 1 illustrates the nitrogen recycling associated with snow NO₃⁻ photolysis as
 320 included in the model. The total flux of snow-sourced NO_x from the snow, F_{NOx} (molec
 321 cm⁻² s⁻¹), is calculated using the wavelength-dependent absorption cross-section for NO₃⁻
 322 photolysis ($\sigma_{NO_3^-}$, cm² molec⁻¹), the temperature (T)- and pH-dependent quantum yield for
 323 NO₃⁻ photolysis (ϕ , molec photon⁻¹), the depth- and wavelength-dependent actinic flux in
 324 the snow photic zone (I , photons cm⁻² s⁻¹ nm⁻¹), and the average NO₃⁻ concentration
 325 ($[NO_3^-]$, molec cm⁻³) over the depth of integration. F_{NOx} is calculated in E7 and converted
 326 into units of ng N m⁻² yr⁻¹ in E8 and E9.

$$327 \quad 328 \quad F_{NOx} = \int_{\lambda_0}^{\lambda_1} \int_{z_0}^{z_{3e}} \sigma_{NO_3^-}(\lambda) \cdot \phi(T, pH) \cdot I(\lambda, z) \cdot [NO_3^-](z) d\lambda dz, \quad E7$$

329
 330 In E7, $\sigma_{NO_3^-}$ is from Burley and Johnston [1992]. The quantum yield from Chu and
 331 Anastasio [2003], assuming T=244K and pH=5 is used for the base case scenario and ϕ
 332 from Zhu et al. [2010] is used for sensitivity studies. The actinic flux (I) is integrated
 333 from the snow surface (z_0) to the depth of the photic zone (z_{3e}). The snow photic zone is
 334 defined as three times the e-folding depth of ultraviolet (UV) actinic flux in snow (z_{3e}),
 335 where 1 e-folding depth is z_e . Below z_{3e} , more than 95% of the radiation has been
 336 attenuated and minimal photochemistry occurs. The flux of snow-sourced NO_x is
 337 integrated over several ultraviolet wavelength bands (298-307 nm, 307-312 nm, 312-320
 338 nm, 320-345 nm), which are then summed to calculate total F_{NOx} from the photolysis of
 339 snow NO₃⁻ between $\lambda=298-345$ nm. We assume that all NO_x formed in E7 is immediately
 340 desorbed into the gas-phase and transported from the LLR to the interstitial air and then
 341 into the overlying boundary layer [*Zatko et al.*, 2013].

Maria Zatko 10/13/15 4:19 AM

Deleted: The calculated boundary layer mixing ratios are insensitive to whether the average mixing ratios in the lowest grid box (total height ~ 100 m) or the three lowest grid boxes (total height ~ 300 m) are used.

Maria Zatko 9/3/15 12:44 PM

Deleted: temperature-dependent

Maria Zatko 9/4/15 1:55 PM

Deleted: ,

Maria Zatko 9/4/15 1:55 PM

Deleted: E10, and

Maria Zatko 9/3/15 12:45 PM

Deleted: T

Maria Zatko 9/8/15 11:49 AM

Deleted:

Maria Zatko 10/13/15 10:03 AM

Deleted:

Maria Zatko 9/3/15 12:50 PM

Deleted: - ... [6]

Maria Zatko 9/8/15 11:43 AM

Deleted:

356

357 2.1.2 Calculating Radiative Transfer in Snow

358 A 2-stream, plane parallel snowpack actinic flux parameterization based on a 4-stream
359 radiative transfer model [Grenfell, 1991] was developed and described in detail in Zatko
360 et al. [2013] and has been implemented into GEOS-Chem for the purposes of this study.
361 The parameterization is simple, broadly applicable, and allows for variation in snow and
362 sky properties (e.g., solar zenith angle, cloud fraction) over time. Ice grains are assumed
363 to be spherical in shape and light-absorbing impurities (LAI), including black carbon,
364 brown carbon, dust, and organics, are assumed to be homogeneously distributed
365 throughout the snow and always external to the ice grain. The snowpack actinic flux
366 parameterization is used to calculate the UV actinic flux ($\text{photons cm}^{-2} \text{s}^{-1} \text{nm}^{-1}$) and the
367 mean austral summer (DJF) e-folding depths (cm) across Antarctica (Figure 3a), which
368 are both needed to calculate F_{NOx} . The snowpack actinic flux parameterization is most
369 sensitive to radiation equivalent mean ice grain radii (r_e) and insoluble LAI in snow
370 [Zatko et al., 2013]; higher concentrations of LAI in the snow and smaller r_e lead to
371 shallower e-folding depths (z_e). Field and satellite measurements suggest significant
372 increases in surface r_e throughout austral summer in Antarctica [Jin et al., 2008, Klein,
373 2014]. The r_e and snow density values used in this study are from observations reported
374 in Gallet et al. [2011] and Klein [2014] and range from 86-360 μm and 260-360 kg m^{-3} ,
375 respectively. The mean Dome C vertical r_e profile from Gallet et al. [2011] is applied
376 across Antarctica for all seasons except austral summer. During austral summer, larger
377 surface r_e values are incorporated across all of Antarctica to simulate the rapid surface r_e
378 growth reported in Klein [2014].

379

380 The concentration of black carbon (BC) in the model (Figure 3b) is calculated by scaling
381 observed BC concentrations (C_{BC}) at Vostok [Grenfell et al., 1994] by the modeled
382 annual average snow accumulation rates ($\text{kg m}^{-2} \text{yr}^{-1}$) from GEOS-Chem. However, high
383 accumulation rates in coastal regions ($700 \text{ kg m}^{-2} \text{yr}^{-1}$) lead to unrealistically low C_{BC} .
384 The minimum C_{BC} values used in the model are 0.08 ng g^{-1} , which is comparable to the
385 C_{BC} values measured in high snow accumulation rate regions in Antarctica, such as in the
386 East Antarctic sea ice zone (0.1 ng g^{-1}) [Bisiaux et al., 2012, Zatko and Warren, 2015].
387 Insoluble non-black carbon species (nonBC) including dust, brown carbon, and organics,
388 are responsible for the majority (up to 89% at $\lambda=305 \text{ nm}$) of the absorption of radiation at
389 UV wavelengths [Zatko et al., 2013] in snow. These nonBC species and their
390 concentrations have not been well quantified in snow. Based on observations reported in
391 Zatko et al. [2013], we scale UV-absorption by insoluble nonBC to the absorption by
392 insoluble black carbon in snow by assuming that at $\lambda=650\text{-}700 \text{ nm}$, which is a wavelength
393 range where black carbon dominates absorption, insoluble black carbon is responsible for
394 70% of the particulate absorption. We also assume that nonBC material has an absorption
395 Ångstrom exponent of 5 [Doherty et al., 2010].

396

397 We neglect the influence of soluble light absorbers in the snow and only consider the
398 influence of insoluble LAI on calculations of actinic flux profiles in snow. To determine
399 whether soluble LAI contribute significantly to light-absorption in the snow, we calculate
400 the total extinction coefficient for insoluble BC, insoluble nonBC, and soluble LAI
401 following section 2.1 of Zatko et al. [2013] and using the absorption coefficients for

Maria Zatko 9/4/15 1:56 PM

Deleted: (Figure 3a)

Maria Zatko 9/4/15 1:58 PM

Deleted:

Maria Zatko 9/4/15 1:56 PM

Deleted: (Figure 3b)

Maria Zatko 9/4/15 1:59 PM

Deleted: , which show good agreement with observations (Figure 2a).

407 soluble material in snow reported in Beine et al., [2011] in northern Alaska. To our
408 knowledge, observations of soluble light-absorbing impurities in Antarctic snow are
409 unavailable. We use soluble LAI observations from the Arctic to provide a general
410 estimate of the importance of soluble LAI in polar snow. The absorption coefficients
411 (0.028 m^{-1} at $\lambda=307 \text{ nm}$) from Beine et al. [2011] are identical to the extinction
412 coefficients because it is assumed that there is no scattering by soluble species. Insoluble
413 C_{BC} (9 ng g^{-1}) from Barrow, Alaska [Doherty et al., 2010] were used to calculate
414 extinction coefficients for BC and nonBC material and therefore the amount of nonBC
415 absorption in the UV and near-visible wavelengths following Zatko et al. [2013].
416 Insoluble nonBC material is responsible for 9-14 times more absorption than soluble
417 material in the wavelength range $\lambda=298\text{-}345 \text{ nm}$. Insoluble BC material is responsible for
418 1.5-10 times more absorption than soluble material in the wavelength range $\lambda=298\text{-}345$
419 nm . The extinction coefficient is not influenced by the addition of a soluble absorber
420 because scattering by snow grains dominates the extinction in snow. The effective co-
421 albedo of single scattering is increased by 6-15% when soluble absorbers are included.
422 The resulting change in z_e is at most 0.5 cm, which represents an increase of 4-9% in the
423 wavelength region of $\lambda=298\text{-}345 \text{ nm}$.

424 2.1.3. Calculating NO_3^- Concentrations in Snow

425 The median value of sub-surface (varied depth resolution) snow NO_3^- concentrations
426 from the ITASE campaign (60 ng g^{-1}) [Berter et al., 2005] is used for modeled sub-
427 surface (from 2-cm depth to the depth of the snow photic zone, z_{3d}) snow NO_3^-
428 concentrations ($[\text{NO}_3^-]_{bot}$) across all of Antarctica. Although there is a large variation in
429 snow NO_3^- concentrations from observations collected during the ITASE campaign
430 (Figure 3d), there is no clear spatial pattern. Since NO_3^- concentrations in the top 2 cm of
431 snow are up to 10 times higher than NO_3^- concentrations below 2-cm depth, the NO_3^-
432 concentrations in the top 2 cm of snow ($[\text{NO}_3^-]_{top}$) are calculated by enhancing $[\text{NO}_3^-]_{bot}$
433 by a factor of 6, the median of observed NO_3^- enhancement factors (EF) in the top 2 cm
434 of snowpack [Dibb et al., 2004, Erbland et al., 2013, Frey et al., 2009, Mayewski and
435 Legrand, 1990, Rothlisberger et al., 2000]. Since NO_3^- concentrations are enhanced by a
436 factor of 6 in the top 2 cm of snow, an equal amount of NO_3^- has been removed from the
437 remainder of the photic-zone depth to maintain mass balance of nitrate within the snow
438 column.

439
440 As mentioned in the introduction, the measured quantum yields for the dominant NO_3^-
441 photolysis pathway (E1) range from 0.003 molec photon $^{-1}$ [Chu and Anastasio, 2003] to
442 0.6 molec photon $^{-1}$ [Zhu et al., 2010] at T=253K. A higher fraction of NO_3^- was likely
443 present on ice surfaces in the Zhu et al. [2010] study compared to the Chu and Anastasio
444 [2003] study due to the different sample preparation methods, and likely explains the 3
445 order-of-magnitude difference in quantum yields. This interpretation suggests NO_3^- on
446 the surface of ice grains is much more photolabile compared to NO_3^- embedded within
447 ice grains, consistent with results from Meusinger et al. [2014]. In this study, we assume
448 that NO_3^- that is wet deposited to the snow surface is more likely to be embedded in the
449 interior of a snow grain compared to NO_3^- that is dry deposited to the surface of the snow
450 grain, which is a simplistic scheme designed to take nitrate recombination chemistry into
451 account. To simulate this effect in an idealized snowpack, we scale snow NO_3^-
452 concentrations by the fraction of dry deposition relative to total (wet + dry) deposition to

Maria Zatko 9/11/15 10:16 AM

Deleted: Although there is a large variation in snow NO_3^- concentrations from observations collected during the ITASE campaign (Figure 3d), there is no clear spatial pattern, likely from the redistribution of NO_3^- resulting from photolysis and subsequent recycling.

Maria Zatko 9/11/15 9:27 AM

Deleted: below 2 cm

Maria Zatko 9/11/15 10:12 AM

Deleted:

Maria Zatko 9/10/15 6:33 PM

Deleted: below this depth

Maria Zatko 9/8/15 2:12 PM

Deleted: 1.3×10^{-3}

Maria Zatko 10/14/15 2:22 PM

Deleted: account for

464 | the Antarctic snow surface, assuming that only the fraction of dry deposited NO_3^- is
465 | photolabile (F_p). The degree of migration of NO_3^- within a snow grain after deposition due
466 | to snow metamorphism is unknown, which may influence the photolability of NO_3^-
467 | [Domine and Shepson, 2002]. Snow NO_3^- concentrations scaled by F_p are shown in
468 | Figure 3d.

469 |
470 | Other modeling studies have attempted to calculate the fraction of photolabile NO_3^- in
471 | snow by estimating the concentration of NO_3^- contained within the liquid-like region
472 | (LLR) on the surface of ice grains (e.g., Thomas et al., 2012). In this work, we do not
473 | explicitly calculate NO_3^- photolysis within the LLR because there are still many
474 | unknowns about the LLR [Domine et al., 2013], including the distribution of NO_3^-
475 | between the bulk snow and the LLR. This distribution is better understood for some
476 | species, such as chloride [Cho et al., 2002], but it is unclear if NO_3^- behaves similarly. In
477 | this study, we have assumed that all NO_x formed in the LLR is transferred to the
478 | boundary layer, which may lead to overestimates in the modeled F_{NO_x} values presented in
479 | this study. The quantum yield for NO_3^- photolysis is dependent on the location of NO_3^- in
480 | snow, and although there are uncertainties surrounding the location of NO_3^- in snow, in
481 | this study we use the full range of measured quantum yields to provide bounds for the
482 | amount of NO_x produced from snow NO_3^- photolysis.

484 | 2.2. Model Sensitivity Studies

485 | Due to uncertainties in our understanding of snow photochemistry [Domine et al., 2013],
486 | we perform a variety of model sensitivity studies, as shown in Table 3. The quantum
487 | yield is varied from 0.002 molec photon⁻¹ (corresponding to T=244 K) [Chu and
488 | Anastasio, 2003] to 0.6 molec photon⁻¹ [Zhu et al., 2010]. Snow NO_3^- concentrations
489 | below 2 cm ($[\text{NO}_3^-]_{\text{bot}}$) are halved and doubled with respect to the base case scenario and
490 | the impact of scaling NO_3^- concentrations by the fraction of photolabile NO_3^- (F_p) is
491 | investigated. The NO_3^- enhancement factor in the top 2 cm of snowpack is varied from 1
492 | to 10, based upon a range of reported observations [Dibb et al., 2004, Frey et al., 2009,
493 | Mayewski and Legrand, 1990, Rothlisberger et al., 2000]. C_{BC} is halved and doubled
494 | with respect to the base case scenario. The r_e profiles are varied in three sensitivity
495 | studies to examine the influence of r_e on the model-calculated mean austral summer
496 | (DJF) flux of snow-sourced NO_x ($\overline{F_{\text{NO}_x}}$). The bulk extinction coefficient for snow
497 | ($K_{\text{ext}_{\text{tot}}}$) is increased and decreased by 20% with respect to the base case scenario because
498 | Libois et al. [2013] suggest that the spherical snow grain assumption overestimates e-
499 | folding depths by a factor of 1.2. These sensitivity studies are used to provide estimates
500 | of the influence of these parameters on $\overline{F_{\text{NO}_x}}$ throughout the Antarctic continent.

502 | 2.3. Estimating the Impact of Snow NO_3^- Photolysis on Boundary Layer Chemistry 503 | and Ice-Core NO_3^- Records

504 | Nitrate photolysis, followed by oxidation, recycling, and redistribution of snow-sourced
505 | NO_x , influences both boundary layer chemistry and the concentration and isotopic
506 | signature of NO_3^- that is ultimately preserved in ice-core records. The preservation of
507 | NO_3^- in ice cores is most dependent on the amount of NO_3^- lost from the snow through
508 | photolysis via transport of snow-sourced NO_x away from the site of primary deposition.

Maria Zatko 9/4/15 2:06 PM

Deleted: (Figure 3c)

Maria Zatko 10/14/15 2:01 PM

Deleted:

Maria Zatko 10/14/15 5:12 PM

Deleted: 2

Maria Zatko 9/8/15 2:29 PM

Deleted: 1.3×10^{-3}

Maria Zatko 9/12/15 8:30 AM

Deleted: preservation of

514 The methods used to explore and quantify nitrogen recycling and photolysis-driven loss
515 of NO_3^- in snow are described in the following sections.

516

517 2.3.1. Reactive Nitrogen Recycling Between the Air and Snow

518 The Nitrogen Recycling Factor (NRF) is a metric originally proposed by Davis et al.
519 [2008] to quantify the degree of reactive nitrogen recycling in snow over 1 year. The
520 NRF is calculated in E8;

521

$$522 \quad NRF = \frac{F_{NOx}}{F_{PRI}}, \quad \text{E8}$$

523

524 In E8, F_{NOx} ($\text{ng N m}^{-2} \text{yr}^{-1}$) is the annual sum of NO_x released from the snow and F_{PRI} (ng
525 $\text{N m}^{-2} \text{yr}^{-1}$) is the annual sum of primary NO_3^- deposited to the snow. Davis et al. [2008]
526 use the NRF to describe nitrogen recycling on both macro-scale (e.g., across the East
527 Antarctic plateau) and micro-scale (e.g., the number of times one molecule of NO_3^- is
528 recycled) levels. An NRF greater than 1 suggests that multiple nitrogen recycling events
529 occur in the snow. NRF represents the average, or “bulk” degree of nitrogen recycling in
530 snow because this global modeling study cannot resolve the degree of nitrogen recycling
531 on a molecular level in the snow; some NO_3^- molecules may never be photolyzed while
532 other NO_3^- molecules may be photolyzed and recycled many times greater than NRF .
533 The NRF has implications for boundary layer chemistry because the continual re-
534 emission of NO_x enhances the effective concentration of NO_x in the boundary layer
535 [Davis et al., 2008]. Additionally, nitrogen recycling between the air and snow may alter
536 the preservation of NO_3^- in ice-core records.

537

538 2.3.2. Export of Snow-sourced Nitrate Away from the Original Site of Photolysis

539 Once snow-sourced NO_x is emitted to the atmosphere, it is subject to transport away from
540 the original site of photolysis. If snow-sourced NO_x is oxidized to HNO_3 and re-deposited
541 back to the snow surface, then there is no net photolysis-driven loss of NO_3^- from the
542 snow. However, if some of the snow-sourced NO_x is transported away from the site of
543 primary deposition, there is a net photolysis-driven loss of NO_3^- from the snow. The
544 fraction of total NO_3^- (photolabile + non-photolabile) lost from the snow driven by
545 photolysis (f) is calculated in E9;

546

$$547 \quad f = \left(\left(\frac{F_R}{F_{NOx}} \right)^{\tau_z} - 1 \right) \cdot F_p \quad \text{E9}$$

548

549 In E9, negative values of f represent loss of NO_3^- from the snow and positive values of f
550 represent gain of NO_3^- to the snow. In E9, F_R ($\text{ng N m}^{-2} \text{yr}^{-1}$) is the total annual flux of
551 recycled NO_3^- to the snow surface and F_{NOx} ($\text{ng N m}^{-2} \text{yr}^{-1}$) is the total annual flux of NO_x
552 released from the snow. F_R is calculated by subtracting the depositional flux of NO_3^- from
553 a model run without snow photochemistry from the depositional flux of NO_3^- from a
554 model run with snow photochemistry. The ratio of F_R to F_{NOx} represents the fraction of
555 photolabile NO_3^- remaining in the snow after 1 year. As long as NO_3^- remains in the
556 photic zone, NO_3^- can continually be lost from the snow by photolysis-driven processes.
557 The preservation of NO_3^- in ice cores is dependent on the fraction of NO_3^- lost from the
558 snow through photolysis during the entire time that NO_3^- remains in the photic zone.

Maria Zatko 9/3/15 1:00 PM

Deleted: r

Maria Zatko 9/3/15 12:57 PM

Deleted: .

Maria Zatko 9/3/15 1:15 PM

Deleted: Similar to the NRF_{yr} in E9, NRF_{τ_z} values greater than 1 suggest that multiple nitrogen recycling events are occurring in the snow before burial beneath the photic zone.

Maria Zatko 9/3/15 1:30 PM

Deleted: We calculate the number of years that NO_3^- remains in the photic zone (τ_z , years) according to E9, where both the depth of the photic zone (cm) and the total annual snow accumulation (α_r) (cm yr^{-1}) are consid... [7]

Maria Zatko 9/3/15 1:34 PM

Deleted: 10

Maria Zatko 10/13/15 9:01 AM

Deleted: 1 –

Maria Zatko 9/3/15 1:34 PM

Deleted: 10

Maria Zatko 9/3/15 1:34 PM

Deleted: 10

575 Provided that there are no major changes in parameters that influence snow
 576 photochemistry (e.g., LAI, overhead ozone abundance) from year to year, the fraction of
 577 photolabile NO_3^- lost from the snow over 1 year will be stable from year to year.

579 τ_z (E10) represents the number of years that NO_3^- remains in the photic zone (τ_z , years)
 580 and in E9, τ_z accounts for the loss of NO_3^- that occurs during the entire time that it
 581 remains in the photic zone. When NO_3^- remains in the photic zone for less than a year (τ_z
 582 < 1), τ_z in E9 is set equal to 1. τ_z is calculated according to E10, where both the depth of
 583 the photic zone (cm) and the total annual snow accumulation (α_r) (cm yr⁻¹) are
 584 considered.

$$586 \tau_z = \frac{z_e}{\alpha_r} \quad \text{E10}$$

588 In E10, z_e (cm) is 1 e-folding depth of UV actinic flux and is used instead of z_{3e} because
 589 87-91% of snow-sourced NO_x is produced within the top 1 e-folding depth. To convert
 590 total annual snow accumulation rate from kg m⁻² yr⁻¹ to cm, a typical snow density for
 591 Antarctica (0.36 g cm⁻³) [Grenfell et al., 1994] is assumed. τ_z is the minimum number of
 592 years on average that NO_3^- remains in the top one-third of the snow photic zone before
 593 burial beneath because nitrogen recycling, which effectively redistributes NO_3^- upwards
 594 in the snow, is not factored into E10. τ_z thus represents the lifetime of NO_3^- in snow in an
 595 average sense and does not resolve photolysis and recycling of individual NO_3^-
 596 molecules.

598 In E9, $\left(\left(\frac{F_R}{F_{\text{NO}_x}}\right)^{\tau_z} - 1\right)$ represents the fraction of photolabile NO_3^- lost from the snow
 599 through photolysis. This fraction is multiplied by F_p to calculate the fraction of total
 600 (photolabile + non-photolabile) NO_3^- lost from the snow through photolysis (f). If f is 0,
 601 then all snow-sourced NO_x is redeposited to the snow and there is no net loss of NO_3^- . f is
 602 also 0 if the net export of snow-sourced NO_x away from the site of original photolysis is
 603 balanced by net import of snow-sourced NO_x from other Antarctic locations. If f is
 604 between -1 and 0 , the export of local snow-sourced NO_x is higher than the deposition of
 605 snow-sourced NO_x from elsewhere in Antarctica, resulting in net photolysis-driven loss
 606 of NO_3^- from the snow. If f is greater than 0, the export of local snow-sourced NO_x is
 607 lower than the deposition of snow-sourced NO_x from elsewhere in Antarctica, resulting in
 608 net photolysis-driven gain of NO_3^- to the snow.

610 f is used to calculate the enrichment in ice-core $\delta^{15}\text{N}(\text{NO}_3^-)$ due solely to the impact of
 611 photolysis-driven loss of NO_3^- in snow. We use a Rayleigh fractionation equation used to
 612 calculate $\delta^{15}\text{N}(\text{NO}_3^-)$ [Blunier et al., 2005]:

$$614 \delta^{15}\text{N}(\text{NO}_3^-) = \delta^{15}\text{N}(\text{NO}_3^-)_{\text{air}} \cdot (1 + f)^\epsilon - 1 \quad \text{E11}$$

616 In E11, $\delta^{15}\text{N}(\text{NO}_3^-)_{\text{air}}$ is the annual-averaged $\delta^{15}\text{N}$ value of boundary layer NO_3^- and ϵ
 617 is the fractionation constant (-47.9‰ [Berhanu et al., 2014]). In this work, we set
 618 $\delta^{15}\text{N}(\text{NO}_3^-)_{\text{air}}$ equal to 0‰ to investigate the enrichment in $\delta^{15}\text{N}(\text{NO}_3^-)$ only from
 619 photolysis-driven loss of NO_3^- from snow.

Maria Zatko 10/15/15 10:52 AM

Deleted: (E10)

Maria Zatko 9/3/15 1:32 PM

Moved (insertion) [1]

Maria Zatko 9/3/15 1:32 PM

Deleted: in E10

Maria Zatko 9/3/15 1:32 PM

Moved up [1]: τ_z in E10 accounts for the loss of NO_3^- that occurs during the entire time that it remains in the photic zone.

Maria Zatko 9/3/15 1:33 PM

Deleted: When NO_3^- remains in the photic zone for less than a year ($\tau_z < 1$), τ_z in E10 is set equal to 1.

Maria Zatko 9/3/15 1:36 PM

Deleted: 10

Maria Zatko 10/13/15 9:08 AM

Deleted: 1 -

Maria Zatko 10/13/15 9:10 AM

Deleted: 0

Maria Zatko 10/13/15 9:10 AM

Deleted: 1

Maria Zatko 10/13/15 9:10 AM

Deleted: less

Maria Zatko 10/13/15 9:04 AM

Deleted: -

634

635 3. Results and Discussion

636 3.1. Parameters that Influence F_{NOX} and its Spatial Redistribution

637 Figure 2a shows modeled total annual snow accumulation rates from GEOS-Chem (kg m^{-2}
 638 yr^{-1}) along with estimated total annual snow accumulation rates ($\text{kg m}^{-2} \text{yr}^{-1}$) in
 639 Antarctica [Erbland et al., 2013, Fegyveresi et al., 2011, Grenfell et al., 1994], ranging
 640 from 10-700 $\text{kg m}^{-2} \text{yr}^{-1}$. The rapid decrease in snow accumulation rate from the coast to
 641 the top of the East Antarctic plateau is attributed to increased distance from the ocean
 642 (moisture source) and increased elevation. Figure 2b shows modeled annual mean surface
 643 wind divergence from May 2009 to May 2010. Figure 2b and Antarctic Mesoscale
 644 Prediction System surface wind output [Figure 3 in Parish and Bromwich, 2007] indicate
 645 that the large-scale airflow pattern in Antarctica flows from the East Antarctic plateau
 646 downslope towards the coast. There are three major regions of wind convergence in
 647 Antarctica, located near the Ross, Ronne, and Amery ice shelves.

649 Figure 3a shows the mean austral summer (DJF) e-folding depth of UV actinic flux in
 650 snow (z_e). z_e ranges from 24 to 69 cm, with the shallowest depths on the East Antarctic
 651 plateau, due to the relatively high C_{BC} values (Figure 3b). Higher C_{BC} in snow results in a
 652 shallower z_e because UV absorption in snow is enhanced as the concentration of LAI
 653 increases [Zatko et al., 2013]. In this study, coastal grid boxes are a mixture of water, sea
 654 ice, and snow-covered surfaces, and since actinic flux profiles are only calculated for
 655 snow-covered surfaces, the average z_e in coastal grid boxes are artificially shallow.
 656 Observations of e-folding depths across Antarctica are limited. France et al. [2011] report
 657 z_e from near-station snow at Dome C ranging from 9-20 cm at 350 nm, which agree well
 658 with our modeled z_e [Zatko et al., 2013]. There are no z_e observations in Antarctica from
 659 snow without station contamination, which is representative of the majority of snow in
 660 Antarctica. Zatko et al. [2013] calculate z_e of 38 cm ($\lambda=298\text{-}345 \text{ nm}$) for remote Dome C
 661 snow due to lower C_{BC} far away from station contamination. The z_e for remote Dome C
 662 snow in this study (48 cm) is a factor of 1.3 larger than reported in Zatko et al. [2013]
 663 because larger radiation equivalent ice grain radii (r_e) are used during austral summer
 664 (based on Klein [2014]), and larger r_e grains lead to deeper z_e .

666 Figure 3b shows snow C_{BC} , ranging from 0.08 to 0.6 ng g^{-1} . Black carbon observations at
 667 WAIS-Divide [Bisiaux et al. 2012], Siple Dome [Chylek et al., 1992], Vostok [Grenfell et
 668 al., 1994], South Pole [Warren and Clarke, 1990], and Dome C [Warren et al., 2006] are
 669 included in Figure 3b. The highest C_{BC} values in Antarctica are found on the East
 670 Antarctic plateau (0.6 ng g^{-1}) and the spatial pattern of C_{BC} is governed by the snow
 671 accumulation rate; higher snow accumulation rates dilute C_{BC} [Doherty et al., 2013]. The
 672 modeled boundary layer black carbon concentrations are relatively uniform across
 673 Antarctica (0.1-0.6 pptv) because the majority of black carbon reaches Antarctica through
 674 long-range transport (with the exception of local production from Antarctic research
 675 stations).

677 Figure 3c shows the fraction of dry-deposited NO_3^- compared to total deposited NO_3^-
 678 across Antarctica. The ratio of dry deposition to total deposition ranges from 0 to 0.2 in
 679 coastal Antarctica and from 0.95 to 0.99 on the East Antarctic plateau. Figure 3d shows

Maria Zatko 10/14/15 4:11 PM
 Deleted: , Sofen et al., 2014

Maria Zatko 9/4/15 2:14 PM
 Deleted: There is good agreement between the modeled total snow accumulation rates in GEOS-Chem and previously reported total annual snow accumulation rates.

Maria Zatko 9/4/15 2:15 PM
 Deleted: ,

Maria Zatko 9/4/15 2:16 PM
 Deleted: which is in general agreement with

Maria Zatko 9/4/15 2:16 PM
 Deleted: from

Maria Zatko 9/4/15 2:18 PM
 Deleted: Figure 3 in

Maria Zatko 9/4/15 2:18 PM
 Deleted: [

Maria Zatko 9/4/15 2:17 PM
 Deleted: . The annual mean surface wind patterns

Maria Zatko 10/13/15 10:17 AM
 Deleted: inaveraged over ,

Maria Zatko 10/15/15 10:52 AM
 Deleted: Byrd

694 the modeled annual mean sub-surface (from 2-cm depth to the bottom of the photic zone,
695 $z_{3\phi}$) snow NO_3^- concentrations ($[\text{NO}_3^-]_{\text{bot}}=60 \text{ ng g}^{-1}$) scaled by F_p compared to averaged
696 multi-year NO_3^- observations from the ITASE campaign [Bertler et al., 2005] and mean
697 asymptotic (sub-photoc zone) NO_3^- mixing ratios from Erbland et al. [2013] and Shi et al.
698 [2014].

3.2. Model Sensitivity Studies

701 Table 3 shows the dependence of mean austral summer (DJF) $\overline{F_{\text{NO}_x}}$ on ϕ , $[\text{NO}_3^-]_{\text{bot}}$, C_{BC} ,
702 F_p , $K_{\text{ext}_{\text{tot}}}$, r_e . The sensitivity study results are compared to $\overline{F_{\text{NO}_x}}$ from the base case
703 scenario, which is also described in Table 3. $\overline{F_{\text{NO}_x}}$ is most sensitive to ϕ , which increases
704 $\overline{F_{\text{NO}_x}}$ by up to a factor of 330 compared to the base case scenario. The second most
705 influential parameter is the concentration of photolabile NO_3^- ($[\text{NO}_3^-]_{\text{bot}}$ and F_p).
706 Assuming that all NO_3^- is photolabile ($F_p=1$) increases $\overline{F_{\text{NO}_x}}$ by up to a factor of 7.4 (at
707 the coasts) with respect to the base case scenario. Variations in r_e , $K_{\text{ext}_{\text{tot}}}$, EF , and C_{BC}
708 influence $\overline{F_{\text{NO}_x}}$ by up to a factor of 1.3 compared to the base case scenario. Appendix A
709 shows model-calculated mean austral summer (DJF) $\overline{F_{\text{NO}_x}}$ throughout Antarctica for the
710 sensitivity studies described in Table 3. The quantum yield for NO_3^- photolysis and the
711 concentration of photolabile NO_3^- are likely related to one another. This highlights the
712 need for field, laboratory, and modeling studies to investigate factors influencing these
713 parameters, such as the location of NO_3^- in ice grains.

714
715 Figure 4 shows model-calculated mean austral summer (DJF) $\overline{F_{\text{NO}_x}}$ for several sensitivity
716 studies compared to previously reported F_{NO_x} at Neumayer [Jones et al., 2001], Halley
717 [Bauguitte et al., 2012, Jones et al., 2011], South Pole [Oncley et al., 2004, Wang et al.,
718 2008, Zatko et al., 2013], Dome C [Frey et al., 2013, Zatko et al., 2013], and WAIS-
719 Divide [Masclin et al., 2013]. The flux of snow-sourced NO_x is overestimated by three
720 orders of magnitude compared to observations when ϕ from Zhu et al. [2010] is used to
721 calculate $\overline{F_{\text{NO}_x}}$. In contrast, model-calculated $\overline{F_{\text{NO}_x}}$ using ϕ from Chu and Anastasio
722 [2003] provides better agreement with the observations, but is lower than the
723 observations by 14-78%. Use of the fraction of dry-deposited NO_3^- (F_p) to scale the
724 concentration of photolabile NO_3^- lowers $\overline{F_{\text{NO}_x}}$ by up to 85% along the coast, but has
725 little impact on the East Antarctic plateau due to the high fraction of dry deposited NO_3^-
726 (Figure 3c). The spatial patterns of $\overline{F_{\text{NO}_x}}$ in Figure 4 are largely governed by the depth of
727 the photic zone (z_e) across Antarctica (Figure 3a), which are inversely related to LAI
728 concentrations. The spatial patterns of $\overline{F_{\text{NO}_x}}$ are also influenced by the fraction of
729 photolabile NO_3^- , which is lowest at the coast in the model.

730
731 Previously reported F_{NO_x} values are calculated from measurements of NO_x concentration
732 gradients and turbulent diffusivity [Jones et al., 2001, 2011, Frey et al., 2013] or
733 calculated based on observed NO gradients and assuming photochemical steady-state
734 [Oncley et al., 2004], by incorporating observations into 1-D multi-phase chemistry
735 models [Bauguitte et al., 2012, Boxe and Saiz-Lopez., 2008, Wang et al., 2008], or by
736 using depth-integrated F_{NO_x} calculations similar to E7 [France et al., 2011, Masclin et al.,
737 2013, Zatko et al., 2013]. Observations of F_{NO_x} represent either noontime maxima
738 [Bauguitte et al., 2012, Frey et al., 2013, Jones et al., 2001, Zatko et al., 2013], daily
739 averages [Jones et al., 2011, Masclin et al., 2013], or averages over the duration of the

Maria Zatko 10/12/15 5:32 PM

Deleted: average

Maria Zatko 9/10/15 6:36 PM

Deleted: below 2 cm

Maria Zatko 10/12/15 5:19 PM

Deleted: (3.7-797 ppb)

Maria Zatko 10/12/15 5:11 PM

Deleted: .

Maria Zatko 10/16/15 5:59 PM

Deleted: .

Maria Zatko 9/6/15 2:18 PM

Deleted: or

Maria Zatko 9/7/15 4:13 PM

Deleted: Boxe et al., 2008

747 field campaign [Oncley et al., 2004, Wang et al., 2008] (see Table 4 in Masclin et al.,
748 [2013]). There is a wide range of reported $\overline{F_{NO_x}}$ at many of these locations; 2.4-17x10⁸
749 molec cm⁻² s⁻¹ at Dome C [France et al., 2011, Frey et al., 2013, Zatko et al., 2013], 3.2-
750 22x10⁸ molec cm⁻² s⁻¹ at South Pole [Oncley et al., 2004, Wang et al., 2008, Zatko et al.,
751 2013], 2.4-12.6x10⁸ molec cm⁻² s⁻¹ at Halley [Bauguitte et al., 2012, Jones et al., 2011],
752 2.1-3.3x10⁸ molec cm⁻² s⁻¹ at Neumayer [Jones et al., 2001], 42.5x10⁸ molec cm⁻² s⁻¹ at
753 WAIS-Divide [Masclin et al., 2013].

754
755 Regardless of the time period that the F_{NO_x} observations represent, all F_{NO_x} values for
756 each location are averaged together and presented in Figure 4c and Figure 4d.
757 Unfortunately, the actinic flux parameterization used here [Zatko et al., 2013] is unable to
758 resolve $\overline{F_{NO_x}}$ directly at the coast because coastal grid boxes are a mixture of ocean, sea
759 ice, and land, which prevents direct comparison of $\overline{F_{NO_x}}$ at Halley and Neumayer. Since
760 the flux of snow-sourced NO_x is overestimated by three orders of magnitude compared to
761 observations when the quantum yield from Zhu et al. [2010] is used, all following results
762 (Figures 5-10) are calculated using the Chu and Anastasio [2003] quantum yield
763 ($\phi=1.3 \times 10^{-3}$). Additionally, to approximate the potential spatial variability in the fraction
764 of NO₃⁻ that is photolabile, we scale snow NO₃⁻ by F_p in Figures 5-10. Figure 4d shows
765 the $\overline{F_{NO_x}}$ values, ranging from 0.5-7.8x10⁸ molec cm⁻² s⁻¹, used in Figures 5-10. All the
766 other parameters used to calculate $\overline{F_{NO_x}}$ in following sections and in Figures 5-10 are
767 described in the base-case scenario in Table 3.

768 3.3. Redistribution and Recycling of Reactive Nitrogen Across Antarctica

769 Figure 5a shows the total annual depositional flux of primary NO₃⁻ (F_{PRI}), which ranges
770 from 0.9-35x10⁵ ng N m⁻² yr⁻¹ and is highest at the coasts due to its relative proximity to
771 NO_x-source regions in lower latitudes. An adjoint modeling study by Lee et al. [2014]
772 suggests that boundary layer NO₃⁻ abundance in Antarctica is dominated by NO₃⁻
773 transport to Antarctica originating from NO_x emissions from 25-65°S during austral
774 winter and by thermal decomposition of peroxyacyl nitrate (PAN) as it descends from the
775 free troposphere in all other seasons. Figure 5b shows the total annual depositional flux
776 of recycled NO₃⁻ (F_R), which ranges from 0.7-31x10⁵ ng N m⁻² yr⁻¹ and is also highest at
777 the coasts due to transport from the Antarctic interior by katabatic winds. F_{PRI} and F_R are
778 comparable in magnitude to the total annual flux of snow-sourced NO_x to the atmosphere
779 (F_{NO_x}), which ranges from 2-23x10⁵ ng N m⁻² yr⁻¹ (Figure 4d). Figure 5c shows that
780 recycled nitrogen (F_R) is the dominant form of NO₃⁻ deposition across Antarctica, except
781 along the coastline where it represents as little as 11% of the deposition flux, and is most
782 important in regions of wind convergence such as the Ronne, Ross, and Amery ice
783 shelves.

784
785
786 To further investigate the role that wind patterns have on the redistribution of NO₃⁻ across
787 Antarctica, we alternately turn off the upward F_{NO_x} in East Antarctica and in West
788 Antarctica to examine the influence of each region on NO₃⁻ redistribution across
789 Antarctica. Figure 6 compares F_R in these sensitivity studies to F_R in the base case
790 scenario. The large reduction in F_R when F_{NO_x} is separately turned off in East and West
791 Antarctica demonstrates that little snow-sourced NO₃⁻ is transported between East and
792 West Antarctica, likely due to the influence of the trans-Antarctic mountains on

Maria Zatko 9/4/15 2:49 PM

Deleted: and comparing the mean $\overline{F_{NO_x}}$ observation at each site with modeled $\overline{F_{NO_x}}$ values in this study allows for a coarse examination of the model-measurement agreement.

Maria Zatko 9/4/15 3:19 PM

Deleted: 3

Maria Zatko 9/12/15 12:26 PM

Deleted: xyac1

800 atmospheric transport. However, recycled NO_3^- is present in West Antarctica where F_{NO_x}
801 has been turned off, suggesting that some snow-sourced NO_3^- from East Antarctica is
802 transported across the trans-Antarctic mountains likely due to the influence of katabatic
803 winds originating from the East Antarctic plateau.

804
805 Figure 7 shows the Nitrogen Recycling Factor (NRF). Across Antarctica, NRF ranges
806 from 0 to 16, indicating that nitrogen is recycled multiple times over the course of 1 year
807 across most of Antarctica, with the exception of the coasts. The spatial pattern of NRF is
808 governed by the flux of snow-sourced NO_x to the atmosphere ($\overline{F_{\text{NO}_x}}$, Figure 4d), which is
809 influenced by the depth of the photic zone (z_e) and the concentration of photolabile
810 nitrate. The spatial pattern of NRF is also dependent on F_{PRI} , which is highest at the coast
811 and lowest on the East Antarctica plateau. NRF values are lowest near the coast because
812 the fraction of photolabile NO_3^- is small and F_{PRI} values are high. The maximum NRF
813 values occur partway up the plateau, corresponding to maximum $\overline{F_{\text{NO}_x}}$ values. [Erbland et al. \[2015\]](#)
814 [use a multi-layer snow chemistry column model along with snow and atmospheric \$\text{NO}_3^-\$ concentration and isotopic measurements to estimate the \$NRF\$ at Dome C. The difference in model-estimates of nitrogen recycling at Dome C in Erbland et al. \[2015\] \(4 recycling events\) and in this study \(9 recycling events\) is at least partially due to the assumption in Erbland et al. that 20% of snow-sourced \$\text{NO}_3^-\$ is transported away from Dome C via katabatic winds. We use our global chemical transport modeling framework to calculate that 25% of snow-sourced \$\text{NO}_3^-\$ is transported away at Dome C, which is slightly larger than the assumption in Erbland et al. \[2015\]. Larger \$\text{NO}_3^-\$ export fractions will lead to larger loss of snow nitrate, which may also lead to a larger number of recycling events via transport and redeposition of snow-sourced \$\text{NO}_x\$ throughout East Antarctica. Davis et al. \[2008\] use estimates of atmospheric \$\text{NO}_x\$ overhead-column burdens and average \$\text{NO}_x\$ atmospheric lifetimes along with primary nitrogen deposition measurements from Legrand and Kirchner \[1990\] to estimate the \$NRF\$ in East Antarctica. Davis et al. \[2008\] estimate an \$NRF\$ of 1.8, which is roughly 3 to 6 times lower than the modeled East Antarctic \$NRF\$ values in this study \(\$NRF=5-10\$ \), although Davis et al. state that their estimated \$NRF\$ value could be factors of 3 to 5 times higher due to uncertainties in primary nitrogen deposition estimates.](#)
815
816
817
818
819
820
821
822
823
824
825
826
827
828
829
830
831

832 **3.4. Impact of Reactive Nitrogen Recycling on Boundary Layer Chemistry**

833 The height of the boundary layer will strongly influence the abundance of NO_3^- , reactive
834 nitrogen oxides, and oxidants emitted or formed at or near the surface. At many Antarctic
835 stations (e.g., Neumayer, South Pole, Dome C, Halley, Kohnen) there is a wide range of
836 observed boundary layer heights during austral summer (10-600 m [[Casasanta et al., 2014](#),
837 [Davis et al., 2004](#), [Handorf, 1996](#), [Jones et al., 2006, 2008](#), [King et al., 2006](#),
838 [Kodama et al., 1985](#), [Konig-Langlo et al., 1998](#), [Neff et al., 2008](#), [Oncley et al., 2004](#),
839 [Travouillon et al., 2008](#), [Weller et al., 1999](#)]), and although modeled boundary layer
840 heights are not systematically biased in one direction compared to observations, they
841 often do not agree well. Therefore, only the relative impacts of snow photochemistry on
842 reactive nitrogen and oxidant abundances are compared in this study. The impact of snow
843 photochemistry on boundary layer chemistry can be examined by considering factor
844 changes in boundary layer NO_x , NO_3^- , OH , and O_3 mixing ratios between simulations
845 with and without snow NO_3^- photolysis. As shown in Figure 8, the inclusion of a snow

Maria Zatko 9/3/15 1:45 PM

Deleted: Figure 7b shows the minimum number of years that snow NO_3^- remains in the photic zone on average, τ_z (E9). Nitrate remains in photic zone for 3 months near the Antarctic coasts and up to 7.5 years on the East Antarctic plateau before burial below the photic zone. The spatial pattern of τ_z is governed by the snow accumulation rate, both directly and indirectly through its influence on C_{BC} . The spatial pattern of τ_z is in agreement with the expectation that NO_3^- remains in the photic zone the longest in areas with low snow accumulation rates.

859 NO_x source leads to factor increases in boundary layer mixing ratios of NO_x from 7.0-
860 31.6, gas-plus aerosol-phase nitrate from 3.9-38.1, OH from 3.6-6.7, and O₃ from 1.3-2.0.
861 The largest factor increases are in West Antarctica, particularly near the Ross and Ronne
862 ice shelves, where winds carrying photo-produced species converge. The surface
863 transport pattern is especially important for the redistribution of the longer-lived species
864 NO₃⁻ and O₃. Other snow photochemical reactions mentioned in the introduction but not
865 included in this modeling study will also impact oxidant abundances, but the effects of
866 each photochemical reaction are not additive due to the highly non-linear nature of
867 oxidant cycling.

868 3.5. Implications for Ice-Core Records of Nitrate Concentrations and Isotopes

869 Figure 9a shows the minimum number of years that snow NO₃⁻ remains in the photic
870 zone on average, τ_z (E9). NO₃⁻ remains in photic zone for 3 months near the Antarctic
871 coasts and up to 7.5 years on the East Antarctic plateau before burial below the photic
872 zone. The spatial pattern of τ_z is governed by the snow accumulation rate, both directly
873 and indirectly through its influence on C_{BC} . The spatial pattern of τ_z is in agreement with
874 the expectation that NO₃⁻ remains in the photic zone the longest in areas with low snow
875 accumulation rates.

876
877
878 Figure 9b shows the fraction of NO₃⁻ gained or lost from the snow through photolysis (f ,
879 E11), which ranges from -0.99 to 0.21. The positive f values indicate regions with net
880 gain of NO₃⁻ to the snow resulting from the spatial redistribution of NO₃⁻ driven by snow
881 photochemistry. In regions of convergence, such as over the Ronne Ice Shelf, and parts of
882 the coast, there is a net gain of snow-sourced NO₃⁻. There is a sharp gradient in f between
883 the plateau and the coast, with the largest loss of snow NO₃⁻ on the East Antarctic
884 plateau. On the East Antarctic plateau, most photolyzed NO₃⁻ is transported away by
885 katabatic winds, but along the coast, the photolysis-driven loss of NO₃⁻ from the snow is
886 minimal due to high snow accumulation rates and transport of snow-sourced NO₃⁻ from
887 the continental interior. The spatial pattern of f is largely influenced by the number of
888 years that NO₃⁻ remains in the photolytic zone (τ_z), the concentration of photolabile NO₃⁻
889 (F_p), and wind patterns across Antarctica.

890
891 Figure 9c shows modeled enrichments in ice-core $\delta^{15}\text{N}(\text{NO}_3^-)$ from photolysis-driven loss
892 of NO₃⁻ in snow, compared to sub-photic zone $\delta^{15}\text{N}(\text{NO}_3^-)$ observations from Erbland et
893 al. [2013], Frey et al. [2009], Jarvis, [2008], Shi et al., [2014], and Sofen et al. [2014].
894 The $\delta^{15}\text{N}(\text{NO}_3^-)$ values at Dome C and along the transect from Dumont d'Urville to
895 Dome C are calculated asymptotic $\delta^{15}\text{N}(\text{NO}_3^-)$ values from Erbland et al. [2013] and Frey
896 et al. [2009], which are representative of snow depths well below the photic zone at
897 Dome C. The $\delta^{15}\text{N}(\text{NO}_3^-)$ values along the transect from Dome A towards Zhongshan are
898 asymptotic $\delta^{15}\text{N}(\text{NO}_3^-)$ values calculated in Shi et al. [2014]. The $\delta^{15}\text{N}(\text{NO}_3^-)$ values at
899 WAIS-Divide [Sofen et al., 2014] and South Pole [Jarvis, 2008] are average ice-core
900 $\delta^{15}\text{N}(\text{NO}_3^-)$ measurements from 1900-2000 CE, which are also representative of
901 $\delta^{15}\text{N}(\text{NO}_3^-)$ values well below the snow photic zone. Model-calculated ice-core
902 $\delta^{15}\text{N}(\text{NO}_3^-)$ values range from 0‰ to 363‰. The modeled enrichments in ice-core
903 $\delta^{15}\text{N}(\text{NO}_3^-)$ values are generally higher than the sub-photic zone $\delta^{15}\text{N}(\text{NO}_3^-)$ observations
904 presented in Figure 9c, however, boundary layer $\delta^{15}\text{N}(\text{NO}_3^-)$ observations are negative in

Maria Zatko 9/3/15 1:46 PM

Deleted: a

Maria Zatko 9/12/15 5:37 PM

Deleted: lost

Maria Zatko 10/13/15 9:12 AM

Deleted: 21

Maria Zatko 10/13/15 9:12 AM

Deleted: 99

Maria Zatko 10/13/15 9:12 AM

Deleted: negative

Maria Zatko 9/3/15 1:46 PM

Deleted: b

Maria Zatko 9/11/15 4:49 PM

Deleted: over much of Antarctica

912 both coastal [Morin et al., 2009, Savarino et al., 2007, Wagenbach et al., 1998] and
913 continental [Erland et al., 2013, Frey et al., 2009] Antarctica, making modeled
914 $\delta^{15}\text{N}(\text{NO}_3^-)$ values biased high by up to $\sim 40\%$ since we assume that the $\delta^{15}\text{N}$ of
915 atmospheric nitrate (NO_3^- and HNO_3) deposited to the snow surface is always equal to
916 0% . The modeled ice-core $\delta^{15}\text{N}(\text{NO}_3^-)$ values resulting from the photolysis-driven loss
917 of snow nitrate are sensitive to the fractionation constant (ϵ). The fractionation constant
918 is varied over the full range of values reported in Erland et al [2013], Frey et al., [2009],
919 and Shi et al. [2014]; an ϵ of -90% increases modeled ice-core $\delta^{15}\text{N}(\text{NO}_3^-)$ by a factor of
920 2 and an ϵ of -10% decreases modeled ice-core $\delta^{15}\text{N}(\text{NO}_3^-)$ by a factor of 5 across
921 Antarctica. Both the modeled and observed $\delta^{15}\text{N}(\text{NO}_3^-)$ values show that $\delta^{15}\text{N}(\text{NO}_3^-)$ is
922 most enriched on the East Antarctic plateau, where the fraction of NO_3^- lost from the
923 snow through photolysis is highest.

924

3.6. Relationship Between Nitrogen Recycling and Photolytic-loss of NO_3^- in Snow

926 The degree of photolysis-driven loss of snow NO_3^- is determined by both rates of
927 photolysis and transport patterns across the Antarctic continent. The spatial patterns of
928 recycling (NR , Figure 7) and loss (f , Figure 9b) differ across Antarctica and Figure 10
929 shows the relationship between f and NR across Antarctica. The magnitude of nitrogen
930 recycling and degree of photolysis-driven loss of snow NO_3^- are well correlated ($r^2 > 0.8$,
931 $p < 0.001$) in regions where NO_3^- remains in the photic zone for less than 3 years ($\tau_z < 3$)
932 (Figure 10a). The relationship between recycling and loss breaks down in locations where
933 NO_3^- remains in the photic zone for more than 3 years (Figure 10b). The relationship
934 between recycling and loss weakens with increasing τ_z because recycling of reactive
935 nitrogen occurs at or near the surface only, while loss of NO_3^- occurs throughout the
936 depth of snow photic zone. The number of years that NO_3^- remains in the snow photic
937 zone (τ_z , E10) is mainly dependent on snow accumulation rates and the concentrations of
938 light-absorbing impurities in snow, which are partially governed by snow accumulation
939 rates. In the present climate, τ_z less than 3 years corresponds to snow accumulation rates
940 higher than $85 \text{ kg m}^{-2} \text{ a}^{-1}$.

941

4. Conclusions

943 We have incorporated the photolysis of snow NO_3^- into a global chemical transport
944 model (GEOS-Chem) for the first time in order to calculate the flux and redistribution of
945 nitrogen in Antarctic snowpack. An important goal of this study is to investigate the
946 impact of snowpack NO_3^- photolysis on boundary layer chemistry and the preservation of
947 NO_3^- concentration and isotopes in Antarctic ice cores.

948

949 The calculated flux of snow-sourced NO_x from Antarctic snow ($0.5\text{-}7.8 \times 10^8 \text{ molec cm}^{-2} \text{ s}^{-1}$)
950 is in general agreement with snow NO_x -flux observations when using a quantum yield
951 for snow NO_3^- photolysis on the order of $10^{-3} \text{ molec photon}^{-1}$ [Chu and Anastasio, 2003].
952 The flux of snow-sourced NO_x is overestimated by 2-3 orders of magnitude when the
953 quantum yield from Zhu et al. [2010] is used along with various assumptions for the
954 amount of photolabile NO_3^- . The modeled spatial pattern of the flux of snow-sourced
955 NO_x is determined by the patterns of light-absorbing impurity concentrations in snow and
956 the fraction of photolabile NO_3^- across Antarctica. In the model, the spatial pattern of
957 light-absorbing impurities is strongly influenced by snow accumulation rates and the

Maria Zatko 9/11/15 4:43 PM

Formatted: Font:Italic

Maria Zatko 9/11/15 4:45 PM

Deleted: [Erland et al., 2013, Frey et al., 2009, Morin et al., 2009, Savarino et al., 2007].

Maria Zatko 9/11/15 4:42 PM

Deleted: 0

Maria Zatko 10/13/15 12:19 PM

Deleted: .

Maria Zatko 9/14/15 5:36 PM

Formatted: Left

Maria Zatko 9/11/15 6:34 PM

Deleted: snow accumulation rate and

Maria Zatko 9/11/15 6:38 PM

Deleted: aerosol

Maria Zatko 9/14/15 5:33 PM

Deleted:

966 spatial pattern of photolabile NO₃⁻ in the model is influenced by the amount of wet
967 deposited NO₃⁻ compared to total deposited NO₃⁻ across Antarctica. Total snow NO₃⁻
968 concentrations were kept spatially constant in this study; however, spatial variations in
969 snow NO₃⁻ concentrations would also influence the spatial pattern of F_{NO_x} across
970 Antarctica. However, observations of snow NO₃⁻ concentrations across Antarctica show
971 no clear spatial pattern. Snow-sourced NO_x is subject to transport across Antarctica, and
972 recycled NO₃⁻ makes up a large fraction of the depositional NO₃⁻ flux across the Antarctic
973 continent, especially in regions of convergence over the Ronne, Ross, and Amery ice
974 shelves.

975
976 The inclusion of snow-sourced NO_x in GEOS-Chem leads to factor increases in boundary
977 layer mixing ratios for NO_x ranging from 7.0-31.6, gas and aerosol phase nitrate ranging
978 from 3.9-38.1, OH ranging from 3.6-6.7, and O₃ ranging from 1.3-2.0. The incorporation
979 of additional snow photochemical reactions into GEOS-Chem will also impact oxidant
980 abundances, but the effects of each photochemical reaction are not be additive due to the
981 highly non-linear nature of oxidant cycling.

982
983 The Nitrogen Recycling Factor (*NRF*) ranges from 0.07 to 15.8, suggesting that nitrogen
984 is recycled multiple times on average over the course of one year across all of Antarctica,
985 except at the coasts where snow accumulation rates are high. Nitrate can remain in the
986 photic zone for up to 7.5 years in Antarctic snow and is recycled multiple times (up to 57,
987 on average) before burial beneath the photic zone in Antarctica. The fraction of NO₃⁻ lost
988 from the snow through photolysis ranges from -0.99 to 0.21, where negative values
989 indicate net loss of NO₃⁻ from the snow. Photolysis of snow NO₃⁻ results in a net gain of
990 NO₃⁻ in parts of West Antarctica, such as near the Ronne Ice Shelf where winds
991 converge. The fraction of NO₃⁻ lost from the snow through photolysis is highest on the
992 East Antarctic plateau (up to -0.99). The fraction of NO₃⁻ lost from the snow through
993 photolysis is used to calculate the enrichment in ice-core δ¹⁵N(NO₃⁻) solely from
994 photolysis-driven NO₃⁻ loss in snow. The modeled enrichment in ice-core δ¹⁵N(NO₃⁻)
995 ranges from 0‰ to 363‰ and are in agreement with the broad-scale spatial patterns of
996 observed sub-photoc zone δ¹⁵N(NO₃⁻) observations. A significant relationship exists
997 between nitrogen recycling and photolysis-driven loss of snow NO₃⁻ when NO₃⁻ remains
998 in the photic zone for less than 3 years (τ_z < 3), corresponding to a snow accumulation
999 rate greater than 85 kg m⁻² a⁻¹ in the present day. Since the spatial variability of Antarctic
1000 ice-core δ¹⁵N(NO₃⁻) is mainly determined by the fractional loss of snow NO₃⁻,
1001 observations of δ¹⁵N(NO₃⁻) in snow and ice can be used to estimate both the degree of
1002 recycling and loss of snow NO₃⁻ in Antarctica as long as this condition is met. The
1003 relationship between recycling and loss can be useful for the interpretation of the oxygen
1004 isotopic composition of ice-core NO₃⁻ (e.g., Sofen et al. [2014]). We note that the
1005 relationship between τ_z and snow accumulation rate may vary in different climates
1006 depending on the concentrations of light-absorbing impurities in snow [Geng et al.,
1007 2015].

1008
1009 This is the first modeling study to incorporate snow NO₃⁻ photolysis into a global
1010 chemical transport model to investigate the impacts of a snow-NO_x source on boundary
1011 layer chemistry and nitrogen recycling and redistribution across Antarctica. Model results

Maria Zatko 9/11/15 6:37 PM

Deleted: .

Maria Zatko 10/12/15 12:33 PM

Deleted: downward

Maria Zatko 10/12/15 12:33 PM

Deleted: yr

Maria Zatko 9/12/15 7:48 AM

Deleted: Along the Antarctic coast, the *NRF*_{τ_z} is less than 1, which suggests that ice-core NO₃⁻ is relatively well preserved in coastal regions.

Maria Zatko 10/13/15 9:14 AM

Deleted: -0.21

Maria Zatko 10/13/15 9:14 AM

Deleted: 99

Maria Zatko 10/13/15 9:15 AM

Deleted: gain

Maria Zatko 10/13/15 9:15 AM

Deleted: to

Maria Zatko 10/15/15 10:55 AM

Deleted: with the magnitude

Maria Zatko 10/15/15 10:55 AM

Deleted: and

Maria Zatko 10/15/15 10:55 AM

Deleted: The agreement between observed and modeled δ¹⁵N(NO₃⁻) suggests that its spatial variability across the Antarctic continent is determined by the degree of photolysis-driven loss of snow NO₃⁻.

Maria Zatko 10/14/15 1:06 PM

Deleted: The variability in the spatial patterns of nitrogen recycling and photolysis-driven NO₃⁻ loss in snow are broadly consistent across much of Antarctica, suggesting that ice-core δ¹⁵N(NO₃⁻) measurements can be used to examine the degree of nitrogen recycling in addition to NO₃⁻ loss in most of Antarctica.

1038 shown here are broadly consistent with observations of the flux of NO_x from the
1039 Antarctic snowpack and snow δ¹⁵N(NO₃⁻), suggesting that the model captures the large-
1040 scale features of nitrogen recycling and loss across the Antarctic continent. Model
1041 sensitivity studies suggest that the flux of snow-sourced NO_x and loss of snow NO₃⁻ is
1042 most sensitive to the quantum yield for NO₃⁻ photolysis and the concentration of
1043 photolabile NO₃⁻, which are likely related to one another. We suggest that future field,
1044 laboratory, and modeling studies continue to focus on gaining a better understanding of
1045 the quantum yield for NO₃⁻ photolysis and the concentration of photolabile NO₃⁻.
1046 Updated information about the quantum yield for NO₃⁻ photolysis and the concentration
1047 of photolabile NO₃⁻ in snow along with additional snow photochemical reactions can be
1048 incorporated into this modeling framework in the future, which will continue to improve
1049 our understanding of the impacts of snow photochemistry on boundary layer chemistry
1050 and the preservation of NO₃⁻ and other photochemically-active species in ice cores.

1051

1052 **Acknowledgments**

1053 We acknowledge support from NSF PLR 1244817, NSF PLR 0944537, NSF PLR
1054 1446904, and an EPA STAR graduate fellowship to M.C. Zatko. The authors thank Steve
1055 Warren, Sarah Doherty, Thomas Grenfell, and Quentin Libois for helpful discussions
1056 about light-absorbing impurities in snow and their influence on snow photochemistry. We
1057 thank Joseph Erbland for many helpful comments and discussions about nitrogen
1058 recycling. Joel Thornton and Lyatt Jaeglé also provided many helpful comments about
1059 this work. We also thank Paul Hezel and Yanxu Zhang for helping M.C. Zatko learn
1060 GEOS-Chem. Lastly, we thank Qianjie Chen for helpful feedback on paper drafts and
1061 Martin Schneebeli for providing useful advice about snow grain profiles in Antarctic
1062 snow.

1063

1064 **References**

1065 Allen, D., Pickering, K., Duncan, B., Damon, M.: Impact of lightning NO emissions on
1066 North American photochemistry as determined using the Global Modeling Initiative
1067 (GMI) model. *J. Geophys. Res.*, 115, D22301, doi:10.1029/2010JD014062, 2010.

1068

1069 Alexander, B., Savarino, J., Kreutz, K.J., Thiemens, M.H.: Impact of preindustrial
1070 biomass burning emissions on the oxidation pathways of tropospheric sulphur and
1071 nitrogen. *J. Geophys. Res.*, 109, D08303, doi:10.1029/2003JD004218, 2004.

1072

1073 Amos, H. M., Jacob, D.J., Holmes, C.D, Fisher, J.A, Wang, Q., Yantosca, R.M., Corbitt,
1074 E.S., Galarneau, E., Rutter, A.P., Gustin, M.S., Steffen, A., Schauer, J.J, Graydon, J.A.,
1075 St. Louis, V.L., Talbot, R.W., Edgerton, E.S., Zhang, Y., Sunderland, E.M.: Gas-Particle
1076 Partitioning of Atmospheric Hg(II) and Its Effect on Global Mercury Deposition, *Atmos.*
1077 *Chem. Phys.*, **12**, 591-603, 2012.

1078

1079 Anastasio, C., Galbavy, E. S., Hutterli, M. A., Burkhart, J. F., Friel, D. K.:
1080 Photoformation of hydroxyl radical on snow grains at Summit, Greenland. *Atmos.*
1081 *Environ.*, 41, 5110-5121, doi:10.1016/j.atmosenv.2006.12.011, 2007.

1082

Maria Zatko 10/15/15 10:56 AM

Deleted: impuritie

1084 Anastasio, C. and Chu, L.: Photochemistry of nitrous acid (HONO) and nitrous acidium
1085 ion (H₂ONO⁺) in aqueous solution and ice. *Environ. Sci. Tech.*, 43, 1108-1114, 2009.
1086
1087 Bauguitte, S.J.-B., Bloss, W.J., Evans, M.J., Salmon, R.A., Anderson, P.S., Jones, A.E.,
1088 Lee, J.D., Saiz-Lopez, A., Roscoe, H.K., Wolff, E.W., Plane, J.M.C.: Summertime NO_x
1089 measurements during the CHABLIS campaign: can source and sink estimates unravel
1090 observed diurnal cycles? *Atmos. Chem. Phys.*, 12, 989-1002, doi:10.5194/acp-12-989-
1091 2012, 2012.
1092
1093 Beine, H., Anastasio, C., Esposito, G., Patten, K., Wilkening, E., Domine, F., Voisin, D.,
1094 Barret, M., Houdier, S., Hall, S.: Soluble, light-absorbing species in snow at Barrow,
1095 Alaska. *J. Geophys. Res.*, 116, D00R05, doi: 10.1029/2011JD016181, 2011.
1096
1097 Berhanu, T. A., Meusinger, C., Erbland, J., Jost, R., Bhattacharya, S. K., Johnson, M. S.,
1098 Savarino, J.: Laboratory study of nitrate photolysis in Antarctic snow. II. Isotopic effects
1099 and wavelength dependence. *J. Chem. Phys.*, 140, 244306, doi:10.1063/1.4882899, 2014.
1100
1101 Bertler, N., Mayewski, P. A., Aristarain, A., Barrett, P., Becagli, S., Bernardo, R., Bo, S.,
1102 Xiao, C., Curran, M., Qin, D., Dixon, D., Ferron, F., Fischer, H., Frey, M., Frezzotti, M.,
1103 Fundel, F., Genthon, C., Gragnani, R., Hamilton, G., Handley, M., Hong, S., Isaksson, E.,
1104 Kang, J., Ren, J., Kamiyama, K., Kanamori, S., Karkas, E., Karlof, L., Kaspari, S.,
1105 Kreutz, K., Kurbatov, A., Meyerson, E., Ming, Y., Zhang, M., Motoyama, H., Mulvaney,
1106 R., Oerter, H., Osterberg, E., Proposito, M., Pyne, A., Ruth, U., Simoes, J., Smith, B.,
1107 Sneed, S., Teinila, K., Traufetter, F., Udisti, R., Virkkula, A., Watanabe, O., Williamson,
1108 R., Winther, J-G., Li, Y., Wolff, E., Li, Z., Zielinski, A.: Snow chemistry across
1109 Antarctica, *Annals of Glaciology*, 41(1), 167- 179, 2005.
1110
1111 Bey, I., Jacob, D.J., Yantosca, R.M., Logan, J.A., Field, B.D., Fiore, A.M., Li, Q., Liu,
1112 H.Y., Mickley, L.J., Schultz, M.G.: Global modeling of tropospheric chemistry with
1113 assimilated meteorology: Model description and evaluation, *J. Geophys. Res.*, 106(D19),
1114 23073-23095, 2001.
1115
1116 Bian, H.S., Prather, M.J.: Fast-J2: Accurate simulation of stratospheric photolysis in
1117 global chemical models. *J. Atmos. Chem.*, 41, 281-296, 2002.
1118
1119 Bisiaux, M. M., Edwards, R., McConnell, J. R., Curran, M. A. J., Van Ommen, T. D.,
1120 Smith, A. M., Neumann, T. A., Pasteris, D. R., Penner, J. E., Taylor, K.: Changes in
1121 black carbon deposition to Antarctica from two high-resolution ice core records, 1850-
1122 2000 AD. *Atmos. Chem. Phys.*, 12, 4107-4115, doi: 10.5194/acp-12-4107-2012, 2012.
1123
1124 Bloss, W.J., Lee, J.D., Heard, D.E., Salmon, R.A., Bauguitte, S.J.-B., Roscoe, H.K.,
1125 Jones, A.E.: Observations of OH and HO₂ radicals in coastal Antarctica. *Atmos. Chem.*
1126 *Phys.*, 7, 4171-4185, 2007.
1127

1128 Boxe, C.S., Colussi, A.J., Hoffmann, M.R., Murphy, J.G., Wollodridge, P.J., Bertram,
1129 T.H., Cohen, R.C.: Photochemical production and release of gaseous NO₂ from nitrate-
1130 doped water ice. *J. Phys. Chem., A*, 109, 8520-8525, 2005.
1131
1132 [Boxe, C.S., Saiz-Lopez, A.: Multiphase modeling of nitrate photochemistry in the quasi-
1133 liquid layer \(QLL\): implications for NO_x release from the Arctic and coastal Antarctic
1134 snowpack. *Atmos. Chem. Phys.*, 8, 4855-4864, 2008.](#)
1135
1136 Blunier, T., Gregoire, F. L., Jacobi, H.-W., and Quansah, E.: Isotopic view on nitrate loss
1137 in Antarctic surface snow. *Geophys. Res. Lett.*, 32, L13501, doi:10.1029/2005GL023011,
1138 2005.
1139
1140 Casasanta, G., Pietroni, I., Petenko, I., Argentini, S.: Observed and modelled convective
1141 mixing-layer height in Dome C, Antarctica. *Boundary-Layer Meteorol.*, 151, 597-608,
1142 doi:10.1007/s10546-014-9907-5, 2014.
1143
1144 Chen, G., Davis, D., Crawford, J., Hutterli, L.M., Huey, L.G., Slusher, D., Mauldin, L.,
1145 Eisele, F., Tanner, D., Dibb, J., Buhr, M., McConnell, J., Lefer, B., Shetter, R., Blake, D.,
1146 Song, C.H., Lombardi, K., Arnoldy, J.: A reassessment of HO_x South Pole chemistry
1147 based on observations recorded during ISCAT 2000. *Atmos. Environ.*, 38, 5451-5461,
1148 2004.
1149
1150 Chu, L., and Anastasio, C.: Quantum Yields of Hydroxyl Radicals and Nitrogen Dioxide
1151 from the Photolysis of Nitrate on Ice. *J. Phys. Chem. A.*, 107, 9594-9602, 2003.
1152
1153 Cho, H., Shepson, P.B., Barrie, L.A., Cowin, J.P., Zaveri, R.: NMR Investigation of the
1154 Quasi-Brine Layer in Ice/Brine Mixtures. *J. Phys. Chem. B.*, 106, 11226-11232, 2002.
1155
1156 Chylek, P., Johnson, B., Wu, H.: Black carbon concentration in Byrd station ice core –
1157 From 13,000 to 700 years before present. *Ann. Geophys.*, 10, 625-629, 1992.
1158
1159 Davis, D., Chen, G., Buhr, M., Crawford, J., Lenschow, D., Lefer, B., Shetter, R., Eisele,
1160 F., Mauldin, L., Hogan, A.: South Pole NO_x Chemistry: an assessment of factors
1161 controlling variability and absolute levels. *Atmos. Environ.*, 38, 5375-5388, 2004.
1162
1163 Davis, D. D., Seelig, J., Huey, G., Crawford, J., Chen, G., Wang, Y., Buhr, M., Helmig,
1164 D., Neff, W., Blake, D., Arimoto, R., Eisele, F.: A reassessment of Antarctic plateau
1165 reactive nitrogen based on ANTCI 2003 airborne and ground based measurements.
1166 *Atmos. Environ.*, 42, 2831-2848, doi:10.1016/j.atmosenv.2007.07.039, 2008.
1167
1168 Dibb, J. E., Huey, G. L., Slusher, D. L., and Tanner, D. J.: Soluble reactive nitrogen
1169 oxides at South Pole during ISCAT 2000. *Atmos. Environ.*, 38, 5399-5409, 2004.
1170
1171 Doherty, S. J., Warren, S. G., Grenfell, T. C., Clarke, A. D., and Brandt, R. E.: Light-
1172 absorbing impurities in Arctic snow. *Atmos. Chem. Phys.*, 10, 11647-11680,
1173 doi:10.5194/acp-10-11647-2010, 2010.

1174
1175 Doherty, S. J., Grenfell, T.C., Forsstrom, S., Hegg, D.L., Brandt, R.E., Warren, S.G.:
1176 Observed vertical redistribution of black carbon and other insoluble light-absorbing
1177 particles in melting snow, *J. Geophys. Res. Atmos.*, 118, 1-17, doi:10.1002/jgrd.50235,
1178 2013.
1179
1180 Domine, F., Shepson, P. B.: Air-snow interactions and atmospheric chemistry, *Science*,
1181 297, 1506–1510, 2002.
1182
1183 Domine, F., Bock, J., Voisin, D., Donaldson, D. J.: Can we model snow photochemistry?
1184 Problems with the current approaches. *J. Phys. Chem. A*, 117, 4733-4749, doi:
1185 10.1021/jp3123314 2013.
1186
1187 Erbland, J., Vicars, W.C., Savarino, J., Morin, S., Frey, M.M., Frosini, D., Vince, E.,
1188 Martins, J.M.F.: Air-snow transfer of nitrate on the East Antarctic Plateau – Part 1:
1189 Isotopic evidence for a photolytically driven dynamic equilibrium in summer. *Atmos.*
1190 *Chem. Phys.*, 13, 6403-6419, doi:10.5194/acp-13-6403-2013, 2013.
1191
1192 Erbland, J., Savarino, J., Morin, S., France, J.L., Frey, M.M., King, M.D.: Air-snow
1193 transfer of nitrate on the East Antarctic plateau – Part 2: An isotopic model for the
1194 interpretation of deep ice-core records. *Atmos. Chem. Phys. Discuss.*, 15,6886-6966,
1195 doi:10.5194/acpd-15-6887-2015, 2015.
1196
1197 [Fegyveresi, J.M., Alley, R.B., Spencer, M.K., Fitzpatrick, J.J., Steig, E.J., White, J.W.C.,](#)
1198 [McConnell, J.R., Taylor, K.C.: Late-Holocene climate evolution at the WAIS Divide site,](#)
1199 [West Antarctica: bubble number-density estimates. *J. Glaciol.*, 57, 204, 2011.](#)
1200
1201 Fisher, J.A., Jacob, D.J., Wang, Q., Bahreini, R., Carouge, C.C., Cubison, M.J., Dibb,
1202 J.E., Diehl, T., Jimenez, J.L., Leibensperger, E.M., Meinders, M.B.T., Pye, H.O.T.,
1203 Quinn, P.K., Sharma, S., van Donkelaar, A., Yantosca, R.M.: Sources, distribution, and
1204 acidity of sulfate-ammonium aerosol in the Arctic in winter-spring, *Atmos. Environ.*, 45,
1205 7301-7318, 2011.
1206
1207 [France, J.L., King, M.D., Frey, M.M., Erbland, J., Picard, G., Preunkert, S., MacArthur,](#)
1208 [A., Savarino, J.: Snow optical properties at Dome C \(Concordia\), Antarctica; implications](#)
1209 [for snow emissions and snow chemistry of reactive nitrogen. *Atmos. Chem. Phys.*, 11,](#)
1210 [9787-9801, doi:10.5194/acp-11-9787-2011, 2011.](#)
1211
1212 Frey, M. M., Savarino, J., Morin, S., Erbland, J., and Martins, J. M. F.: Photolysis imprint
1213 in the nitrate stable isotope signal in snow and atmosphere of East Antarctica and
1214 implications for reactive nitrogen cycling. *Atmos. Chem. Phys.*, 9, 8681-8696, 2009.
1215
1216 Frey, M. M., Brough, N., France, J. L., Anderson, P.S., Traulle, O., King, M.D., Jones,
1217 A.E., Wolff, E.W., Savarino, J.: The diurnal variability of atmospheric nitrogen oxides
1218 (NO and NO₂) above the Antarctic Plateau driven by atmospheric stability and snow
1219 emissions. *Atmos. Chem. Phys.*, 13, 3045-3062, doi:10.5194/acp-13-3045-2013, 2013.

1220
1221 Freyer, H. D., Kley, D., Voiz-Thomas, A., Kobel, K.: On the interaction of isotopic
1222 exchange processes with photochemical reactions in atmospheric oxides of nitrogen. *J.*
1223 *Geophys. Res. Atmos.*, 98(D8), 14791-14796, 1993.
1224
1225 Gallet, J.-C., Domine, F., Arnaud, L., Picard, G., and Savarino, J.: Vertical profiles of the
1226 specific surface area and density of the snow at Dome C and on a transect to Dumont
1227 D'Urville, Antarctica – albedo calculations and comparison to remote sensing products.
1228 *The Cryosphere.*, 5, 631-649, doi: 10.5194/tc-5-631-2011, 2011.
1229
1230 Geng, L., Alexander, B., Cole-Dai, J., Steig, E.J., Savarino, J., Sofen, E.D., Schauer, A.J.:
1231 Nitrogen isotopes in ice core nitrate linked to anthropogenic atmospheric acidity change.
1232 *Proc. Natl. Acad. Sci.*, 111, 16, 5808-5812, doi:10.1073/pnas.1319441111, 2014a.
1233
1234 Geng, L., Cole-Dai, J., Alexander, B., Erbland, J., Savarino, J., Schauer, A. J., Steig, E.J.,
1235 Lin, P., Fu, Q., Zatzko, M.C.: On the origin of the occasional springtime nitrate
1236 concentration maximum in Greenland. *Snow. Atmos. Chem. Phys.*, 14, 13361-13376,
1237 doi:10.5194/acp-14-13361-2014, 2014b.

1238 [Geng, L., Zatzko, M.C., Alexander, B., Fudge, T.J., Schauer, A.J., Murray, L.T., Mickley,](#)
1239 [L.J.: Effects of post-depositional processing on nitrogen isotopes of nitrate in the](#)
1240 [Greenland Ice Sheet Project 2 \(GISP2\) ice core. *Geophys. Res. Lett.*,](#)
1241 [doi:10.1002/2015GL064218, 2015.](#)

1242 Grannas, A. M., Jones, A. E., Dibb, J., Ammann, M., Anastasio, C., Beine, H. J., Bergin,
1243 M., Bottenheim, J., Boxe, C. S., Carver, G., Chen, G., Crawford, J. H., Domine, F., Frey,
1244 M. M., Guzman, M. I., Heard, D. E., Helmig, D., Hoffman, M. R., Honrath, R. E., Huey,
1245 L. G., Hutterli, M., Jacobi, H. W., Klan, P., Lefer, B., McConnell, J., Plane, J., Sander,
1246 R., Savarino, J., Shepson, P. B., Simpson, W. R., Sodeau, J. R., von Glasow, R., Weller,
1247 R., Wolff, E. W., Zhu, T.: An overview of snow photochemistry: evidence, mechanisms
1248 and impacts. *Atmos. Chem. Phys.*, 7, 4329-4373, 2007.
1249
1250 Grenfell, T. C.: A Radiative Transfer Model for Sea Ice With Vertical Structure
1251 Variations. *J. Geophys. Res.*, 96, 16991-17001, 1991.
1252
1253 Grenfell, T.C., Warren, S.G, Mullen, P.C.: Reflection of solar radiation by the Antarctic
1254 snow surface at ultraviolet, visible, and near-infrared wavelengths. *J. Geophys. Res.*, 99,
1255 18669-18684, 1994.
1256
1257 Handorf, D., Foken, T., Kottmeier, C.: The stable atmospheric boundary layer over an
1258 Antarctic ice sheet. *Boundary-Layer Meteorol.*, 91, 165-189, 1999.
1259
1260 Hastings, M.G., Sigman, D.M., Steig, E.J.: Glacial/interglacial changes in the isotopes of
1261 nitrate from the Greenland Ice Sheet Project (GISP2) ice core. *Global Biogeochem.*
1262 *Cycles*, 19:GB4024, doi:10.1029/2005GB002502, 2005.
1263

1264 Heaton, T. H. E., Spiro, B., Robertson, M. C. S.: Potential canopy influences on the
1265 isotopic composition of nitrogen and sulphur in atmospheric deposition. *Oecologia*, 109,
1266 4, 600-607, 1997.
1267
1268 Helmig, D., Johnson, B., Oltmans, S.J., Neff, W., Eisele, F., Davis, D.: Elevated ozone in
1269 the boundary layer at South Pole. *Atmos. Environ.*, 42, 2788-2803, 2008.
1270
1271 Holtslag, A.A.M., Boville, B.: Local versus nonlocal boundary layer diffusion in a global
1272 climate model. *J. Clim.*, 6, 1825-1842, 1993.
1273
1274 Hudman, R.C., N.E. Moore, R.V. Martin, A.R. Russell, A.K. Mebust, L.C. Valin, and
1275 R.C. Cohen, A mechanistic model of global soil nitric oxide emissions: implementation
1276 and space based-constraints, *Atmos. Chem. Phys.*, 12, 7779-7795, doi:10.5194/acp-12-
1277 7779-2012, 2012.
1278
1279 Jarvis, J. C.: Isotopic studies of ice core nitrate and atmospheric nitrogen oxides in polar
1280 regions. Ph.D. Thesis, University of Washington, publication number 3328411, 2008.
1281
1282 [Jin, Z., Charlock, T.P., Yang, P., Xie, Y., Miller, W.: Snow optical properties for](#)
1283 [different particle shapes with application to snow grain size retrieval and MODIS/CERES](#)
1284 [radiance comparison over Antarctica. *Remote. Sens. Environ.*, 112, 3563-3581, 2008.](#)
1285
1286 Jones, A., Weller, R., Anderson, P., Jacobi, H., Wolff, E., Schrems, O., Miller, H.:
1287 Measurements of NO_x emissions from the Antarctic snowpack. *Geophys. Res. Lett.*, 28,
1288 1499-1502, doi: 10.1029/2000GL011956, 2001.
1289
1290 Jones, A.E., Anderson, P.S., Wolff, E.W., Turner, J., Rankin, A.M., Colwell, S.R.: A role
1291 for newly forming sea ice in springtime polar tropospheric ozone loss? Observational
1292 evidence from Halley station, Antarctica. *J. Geophys. Res.*, 111, D08306,
1293 doi:10.1029/2005JD006566, 2006.
1294
1295 Jones, A.E., Wolff, E.W., Salmon, R.A., Bauguitte, S.J.-B., Roscoe, H.K., Anderson,
1296 P.S., Ames, D., Clemitshaw, K.C., Fleming, Z.L., Bloss, W.J., Heard, D.E., Lee, J.D.,
1297 Read, A.K., Hamer, P., Shallcross, D.E., Jackson, A.V., Walker, S.L., Lewis, A.C.,
1298 Mills, G.P., Plane, J.M.C., Saiz-Lopez, A., Sturges, W.T., Worton, D.R.: Chemistry of
1299 the Antarctic Boundary Layer and the Interface with Snow: an overview of the
1300 CHABLIS campaign. *Atmos. Chem. Phys.*, 8, 3789-3803, 2008.
1301
1302 Jones, A.E., Wolff, E.W., Ames, D., Bauguitte, S. J.-B., Clemitshaw, K.C., Fleming, Z.,
1303 Mills, G.P., Saiz-Lopez, A., Salmon, R.A., Sturges, W.T., Worton, D.R.: The multi-
1304 seasonal NO_y budget in coastal Antarctica and its link with surface snow and ice core
1305 nitrate: results from the CHABLIS campaign. *Atmos. Chem. Phys.*, 11, 9271-9285,
1306 doi:10.5194/acp-11-9271, 2011, 2011.
1307

1308 King, J.C., Argentini, S.A., Anderson, P.S.: Contrasts between the summertime surface
1309 energy balance and boundary layer structure at Dome C and Halley stations, Antarctica.
1310 *J. Geophys. Res.*, 111, D02105, doi:10.1029/2005JD006130, 2006.
1311
1312 Klein, K.: Variability in dry Antarctic firn; Investigations on spatially distributed snow
1313 and firn samples from Dronning Maud Land, Antarctica. Ph.D. Thesis, Universitat
1314 Bremen. hdl: 10013/epic.44893. <http://nbn-resolving.de/urn:nbn:de:gbv:46-00104117-15>,
1315 date last access: April 15, 2014.
1316
1317 Kodama, Y., Wendler, G., Ishikawa, N.: The diurnal variation of the boundary layer in
1318 summer in Adelie Land, Eastern Antarctica. *J. Appl. Met.*, 28, 16-24, 1989.
1319
1320 Konig-Langlo, G., King, J., Petre, P., Climatology of the three coastal Antarctic stations
1321 Durmont D'urville, Neumayer, and Halley. *J. Geophys. Res.*, D9, 103, 10935-10946,
1322 1998.
1323
1324 Lee, H., Henze, D.K., Alexander, B., Murray, L.T.: Investigating the sensitivity of
1325 surface-level nitrate seasonality in Antarctica to primary sources using a global model.
1326 *Atmos. Environ.*, 89, 757-767, doi:10.1016/j.atmosenv.2014.03.003, 2014.
1327
1328 [Legrand, M.R., Kirchner, S.: Origins and variations of nitrate in South Polar](#)
1329 [precipitation. *J. Geophys. Res.*, 95, 3493-3507, 1990.](#)
1330
1331 Levy, H., Moxim, W.J., Klonecki, A.A., Kasibhatla, P.S.: Simulated tropospheric NOx:
1332 Its evaluation, global distribution and individual source contributions. *J. Geophys. Res.*,
1333 104, 26279-26306, 1999.
1334
1335 Libois, Q., Picard, G., France, J. L., Arnaud, L., Dumont, M., Carmagnola, C. M., King,
1336 M. D.: Grain shape influence on light extinction in snow. *The Cyrosphere*, 7, 1803-1818,
1337 doi:10.5194/tc-7-1803-2013, 2013.
1338
1339 [Lin, S.J., Rood, R.B.: Multidimensional flux form semi-Lagrangian transport schemes.](#)
1340 [*Mon. Wea. Rev.*, 124, 2046-2070, 1996.](#)
1341
1342 Lin, J. T., McElroy, M.B.: Impacts of boundary layer mixing on pollutant vertical profiles
1343 in the lower troposphere: Implications to satellite remote sensing. *Atmos. Environ.*, 44,
1344 1726-1749, doi:10.1016/j.atmosenv.2010.02.009, 2010.
1345 Liu, H., Jacob, D.J., Bey, I., Yantosca, R.M.: Constraints from ²¹⁰Pb and ⁷Be on wet
1346 deposition and transport in a global three-dimensional chemical tracer model driven by
1347 assimilated meteorological fields, *J. Geophys. Res.*, 106(D11), 12,109-112,128, 2001.
1348 Logan, J.A., Nitrogen oxides in the troposphere: Global and regional budgets. *J.*
1349 *Geophys. Res.*, 88(C15), 10785-10807, doi:10.1029/JC088iC15p10785, 1983.
1350
1351 Mack, J., and Bolton, J. R.: Photochemistry of nitrite and nitrate in aqueous solution: A
1352 review. *J. Photochem. Photobiol. A.*, 128, 1-13, 1999.
1353

1354 Mao, J., Jacob, D.J., Evans, M.J., Olson, J.R., Ren, X., Brune, W.H., St. Clair, J.M.,
1355 Crounse, J. D., Spencer, K.M., Beaver, M.R., Wennberg, P.O., Cubison, M.J., Jimenez,
1356 J.L., Fried, A., Weibring, P., Walega, J.G., Hall, S.R., Weinheimer, A.J., Cohen, R.C.,
1357 Chen, G., Crawford, J.H., Jaegle, L., Fisher, J.A., Yantosca, R.M., Le Sager, P., Carouge,
1358 C.: Chemistry of hydrogen oxide radicals (HO_x) in the Arctic troposphere in spring.
1359 *Atmos. Chem. Phys.*, 10, 5823-5838, doi:10.5194/acp-10-5823-2010, 2010.
1360
1361 Masclin, S., Frey, M. M., Rogge, W. F., Bales, R. C.: Atmospheric nitric oxide and ozone
1362 at the WAIS Divide deep coring site: a discussion of local sources and transport in West
1363 Antarctica. *Atmos. Chem. Phys.*, 13, 8857-8877, doi:10.5194/acp-13-8857-2013, 2013.
1364
1365 Mayewski, P. A., and Legrand, M. R.: Recent increase in nitrate concentration of
1366 Antarctic snow. *Nature*, 346, 258-260, 1990.
1367
1368 Meusinger, C., Berhanu, T.A., Erbland, J., Savarino, J., Johnson, M.S.: Laboratory study
1369 of nitrate photolysis in Antarctic snow. I. Observed quantum yield, domain of photolysis,
1370 and secondary chemistry. *J. Chem. Phys.*, 140, 244305, doi:10.1063/1.4882898, 2014.
1371
1372 Morin, S., Savarino, J., Frey, M.M., Domine, F., Jacobi, H.-W., Kaleschke, L., Martins,
1373 J.M.F.: Comprehensive isotopic composition of atmospheric nitrate in the Atlantic Ocean
1374 boundary layer from 65°S to 79°N. *J. Geophys. Res.*, 114, D05303,
1375 doi:10.1029/2008JD010696, 2009.
1376
1377 Mulvaney, R., Wagenbach, D., Wolff, E.W.: Postdepositional change in snowpack nitrate
1378 from observation of year-round near-surface snow in coastal Antarctica. *J. Geophys. Res.*,
1379 103, 11021-11031, 1998.
1380
1381 Murray, L.T., Jacob, D.J., Logan, J.A., Hudman, R.C., Koshak, W.J.: Optimized regional
1382 and interannual variability of lightning in a global chemical transport model constrained
1383 by LIS/OTD satellite data, *J. Geophys. Res.*, 117, D20307, 2012.
1384 Neff, W., Helmig, D., Grachev, A., Davis, D.: A study of boundary layer behaviour
1385 associated with high concentrations at the South Pole using a minisoder, tethered balloon,
1386 and a sonic anemometer. *Atmos. Environ.*, 42, 2762-2779, doi:10.1029/2012JD017934,
1387 2008.
1388
1389 Oliver, J.G.J., Van Aardenne, J.A., Dentener, F.J., Pagliari, V., Ganzeveld, L.N., Peters,
1390 J.A.H.W.: Recent trends in global greenhouse gas emissions: regional trends 1970-2000
1391 and spatial distribution of key sources in 2000. *Env. Sci.*, 2(2-3), 81-99,
1392 doi:10.1080/15693430500400345, 2005.
1393
1394 Oncley, S., Buhr, M., Lenschow, D., Davis, D., Semmer, S.: Observations of summertime
1395 NO fluxes and boundary-layer height at the South Pole during ISCAT 2000 using scalar
1396 similarity. *Atmos. Environ.*, 38, 5389-5398, doi:10.1016/j.atmosenv.2004.05.053, 2004.
1397

1398 Parish, T. R., and D. H. Bromwich (2007), Reexamination of the near-surface airflow
1399 over the Antarctic continent and implications on atmospheric circulations at high
1400 southern latitudes, *Monthly Weather Review*, 135, 1961-1973.
1401
1402 Parrella, J.P., Jacob, D.J., Liang, Q., Zhang, Y., Mickley, L.J., Miller, B., Evans, M.J.,
1403 Yang, X., Pyle, J.A., Theys, N., Van Roozendael, M.: Tropospheric bromine chemistry:
1404 implications for present and pre-industrial ozone and mercury. *Atmos. Chem. Phys.*, 12,
1405 6723-6740, doi:10.5194/acp-12-6723-2012, 2012.
1406
1407 Pratt, K. A., Custard, K. D., Shepson, P. B., Douglas, T. A., Pohler, D., General, S.,
1408 Zielcke, J., Simpson, W. R., Platt, U., Tanner, D. J., Huey, L. G., Carlsen, M., Stirm, B.
1409 H.: Photochemical production of molecular bromine in Arctic surface snowpacks.
1410 *Nature*, 6, 351-356, doi:10.1038/NGEO1779, 2013.
1411
1412 Price, C., Rind, D.: A simple lightning parameterization for calculating global lightning
1413 distributions. *J. Geophys. Res.*, 97, 9919-9933, 1992.
1414
1415 Rothlisberger, R., Hutterli, M. A., Sommer, S., Wolff, E. W., and Mulvaney, R.: Factors
1416 controlling nitrate in ice cores: Evidence from the Dome C deep ice core. *J. Geophys.*
1417 *Res.*, 105, 20565-20572, 2000.
1418
1419 Sander, S. P., Friedl, R.R., Golden, D.M., Kurylo, M.J., Moortgat, G.K., Keller-Rudek,
1420 H., Wine, P.J., Ravishankara, A.R., Kolb, C.E., Molina, M.J., Finalyson-Pitts, B.J., Huie,
1421 R.E., Orkin, V.L.: Chemical kinetics and photochemical data for use in atmospheric
1422 studies evaluation number 15. JPL Publications, Pasadena, 1-523, 06-2, 2006.
1423
1424 Savarino, J., Kaiser, J., Morin, S., Sigman, D.M., Thiemens, M.H.: Nitrogen and oxygen
1425 isotopic constraints on the origin of atmospheric nitrate in coastal Antarctica. *Atmos.*
1426 *Chem. Phys.*, 7, 1925-1945, 2007.
1427
1428 Simpson, W. R., von Glasow, R., Riedel, K., Anderson, P., Ariya, P., Bottenheim, J.,
1429 Burrows, J., Carpenter, L. J., Friess, U., Goodsite, M. E., Heard, D., Hutterli, M., Jacobi,
1430 H.-W., Kaleschke, L., Neff, B., Plane, J., Platt, U., Richter, A., Roscoe, H., Sander, R.,
1431 Shepson, P., Sodeau, J., Steffen, A., Wagner, T., Wolff, E.: Halogens and their role in
1432 polar boundary-layer ozone depletion. *Atmos. Chem. Phys.*, 7(16):4375-4418, 2007.
1433
1434 Slusher, D. L., Huey, L. G., Tanner, D. J., Chen, G., Davis, D. D., Buhr, M., Nowak, J.
1435 B., Eisele, F. L., Kosciuch, E., Mauldin, R. L., Lefer, B. L., Shetter, R. E., Dibb, J. E.:
1436 Measurements of pernitric acid at the South Pole during ISCAT 2000. *Geophys. Res.*
1437 *Lett.*, 29, 21, doi:10.1029/2002GL015703, 2002.
1438
1439 Shi, G., Buffen, A.M., Hastings, M.G., Li, C., Ma, H., Li, Y., Sun, B., An, C., Jiang, S.:
1440 Investigation of post-depositional processing of nitrate in East Antarctica snow: isotopic
1441 constraints on photolytic loss, re-oxidation, and source inputs. *Atmos. Chem. Phys.*
1442 *Discuss.*, 14, 31943-31986, doi: 10.5194/acpd-14-31943-2014, 2014.
1443

1444 Sjostedt, S.J., Huey, L.G., Tanner, D.J., Peischl, J., Chen, G., Dibb, J.E., Lefer, B.,
1445 Hutterli, M.A., Beyersdorf, A.J., Blake, N.J., Blake, D.R., Sueper, D., Ryerson, T.,
1446 Burkhardt, J., Stohl, A.: Observations of hydroxyl and the sum of peroxy radicals at
1447 Summit, Greenland during summer 2003. *Atmos. Environ.*, 41, 5122-5137, 2007.
1448
1449 Sofen, E.D., Alexander, B., Steig, E.J., Thiemens, M.H., Kunasek, S.A., Amos, H.M.,
1450 Schauer, A.J., Hastings, M.G., Bautista, J., Jackson, T.L., Vogel, L.E., McConnell, J.R.,
1451 Pasteris, D.R., Saltzman, E.S.: WAIS Divide ice core suggests sustained changes in the
1452 atmospheric formation pathways of sulfate and nitrate since the 19th century in the
1453 extratropical Southern Hemisphere. *Atmos. Chem. Phys.*, 14, 5749-5769,
1454 doi:10.5194/acp-14-5749-2014, 2014.
1455
1456 Thomas, J. L., Dibb, J. E., Huey, L. G., Liao, J., Tanner, D., Lefer, B., von Glasow, R.,
1457 Stutz, J.: Modeling chemistry in and above snow at Summit, Greenland – Part 2: Impact
1458 of snowpack chemistry on the oxidation capacity of the boundary layer. *Atmos. Chem.*
1459 *Phys.*, 12, 6537-6554, doi:10.5194/acp-12-6537-2012, 2012.
1460
1461 Thompson, A.M., The oxidizing capacity of the Earth's atmosphere: Probable past and
1462 future changes. *Science*, 256, 1157-1165, 1992.
1463
1464 Travouillon, T., Ashley, M.C.B., Burton, M.G., Storey, J.W.V., Loewenstein, R.F.:
1465 Atmospheric turbulence at the South Pole and its implications for astronomy. *Astronom.*
1466 *And Astrophys.*, 400, 1163-1172, doi:10.1051/0004-6361:20021814, 2003.
1467
1468 UNEP/WMO. Integrated Assessment of Black Carbon and Tropospheric Ozone:
1469 Summary for Decision Makers, UNON/Publishing Services Section/Nairobi, ISO
1470 14001:2004, 2011.
1471
1472 van Donkelaar, A., R. V. Martin, W. R. Leitch, A.M. Macdonald, T. W. Walker, D. G.
1473 Streets, Q. Zhang, E. J. Dunlea, J. L. Jimenez, J. E. Dibb, L. G. Huey, R. Weber, and M.
1474 O. Andreae. Analysis of Aircraft and Satellite Measurements from the Intercontinental
1475 Chemical Transport Experiment (INTEX-B) to Quantify Long-Range Transport of East
1476 Asian Sulfur to Canada. *Atmos. Chem. Phys.*, 8, 2999-3014, 2008.
1477
1478 van der Werf, G.R., Morton, D.C., DeFries, R.S., Giglio, L., Randerson, J.T., Collatz,
1479 G.J., Kasibhatla, P.S.: Estimates of fire emissions from an active deforestation region in
1480 the southern Amazon based on satellite data and biogeochemical
1481 modeling. *Biogeosciences*, 6 (2):235-249, 2009.
1482
1483 [Wagenbach, D., Legrand, M., Fischer, H., Pichlmayer, F., Wolff, E.W.: Atmospheric](#)
1484 [near-surface nitrate at coastal Antarctic sites. *J. Geophys. Res.*, 103, 11007-11020, 1998.](#)
1485
1486 Wang, Y. H., Jacob, D.J., Logan, J.A.: Global simulation of tropospheric O₃-NO_x
1487 hydrocarbon chemistry 1. Model formulation, *J. Geophys. Res.*, 103, 7113-7107, 25,
1488 1998.
1489

1490 Wang, Y., Choi, Y., Zeng, T., Davis, D., Buhr, M., Huey, G. L., and Neff, W.: Assessing
1491 the photochemical impact of snow NO_x emissions over Antarctica during ANTCI 2003.
1492 *Atmos. Environ.*, 41, 3944-3958, doi:10.1016/j.atmosenv.2007.01.056, 2008.
1493
1494 Wang, Q., Jacob, D.J., Fisher, J.A., Mao, J., Leibensperger, E.M., Carouge, C.C., Le
1495 Sager, P., Kondo, Y., Jimenez, J. L., Cubison, M. J., Doherty, S.: Sources of
1496 carbonaceous aerosols and deposited black carbon in the Arctic in winter-spring:
1497 implications for radiative forcing. *Atmos. Chem. Phys.*, 11, 12453-12473,
1498 doi:10.5194/acp-11-12453-2011, 2011.
1499
1500 Warren, S.G., Clarke, A.D.: Soot in the atmosphere and snow surface of Antarctica. *J.*
1501 *Geophys. Res.*, 95, 1811-1816, 1990.
1502
1503 Warren, S. G., Brandt, R. E., and Grenfell, T. C.: Visible and near-ultraviolet absorption
1504 spectrum of ice from transmission of solar radiation into snow. *Appl. Opt.*, 45, 5320-
1505 5334, 2006.
1506
1507 Weller, R., Minikin, A., Konig-Langlo, G., Schrems, O., Jones, A.E., Wolff, E.W.,
1508 Anderson, P.S.: Investigating possible causes of the observed diurnal variability in
1509 Antarctica NO_y. *Geophys. Res. Lett.*, 26, 18, 2853-2856, 1999.
1510
1511 Wesely, M. L.: Parameterization of surface resistances to gaseous dry deposition in
1512 regional-scale numerical-models, *Atmos. Env.*, 23, 1293-130, 1989.
1513
1514 Wild, O., Q. Zhu, and M. J. Prather (2000), Fast-J: Accurate simulation of in- and below-
1515 cloud photolysis in global chemical models, *J. Atm. Chem.*, 37, 245-282.
1516
1517 Wolff, E.W.: Nitrate in polar ice, in *Ice Core Studies of Global Biogeochem. Cycles*,
1518 NATO ASI Ser., Ser. I, pp. 195-224, edited by R.J. Delmas, Springer, New York, 1995.
1519
1520 Wolff, E.W., Jones, A.E., Bauguitte, S. J.-B., Salmon, R.A.: The interpretation of spikes
1521 and trends in concentration of nitrate in polar ice cores, based on evidence from snow and
1522 atmospheric measurements. *Atmos. Chem. Phys.*, 8, 5627-5634, 2008.
1523
1524 [Xu, L., Penner, J.E.: Global simulations of nitrate and ammonium aerosols and their](#)
1525 [radiative effects. *Atmos. Chem. Phys.*, 12, 9479-9504, doi:10.5194/acp-12-9479-2012,](#)
1526 [2012.](#)
1527
1528 Zatzko, M.C., Grenfell, T.C., Alexander, B., Doherty, S.J., Thomas, J.L., Yang, X., The
1529 influence of snow grain size and impurities on the vertical profiles of actinic flux and
1530 associated NO_x emissions on the Antarctic and Greenland ice sheets. *Atmos. Chem.*
1531 *Phys.*, 13, 3547-3567, doi:10.5194/acp-13-3547-2013, 2013.
1532
1533 Zatzko, M.C. and Warren, S.G.: East Antarctic sea ice in spring: spectral albedo of snow,
1534 nilas, frost flowers, and slush; and light-absorbing impurities in snow. *Ann. Glaciol.*

1535 *Special Issue: Sea ice in a changing environment*, 56(69), 53-64,
1536 doi:10.3189/2015AoG69A574, 2015.
1537
1538 Zhang, L., S. Gong, J. Padro, and L. Barrie.: A size-segregated particle dry deposition
1539 scheme for an atmospheric aerosol module, *Atmos. Env.*, 35, 549-560, 2001.
1540
1541 Zhu, C., Xiang, B., Chu, L.T., Zhu, L.: 308 nm Photolysis of Nitric Acid in the Gas
1542 Phase, on Aluminum Surfaces, and on Ice Films. *J. Phys. Chem. A.*, 114, 2561-2568, doi:
1543 10.1021/jp909867a, 2010.
1544
1545
1546
1547
1548
1549
1550
1551
1552
1553
1554
1555
1556
1557
1558
1559
1560
1561
1562
1563
1564
1565
1566
1567
1568
1569
1570
1571
1572
1573
1574
1575
1576
1577
1578
1579
1580

1581 | Table 1. Glossary of variables used in this paper.

Variable	Unit	Description
λ	nm	Wavelength
ϕ	molec photon ⁻¹	Quantum yield for NO ₃ ⁻ photolysis
$\sigma_{NO_3^-}$	cm ²	Absorption cross-section for NO ₃ ⁻ photolysis
I	photons cm ⁻² s ⁻¹ nm ⁻¹	Actinic flux of UV radiation
z_e	cm	e-folding depth of UV actinic flux in snow
z_{3e}	cm	Depth of snow photic zone
α_r	kg m ⁻² yr ⁻¹	Total annual snow accumulation rate
C_{BC}	ng g ⁻¹	Annual mean snow black carbon concentration
r_e	μm	Radiation equivalent mean ice grain radii
$K_{ext_{tot}}$	cm ⁻¹	Bulk extinction coefficient for snow
$[NO_3^-]_{top}$	ng g ⁻¹	Mean NO ₃ ⁻ concentration in top 2 cm of snow
$[NO_3^-]_{bot}$	ng g ⁻¹	Mean NO ₃ ⁻ concentration from 2-cm depth to the bottom of the snow photic zone
EF	unitless	NO ₃ ⁻ enhancement factor in top 2 cm of snow
F_p	fraction	Fraction of photolabile NO ₃ ⁻ in snow
$\Delta^{17}O(NO_3^-)$	‰	Oxygen isotopic composition of NO ₃ ⁻
$\delta^{15}N(NO_3^-)$	‰	Nitrogen isotopic composition of NO ₃ ⁻
ϵ	‰	Fractionation constant for NO ₃ ⁻ photolysis
$\overline{F_{NO_x}}$	molec cm ⁻² s ⁻¹	Mean austral summer flux of snow-sourced NO _x
F_{NO_x}	ng N m ⁻² yr ⁻¹	Annual sum of snow-sourced NO _x flux
F_{PRI}	ng N m ⁻² yr ⁻¹	Annual sum of primary NO ₃ ⁻ deposited to snow
F_R	ng N m ⁻² yr ⁻¹	Annual sum of recycled NO ₃ ⁻ to snow
NRF_{yr}	unitless	Metric to assess degree of nitrogen recycling in 1 year
NRF_{τ_z}	unitless	Metric to assess degree of nitrogen recycling before NO ₃ ⁻ burial below snow photic zone
τ_z	years	Years NO ₃ ⁻ remains in snow photic zone
f	fraction	Fraction of photolysis-driven loss of NO ₃ ⁻ from snow

Maria Zlatko 9/10/15 6:41 PM

Deleted: in below 2 cm snow depth

1582
1583
1584
1585
1586
1587
1588
1589
1590
1591
1592
1593
1594
1595
1596
1597

1599
1600

Table 2. Value(s) of parameters used in the model.

Variable	Value(s) used in model	References
ϕ	0.002 molec photon ^{-1a}	Chu and Anastasio [2003]
$\sigma_{NO_3^-}$	2.7x10 ⁻²⁰ cm ² (λ =298-307 nm) 2.4x10 ⁻²⁰ cm ² (λ =307-312 nm) 1.9x10 ⁻²⁰ cm ² (λ =312-320 nm) 2.3x10 ⁻²¹ cm ² (λ =320-345 nm)	Sander et al. [2006]
ϵ	-47.9‰	Berhanu et al. [2014]
r_e	Jan: 332.0 μm^b Dec-Feb: 198-332.0 μm^b Mar-Nov: 86.0-332.0 μm^b	Gallet et al. [2011] Klein [2014]
ρ_{snow}	260-360 kg m ^{-3c}	Gallet et al. [2011]
EF^b	6 ^d	Dibb et al. [2004] Erbland et al. [2013] Frey et al. [2009] Mayewski and Legrand [1990] Rothlisberger et al. [2000]
$[NO_3^-]_{bot}$	60 ng g ^{-1e}	Bertler et al. [2005]

1601
1602
1603
1604
1605
1606
1607
1608
1609
1610
1611
1612
1613
1614
1615
1616
1617
1618
1619
1620
1621
1622
1623
1624
1625
1626
1627

^aAt temperature (T) = 244K
^b r_e is varied vertically and temporally, but uniformly across Antarctica based on Gallet et al. [2011] and Klein [2014]. In January, r_e is constant with depth (332 μm), in December and February, r_e ranges from 198 μm at the snow surface to 332 μm at 300 cm depth, and from March to November, r_e ranges from 86 μm at the surface to 360 μm at 300 cm depth.
^cThe mean vertical ρ_{snow} profile from several Dome C snowpits are used in this study (see Figure 11 in Gallet et al. [2011]).
^dMedian of observed NO_3^- enhancement factors.
^eMedian of observed sub-surface snow NO_3^- mixing ratios from the ITASE campaign.

1628

1629 Table 3. Dependence of mean austral summer (DJF) flux of snow-sourced NO_x ($\overline{F_{\text{NO}_x}}$) on
 1630 quantum yield (ϕ), the fraction of photolabile NO_3^- (F_p), snow NO_3^- concentrations below
 1631 2 cm ($[\text{NO}_3^-]_{\text{bot}}$), the radiation equivalent ice grain radius (r_e), the bulk snow extinction
 1632 coefficient ($K_{\text{ext}_{\text{tot}}}$), the NO_3^- concentration enhancement factor in the top 2 cm (EF), and
 1633 snow black carbon concentration (C_{BC}).

Parameter	Base case values ^a	Values used in sensitivity studies	$\overline{F_{\text{NO}_x}}$ range in sensitivity studies ($\times 10^8 \text{ molec cm}^{-2} \text{ s}^{-1}$)	Corresponding Figures
Quantum yield (ϕ)	0.002 molec photon ⁻¹ ^b	0.6 molec photon ⁻¹	5-2600	Fig. 4a, b, c, d Fig. 1Aa
Fraction of photolabile NO_3^- (F_p)	0.01-0.99 (spatial variation, Figure 3c)	Set to 1 everywhere	3.7-9.6	Fig. 4c, d
Sub-surface snow NO_3^- ($[\text{NO}_3^-]_{\text{bot}}$)	60.0 ng g ⁻¹ ^c	30-120 ng g ⁻¹	0.3-15.8	Fig. 1Ab, c
Radiation equivalent mean ice grain radii (r_e)	Jan: 332.0 μm ^d Dec-Feb: 198-332.0 μm ^d Mar-Nov: 86.0-332.0 μm ^d	Study 1: 332.0 μm ^e Study 2: 198-332.0 μm ^e Study 3: 86.0-332.0 μm ^e	0.5-10.2	Fig. 1Aj, k, l
Bulk snow extinction coefficient ($K_{\text{ext}_{\text{tot}}}$)	1.7-6.9 $\times 10^3 \text{ m}^{-1}$ (spatial variation)	$\pm 20\%$ with respect to base case values	0.5-9.4	Fig. 1Ah, i
NO_3^- enhancement factor in top 2 cm (EF)	6.0 ^f	1-10	0.5-9.3	Fig. 1Af, g
Snow black carbon (C_{BC})	0.08-0.6 ng g ⁻¹ (spatial variation, Figure 3b)	\pm factor of 2 with respect to base case values	0.5-8.6	Fig. 1Ad, e

1634 ^abase case $F_{\text{NO}_x}=0.5-7.8 \times 10^8 \text{ molec cm}^{-2} \text{ s}^{-1}$ (Figure 4d)

1635 ^bfrom Chu and Anastasio [2003] at $T=244\text{K}$

1636 ^cmedian of ITASE campaign [Bertler *et al.*, 2005]

1637 ^d r_e is varied vertically and temporally, but uniformly across Antarctica based on Gallet *et al.* [2011] and Klein [2014]. In January, r_e is constant with depth (332 μm), in December and February, r_e ranges from 198 μm at the snow surface to 332 μm at 300 cm depth, and
 1639 from March to November, r_e ranges from 86 μm at the surface to 360 μm at 300 cm
 1640 depth.
 1641

1642 ^ein r_e sensitivity study 1, the base-case ‘January’ r_e profile is applied for every month. In
 1643 r_e sensitivity study 2, the base-case ‘December and February’ r_e profile is applied for
 1644 every month. In r_e sensitivity study 3, the base-case ‘March-November’ r_e profile is
 1645 applied for every month.

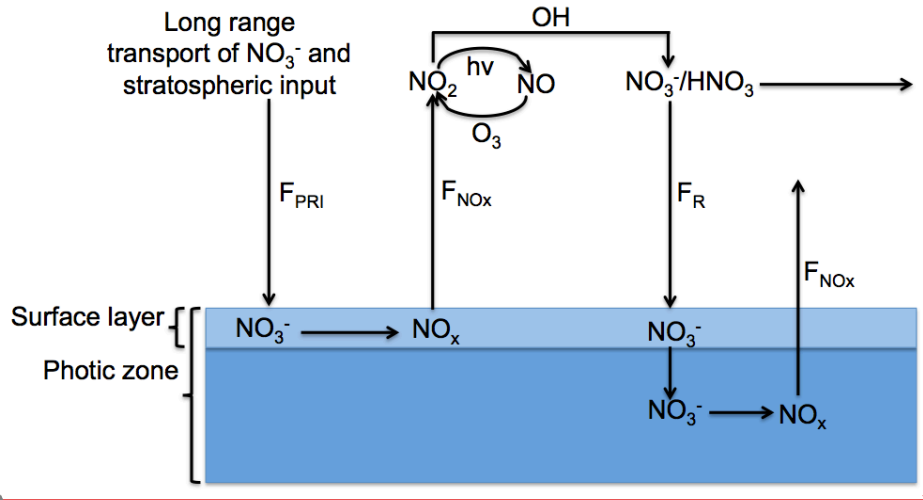
1646 ^fmedian of observed EF [Dibb *et al.*, 2004, Frey *et al.*, 2009, Mayewski and Legrand,
 1647 1990, Rothlisberger *et al.*, 2000].

1648

1649

1650

1651



1652

1653 Figure 1. Schematic showing the nitrogen recycling associated with NO_3^- photolysis as
1654 included in the model. F_{PRI} ($\text{ng N m}^{-2} \text{yr}^{-1}$) is the downward, primary flux of NO_3^- to
1655 Antarctica originating from long-range transport and the stratosphere, F_{NOx} ($\text{ng N m}^{-2} \text{yr}^{-1}$)
1656 ¹) is the upward flux of snow-sourced NO_x to the boundary layer, and F_R ($\text{ng N m}^{-2} \text{yr}^{-1}$)
1657 is downward, recycled flux of HNO_3 to the snow surface. The surface snow layer (top 2
1658 cm) is distinguished from the rest of the photic zone because 30-65% of snow-sourced
1659 NO_x is produced in the **top 2 cm of snowpack** [Zatko *et al.*, 2013], and because both NO_3^-
1660 concentrations and actinic flux are much higher in the top surface layer compared to
1661 deeper layers.

1662

1663

1664

1665

1666

1667

Unknown

Formatted: Font:(Default) Times New Roman

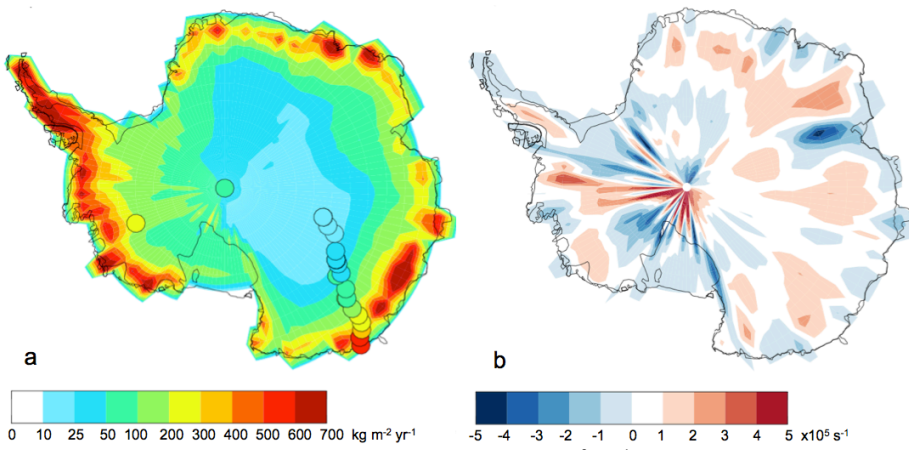
Maria Zatko 10/12/15 6:44 PM

Deleted: -

... [8]

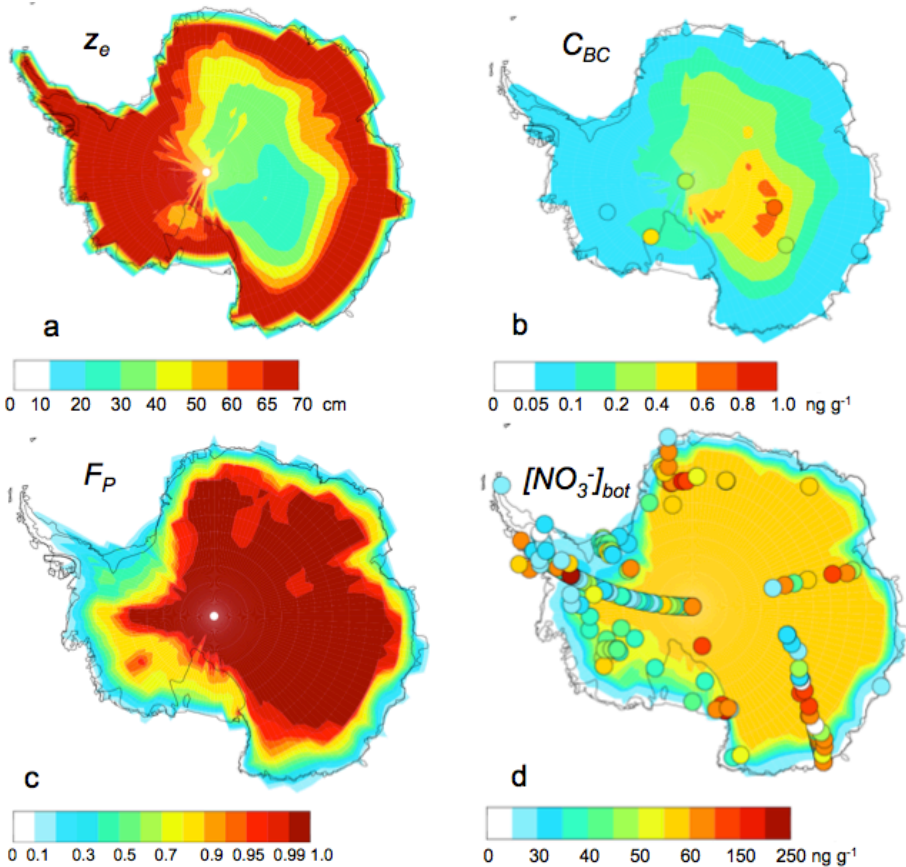
Unknown

Formatted: Font:(Default) Times New Roman



1670
 1671 Figure 2. (a) Annual total snow accumulation rate ($\text{kg m}^{-2} \text{yr}^{-1}$) in GEOS-Chem from May
 1672 2009 to May 2010 with annual snow accumulation rates (circles) estimated in Erbland et
 1673 al. [2013], [Fegyveresi et al. \[2011\]](#), and Grenfell et al. [1994]. (b) Annual mean surface
 1674 wind divergence (s^{-1}) in GEOS-Chem from May 2009 to May 2010. Blue regions indicate
 1675 regions of convergence.
 1676
 1677

Maria Zatko 10/14/15 4:11 PM
 Deleted: , and Sofen et al. [2014].



1679
1680
1681
1682
1683
1684
1685
1686
1687
1688
1689
1690
1691
1692
1693
1694
1695
1696

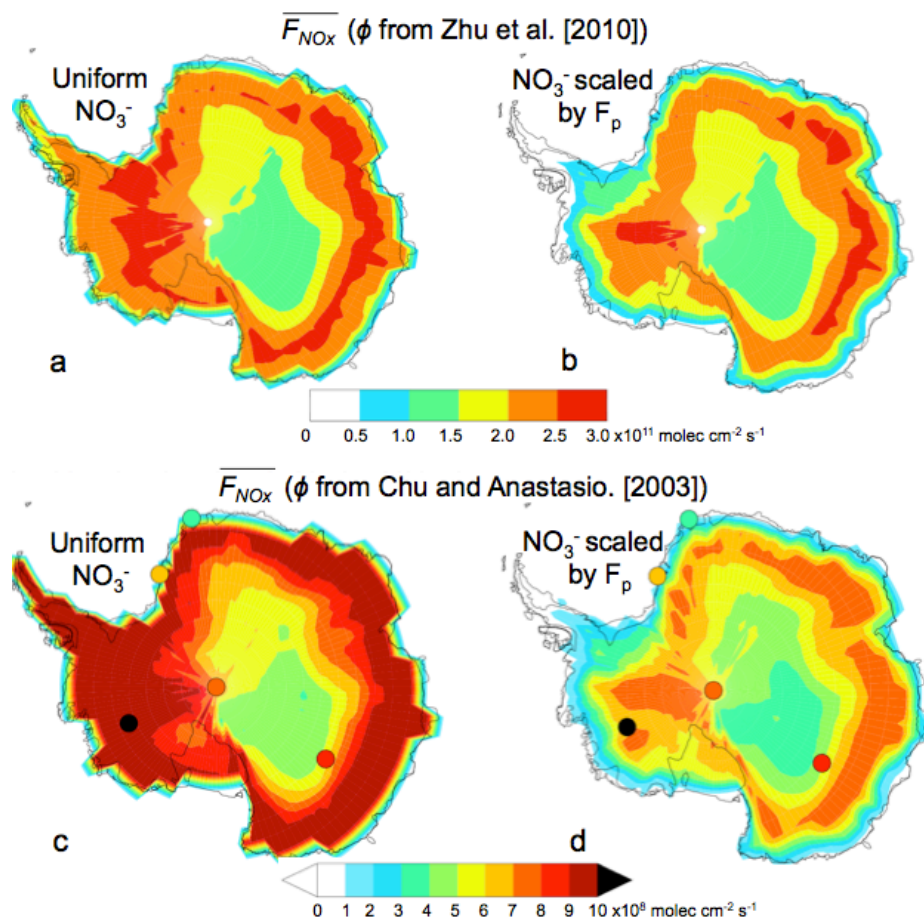
Figure 3. (a) Calculated mean austral summer (DJF) UV e-folding depth (z_e). (b) Modeled and observed (circles) annual mean snow black carbon concentrations (C_{BC}), with observations from WAIS-Divide and Law Dome [Bisiaux *et al.*, 2013], Siple Dome [Chylek *et al.*, 1992], Vostok [Grenfell *et al.*, 1994], South Pole [Warren and Clarke, 1990], and Dome C [Warren *et al.*, 2006]. (c) Ratio of annual dry-deposited NO_3^- to annual total deposited NO_3^- , F_P . (d) Annual sub-surface snow NO_3^- concentrations ($[NO_3^-]_{bot}$) from 2-cm depth to the bottom of the snow photic zone (z_{3e}) used in the model scaled by F_P . Mean sub-surface, multi-year NO_3^- observations from the ITASE campaign along with mean asymptotic (sub-photic zone) NO_3^- mixing ratios from Erbland *et al.* [2013] and Shi *et al.* [2014] (circles) are also included in Figure 3d [Bertler *et al.*, 2005].

Maria Zatko 10/12/15 6:29 PM

Deleted: Unknown
Formatted: Font:(Default) Times New Roman

Maria Zatko 9/11/15 8:58 AM
Deleted: along with
Maria Zatko 9/11/15 8:58 AM
Deleted: average
Maria Zatko 9/11/15 8:58 AM
Deleted: d

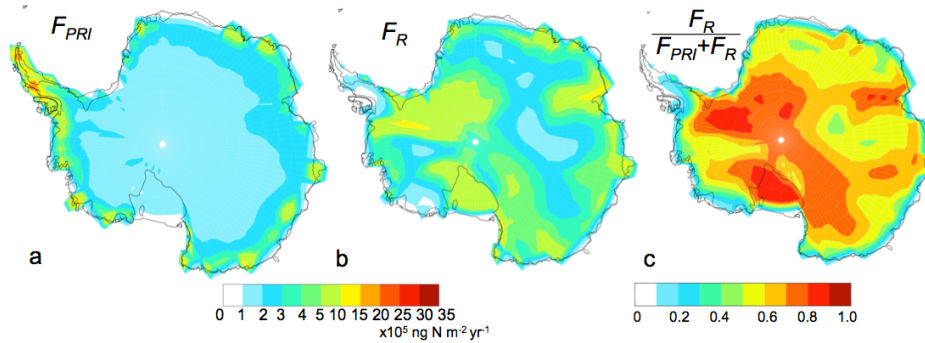
1701
1702



1703
1704
1705
1706
1707
1708
1709
1710
1711
1712
1713
1714
1715
1716

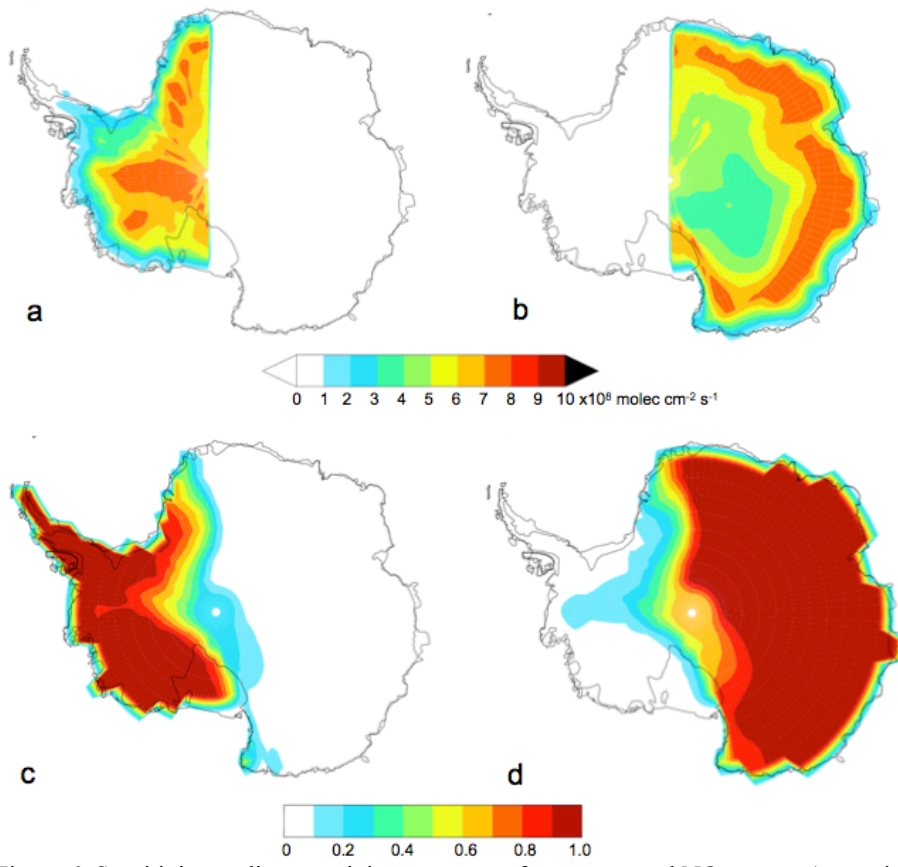
Figure 4. Mean austral summer (DJF) flux of snow-sourced NO_x from the snow ($\overline{F_{NO_x}}$) with previously reported F_{NO_x} observations from Neumayer [Jones et al., 2001], Halley [Jones et al., 2011, Bauguitte et al., 2012], South Pole [Oncley et al., 2004, Wang et al., 2008, Zatzko et al., 2013], WAIS-Divide [Masclin et al., 2013], and Dome C [Frey et al., 2013, Zatzko et al., 2013]. (a) $\overline{F_{NO_x}}$ calculated using ϕ from Zhu et al. [2010] and uniform snow NO_3^- concentrations ($[NO_3^-]_{top}=360 \text{ ng g}^{-1}$, $[NO_3^-]_{bot}=60 \text{ ng g}^{-1}$). (b) $\overline{F_{NO_x}}$ calculated using ϕ from Zhu et al. [2010] and uniform snow NO_3^- concentrations ($[NO_3^-]_{top}=360 \text{ ng g}^{-1}$, $[NO_3^-]_{bot}=60 \text{ ng g}^{-1}$) scaled by the ratio of annual dry-deposited NO_3^- to annual total deposited NO_3^- (F_p , Figure 3c) (c) $\overline{F_{NO_x}}$ calculated using ϕ from Chu and Anastasio [2003] and uniform snow NO_3^- concentrations ($[NO_3^-]_{top}=360 \text{ ng g}^{-1}$, $[NO_3^-]_{bot}=60 \text{ ng g}^{-1}$). (d) Base case: $\overline{F_{NO_x}}$ calculated using ϕ from Chu and Anastasio [2003] and uniform snow NO_3^- concentrations ($[NO_3^-]_{top}=360 \text{ ng g}^{-1}$, $[NO_3^-]_{bot}=60 \text{ ng g}^{-1}$) scaled by the ratio of annual dry-deposited NO_3^- to annual total deposited NO_3^- (F_p).

1717
1718
1719
1720



1721
1722 Figure 5. (a) Annual wet plus dry deposition flux of primary NO_3^- to the snow (F_{PRI}). (b)
1723 Annual wet plus dry deposition flux of recycled NO_3^- to the snow (F_R). (c) Ratio of F_R
1724 to the total downward NO_3^- flux ($\frac{F_R}{F_{PRI}+F_R}$) for the base case scenario.

1725
1726
1727
1728
1729
1730
1731
1732
1733
1734
1735
1736
1737



1738
 1739
 1740
 1741
 1742
 1743
 1744
 1745
 1746
 1747

Figure 6. Sensitivity studies examining transport of snow-sourced NO_x across Antarctica. Mean austral summer (DJF) $\overline{F_{NO_x}}$ across Antarctica when $\overline{F_{NO_x}}$ set to 0 (a) in East Antarctica and (b) in West Antarctica. Ratio of recycled NO_3^- flux (F_R) to F_R in the base case scenario when $F_{NO_x}=0$ in (c) East Antarctica and (d) in West Antarctica.

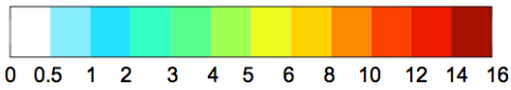
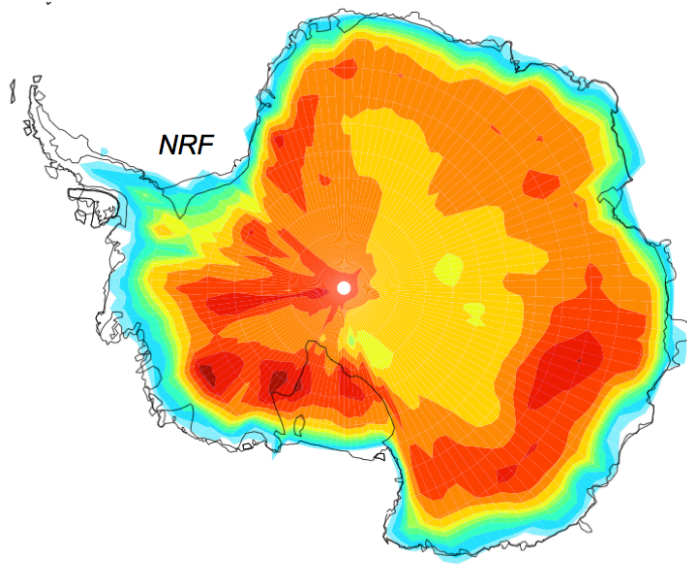
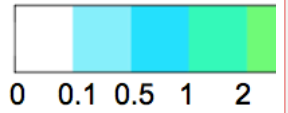
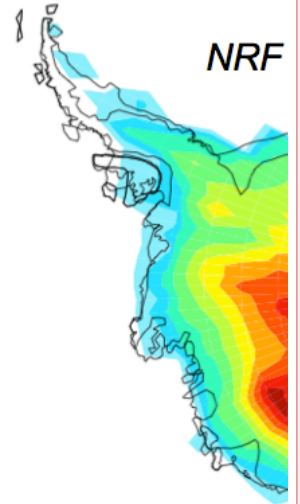


Figure 7. Nitrogen recycling factor (NRF_{E8}).

1748
1749
1750
1751
1752
1753
1754
1755
1756
1757
1758
1759
1760
1761

Unknown
Formatted: Font:(Default) Times New Roman

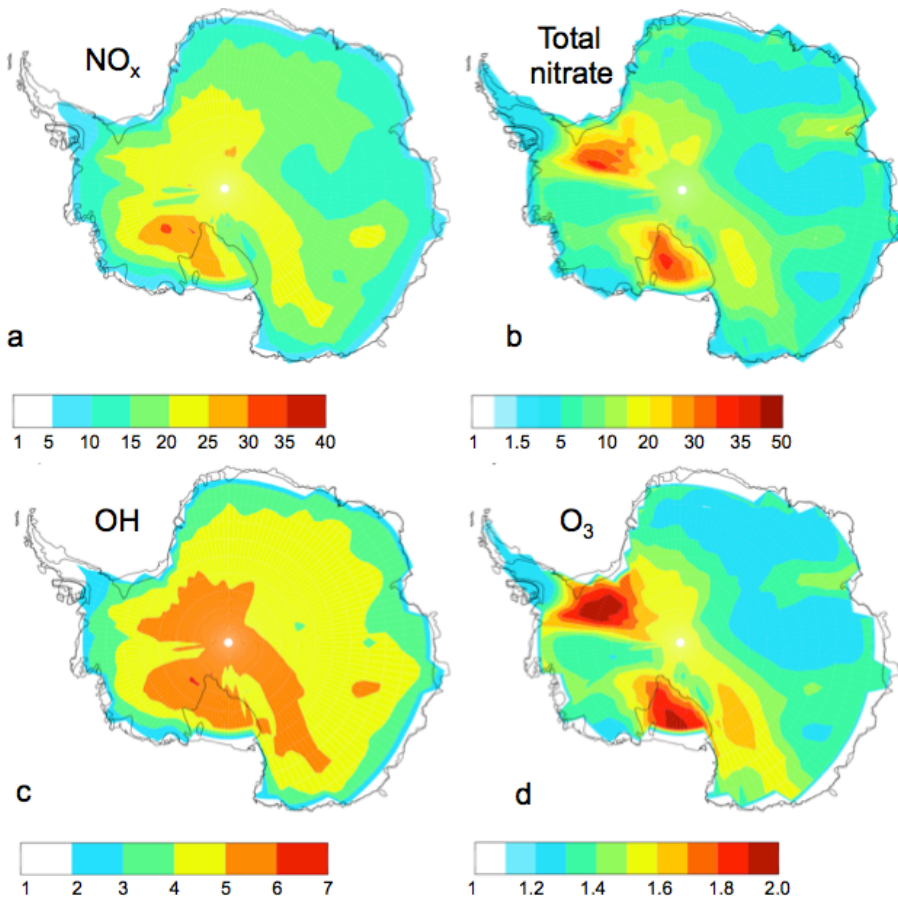
Maria Zatko 10/14/15 8:55 AM



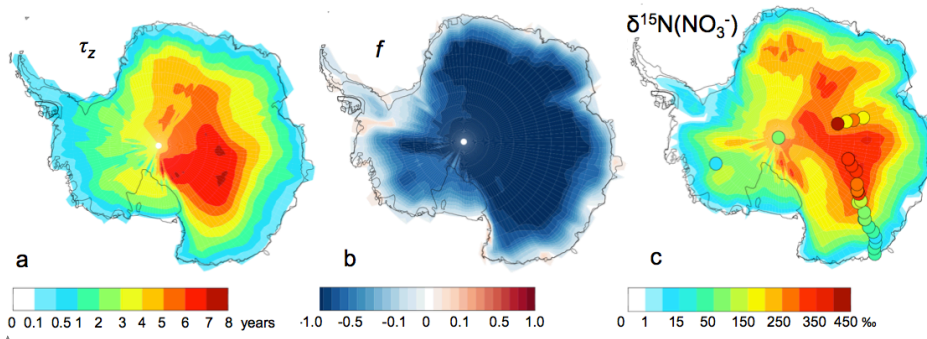
Deleted:

Maria Zatko 10/13/15 10:22 AM

Deleted: _{yr}



1764
 1765 Figure 8. Factor increase in mean austral summer (DJF) boundary layer (a) NO_x , (b)
 1766 gas+aerosol phase nitrate, (c) OH, and (d) O_3 mixing ratios between model runs with
 1767 F_{NO_x} compared to without F_{NO_x} .
 1768
 1769
 1770
 1771

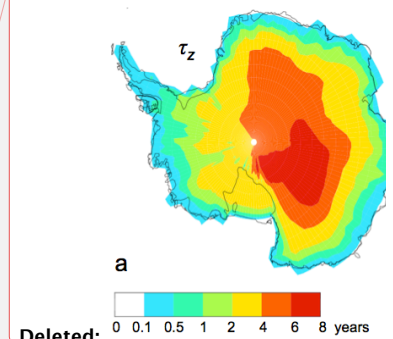


1772
 1773
 1774
 1775
 1776
 1777
 1778
 1779
 1780
 1781
 1782
 1783
 1784
 1785
 1786
 1787
 1788
 1789
 1790
 1791
 1792
 1793

Figure 9. (a) Minimum years NO_3^- remains in photolytic zone (τ_z , years, E10). (b) Fraction of NO_3^- gained (positive values) or lost (negative values) from the snow through photolysis (f , E9). (c) Modeled enrichment in ice-core $\delta^{15}\text{N}(\text{NO}_3^-)$ (E11) due to photolysis-driven loss of NO_3^- in snow compared to sub-photic zone $\delta^{15}\text{N}(\text{NO}_3^-)$ observations [Erbland *et al.*, 2013, Frey *et al.*, 2009, Jarvis, 2008, Shi *et al.*, 2014, Sofen *et al.*, 2014].

Unknown
 Formatted: Font:(Default) Times New Roman

Maria Zatko 10/13/15 8:02 AM



Deleted: 0 0.1 0.5 1 2 4 6 8 years

Maria Zatko 9/12/15 5:43 PM

Deleted: lost

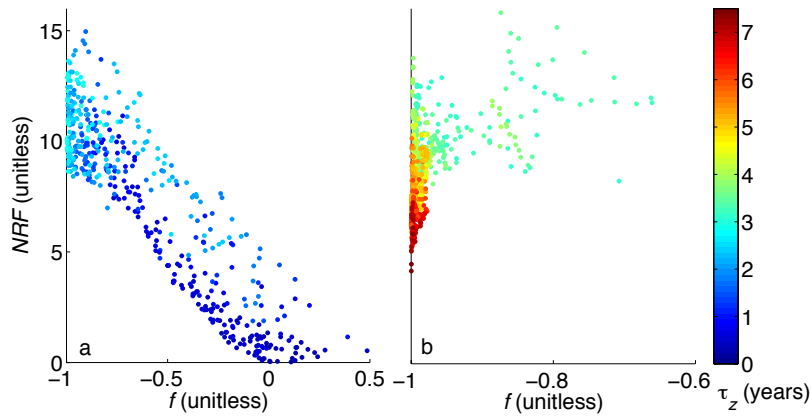
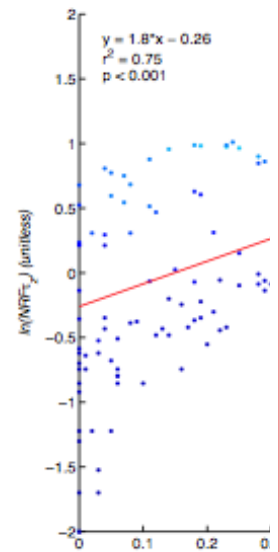
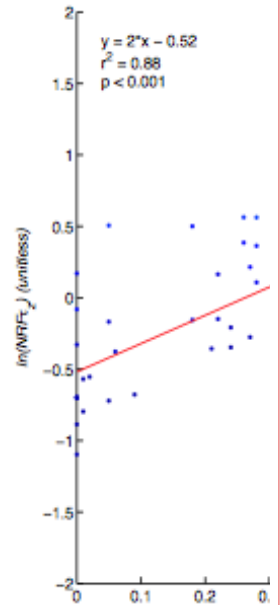


Figure 10. *NRF* versus *f* values across Antarctica. (a) Regions where NO_3^- remains in the photic zone for 3 years or less. (b) Regions where NO_3^- remains in the photic zone for more than 3 years. The color scale represents the number of years NO_3^- remains in the photic zone (τ_z). Note the different x-axis range for (a) and (b).

1796
1797
1798
1799
1800
1801
1802
1803
1804
1805
1806
1807
1808
1809
1810
1811
1812
1813
1814
1815
1816
1817
1818
1819
1820
1821
1822
1823
1824
1825
1826
1827

Maria Zatko 10/14/15 9:45 AM



Deleted:

Unknown

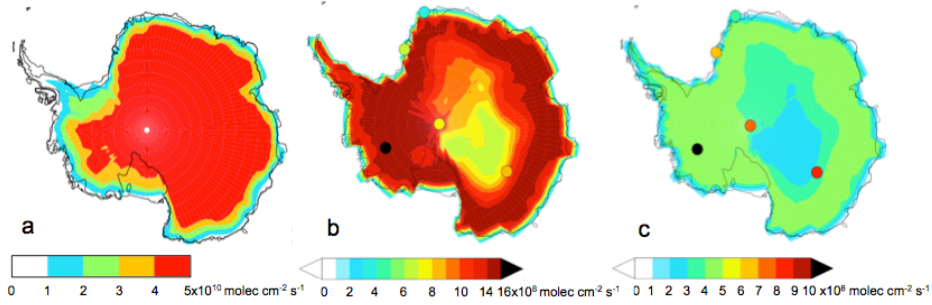
Formatted: Font:(Default) Times New Roman

Maria Zatko 10/14/15 9:46 AM

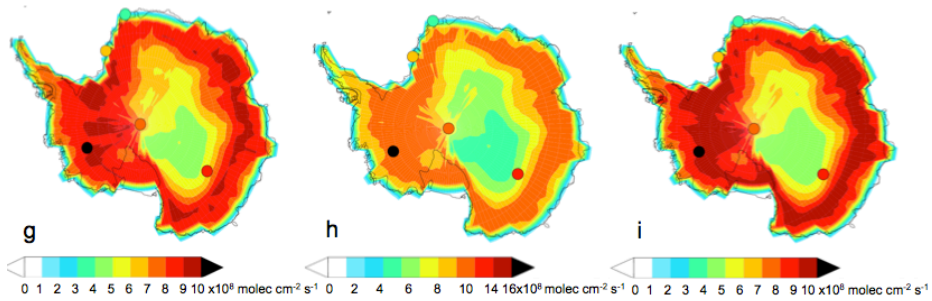
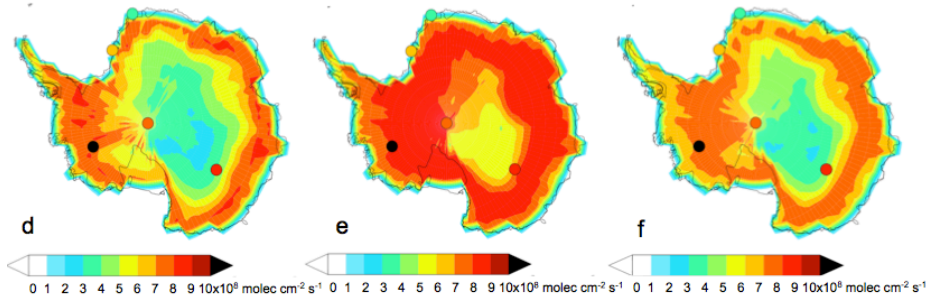
Deleted: The linear regression line, r^2 , and p value for all Antarctica data (East Antarctica + West Antarctica) is $y=1.8x - 0.32$, 0.80, and 0.001, respectively.

1833
1834

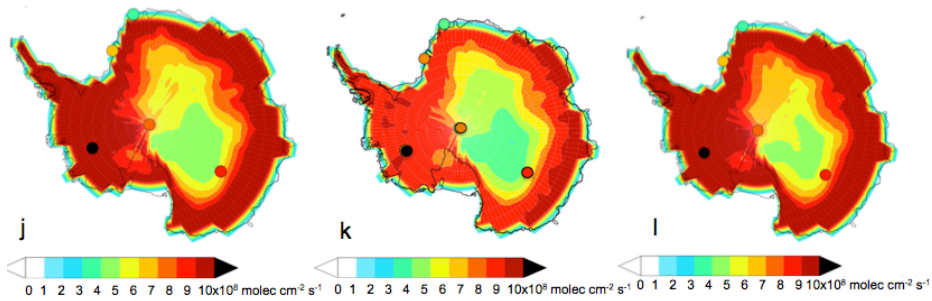
Appendix A



1835
1836



1837
1838



1839 Figure 1A. Results of sensitivity studies that show how the average austral summer (DJF)
1840 flux of snow-sourced NO_x ($\overline{F_{\text{NO}_x}}$) in Antarctic snowpacks is altered by changes in
1841 variables relevant to snow NO_3^- photolysis. The standard set of variables in the above
1842 figures are quantum yield (ϕ) = 0.002 molec photon⁻¹, fraction of photolabile NO_3^- (F_p) =
1843 1, annual mean sub-surface snow NO_3^- ($[\text{NO}_3^-]_{\text{bot}}$) = 60 ng g⁻¹, radiation equivalent mean
1844 ice grain radii (r_e) = 332 μm , NO_3^- enhancement factor (EF) = 6, bulk snow extinction
1845 coefficient ($K_{\text{ext}_{\text{tot}}}$) = 1.7x10⁻³ to 6.9x10⁻³ (spatial variability), and annual mean snow
1846 black carbon (C_{BC}) = 0.08 to 0.6 ng g⁻¹ (spatial variability). Observed $\overline{F_{\text{NO}_x}}$ values are
1847 overplotted (see Figure 4 for references). In (a), for the top centimeter of snow, the Zhu et
1848 al. [2010] ϕ is applied to all dry-deposited NO_3^- and the Chu and Anastasio [2003] ϕ is
1849 applied to all wet-deposited NO_3^- . Below 1 cm, the Chu and Anastasio [2003] ϕ is applied
1850 to all NO_3^- . In (b), $[\text{NO}_3^-]_{\text{bot}}$ is doubled from the base case value and in (c), $[\text{NO}_3^-]_{\text{bot}}$ is
1851 halved from the base case value. In (d), the C_{BC} is doubled from base case values and in
1852 (e) the C_{BC} is halved from base case values. In (f), $EF=1$ and in (g), $EF=10$. In (h), $K_{\text{ext}_{\text{tot}}}$
1853 is a factor of 1.2 higher than the base case value. In (i), $K_{\text{ext}_{\text{tot}}}$ is a factor of 0.8 than the
1854 base case value. In (j), r_e is representative of austral mid-summer (January) conditions is
1855 used (see Table 3 footnote). In (k), r_e is representative of austral spring, fall, and winter
1856 (March-November) conditions. In (l), r_e is representative of austral early summer and
1857 late summer (December, February) conditions. Note different color scales.

1858
1859
1860
1861
1862
1863
1864
1865
1866
1867
1868
1869
1870
1871
1872
1873
1874